coatings

MDPI

Review

Copper-Based Composite Coatings by Solid-State Cold Spray Deposition: A Review

Huipeng Wang [1], Peng Li [1,2], Weiling Guo [2,*], Guozheng Ma [2,*] and Haidou Wang [2,3]

[1] School of Mechanical and Electrical Engineering, Jiangxi University of Science and Technology, Ganzhou 341000, China
[2] National Key Laboratory of Remanufacturing, Army Academy of Armored Force, Beijing 100072, China
[3] National Engineering Research Center for Remanufacturing, Army Academy of Armored Force, Beijing 100072, China
* Correspondence: guoweiling_426@163.com (W.G.); magz0929@163.com (G.M.)

Abstract: Copper (Cu)-based composite coatings have been widely applied in all kinds of important industry fields due to their outstanding comprehensive properties. The preparation temperature of a composite coating is the key factor affecting the properties, so the cold spray (CS) technology is characterized by low-temperature solid-state deposition, which ensures its emergence as the most promising technology for preparing the Cu-based composite coatings. In this paper, first, the principle of CS technology and the deposition mechanism of the coatings are introduced. On this basis, the deposition mechanism of Cu-based metal/ceramic composite coatings is further explored. Secondly, the effects of key CS process parameters (particle velocity, particle morphology, and substrate state) on the quality of the Cu-based composite coatings are summarized, and the current research status of cold-sprayed Cu-based composite coatings in the fields of corrosion resistance, wear resistance, self-lubricating properties, and electrical conductivity is reviewed. Moreover, the improvement of the performance of Cu-based composite coatings by various post-process treatments of coatings, such as heat treatment (HT) and friction stir processing (FSP), is elaborated. Finally, the future development of Cu-based composite coatings and CS technology is prospected.

Keywords: cold spraying; copper-based composite coating; deposition mechanism; spraying parameters; post-processing technology

Citation: Wang, H.; Li, P.; Guo, W.; Ma, G.; Wang, H. Copper-Based Composite Coatings by Solid-State Cold Spray Deposition: A Review. *Coatings* **2023**, *13*, 479. https://doi.org/10.3390/coatings13030479

Academic Editor: Philipp Vladimirovich Kiryukhantsev-Korneev

Received: 6 February 2023
Revised: 14 February 2023
Accepted: 16 February 2023
Published: 21 February 2023

1. Introduction

Copper (Cu) and Cu alloys are unique regarding ductility, thermal conductivity, and electrical conductivity, which ensures their wide application in energy, electric power, rail transit, aerospace, military machinery, and other industrial fields [1,2]. However, the hardness, strength and wear resistance of Cu and Cu alloys are relatively unsatisfactory. Currently, appropriate surface treatment technologies are mainly adopted for the preparation of high-performance coatings on the surfaces of Cu and Cu alloys to improve the performance and service life of these materials. An in-depth exploration of the technical principles and process parameters of CS, the deposition mechanisms and application of Cu-based functional coatings, and the post-treatment processes of the coatings has been made by researchers, aiming to further improve the comprehensive performance of the coatings under high temperature, high salinity, high electric current, heavy load, and other adverse working conditions [3–6]. It has been shown that the Cu-based composite coatings, prepared with Cu as the main phase and hard ceramics, amorphous material, diamond, graphene, carbon nanotubes, and other metal particles as the reinforcing phase, takes the advantage of both the metallic phase (good tenacity and machinability) and the reinforcing ceramic phase (high hardness and good wear resistance), which is characterized by low porosity, high hardness, and high bonding strength. There is no doubt that the Cu-based

composite coatings exhibit excellent corrosion resistance, wear resistance, electrical conductivity, and self-lubricating properties, as well as ideal mechanical properties, manifesting its wide application prospect in industrial fields [7,8].

At present, the preparation technologies of Cu-based composite coatings dominated by powder metallurgy, vapor deposition, electrospark deposition, laser cladding, and thermal spray require high temperature and high pressure [9]. Cu-based composite coatings prepared by the methods above show certain defects. For example, the mechanical bonding between the coating prepared by powder metallurgy and the substrate shows a low bonding strength and poor coating quality. There is a low bonding strength between the coating prepared by thermal spray and the corresponding substrate, making the coating potentially defective. Additionally, the coating prepared by vapor deposition technology is very thin and displays other defects, which results in the poor comprehensive performance of Cu-based composite coatings and the stagnation of most of them in the laboratory phase. The above-mentioned defects inhibit the application of these conventional surface strengthening technologies in the manufacture of Cu-based composite coatings used in practical engineering under heavy load and special service conditions. Therefore, it is crucial to find a more cost-effective method for surface strengthening of copper and copper alloys [10,11].

CS, with no defects similar to the above-mentioned technologies, has attracted extensive attention from researchers, as it helps deposit solid particles onto substrates with no need for high-temperature phase transition or oxidation. The CS process is achieved using high-pressure gas, during which the solid particles are regulated to impact the substrate at a supersonic speed and then deposited on the substrate surface to form a coating through severe plastic deformation [12,13]. As a low-temperature solid-state deposition method, CS is characterized by a low deposition temperature, a low oxidation ratio of powder, a high deposition efficiency, little thermal influence on the substrate, etc., by which coatings with low porosity, high compactness, and controllable thickness can be prepared, establishing its indispensable position among coating preparation technologies [14,15]. In recent years, CS has been adopted to prepare the Cu-based composite coatings with corrosion resistance, wear resistance, self-lubricating properties, and high electrical conductivity that can be applied under different working conditions, which not only expands the application of Cu-based composite coatings but also promotes the rapid development of CS in industrial fields. Nonetheless, the high brittleness, poor ductility, and weak cohesion of cold-sprayed coatings caused by dislocations and residual stresses make it impossible to prepare parts and components capable of displaying the advantages of high-performance Cu-based composite coatings [16,17]. Therefore, post-process treatments may also be required in order to promote the comprehensive performance of Cu-based composite coatings [18,19]. The application of CS technology to prepare high-performance metal protective coatings, repair failed metal parts and components, and manufacture additive materials has become a research hotspot in related fields [20–22].

In this paper, the recent research progress of CS technology in the preparation of Cu-based composite coatings is summarized mainly from the following aspects: the principle of CS technology, the deposition mechanism of cold-sprayed coatings, the deposition mechanism of Cu-based composite coatings, the influence of CS process parameters on coating quality, the application status of Cu-based composite coatings in corrosion resistance, wear resistance, self-lubricating properties, and electrical conductivity, and the influence of post-process treatments on the performance of Cu-based composite coatings. Finally, the future development of cold-sprayed Cu-based composite coatings is prospected, aiming to provide references for the research and application of cold-sprayed Cu-based composite coatings.

2. Principle of CS Technology and the Deposition Mechanism of Coatings

2.1. Principle of CS Technology

In the late 1980s, Anatolii Papyrin, a scientist from the former Soviet Union, and his team conducted wind tunnel experiments and revealed a phenomenon that the effect of tracer particles on the target surface changes from erosion-targeted to deposition-targeted when the speed exceeds a certain critical value, contributing to the close binding between the tracer particles and the target. Based on this phenomenon, the concept of CS was put forward [23]. The CS technology is highly valuable by virtue of its potential applications based on its performance in low-temperature solid-state deposition and its advantages in preparing coatings on metal surfaces, which has aroused worldwide interest, enabling its rapid development among coating preparation technologies. Large quantities of studies have been conducted on the research and development of CS equipment, material system design, numerical simulation, deposition mechanism of coatings, and optimization of spray process parameters over the past two decades. These achievements have accelerated the experimental process of CS technology and made it a reliable surface-strengthening technology, substantially promoting the development and application of CS technology [24].

CS is a novel technology for preparing a coating, and its principle is shown in Figure 1. During the CS, solid particles (particle size: 5–50 μm) undergo convergence and divergence through scaled de Laval nozzles under the action of a working gas (helium, nitrogen, air, gas mixtures, etc.) with a certain temperature and pressure to produce a supersonic biphasic flow (generally 300–1200 m/s), which collides with the substrate surface at high speed [25]. When the impact velocity of the feedstock particles reaches or exceeds their critical deposition velocity (v_{crit}), the solid particles impact the substrate to trigger "adiabatic shear instability (ASI)" at the interface to cause severe plastic flow deformation, thereby forming a coating on the substrate surface [26].

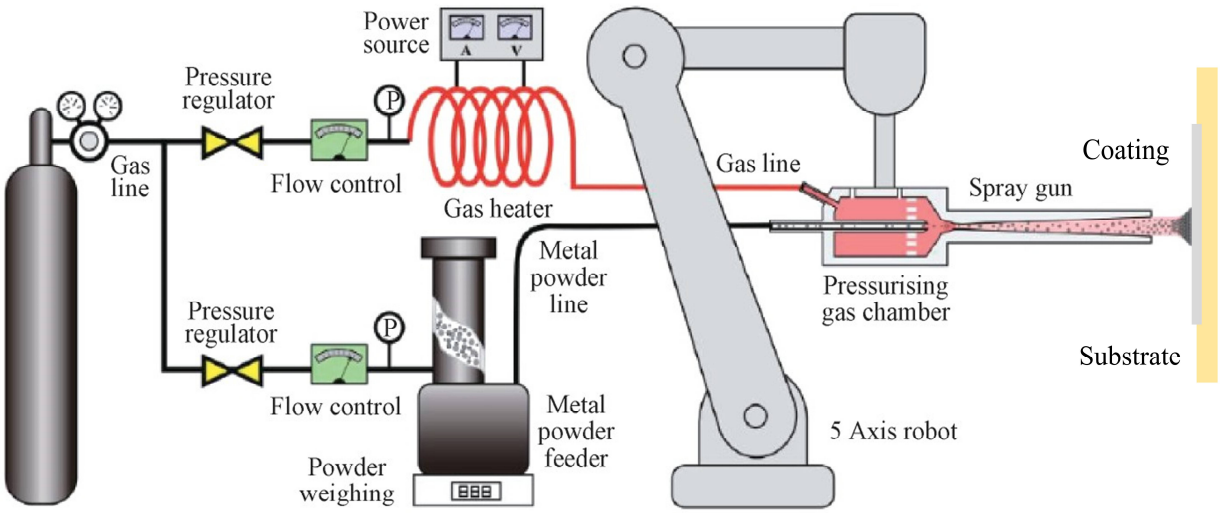

Figure 1. Schematic diagram of a typical cold spraying principle [25].

As the CS technology has been continuously developed and gradually becomes mature, many new "CS + assistive technologies", such as laser-assisted, shot-peening-assisted, magnetic-field-assisted, friction stir processing (FSP)-assisted, and pulse-assisted CS technologies, have been developed through the combination of the original single CS technology and other technologies [27]. Different types of CS technologies can be adopted in light of the actual application requirements of different engineering projects, laying crucial foundations for the design, preparation, and application of high-performance Cu-based composite coatings.

2.2. Deposition Mechanism of Cold-Sprayed Coatings

The bonding mechanism of cold-sprayed coatings has always been a hot research topic. Up to now, no consensus has been reached on the deposition mechanism of coatings. Nowadays, the theory of ASI proposed by Assadi et al. [28] is the most recognized coating deposition theory. The high-velocity impact of particles on the substrate causes severe plastic deformation at the interface of the impact, leading to the work hardening effect of the material. As the impact time is extremely short, most of the kinetic energy of the particles is converted into heat energy, and there is not enough time for energy transfer. Therefore, the heat energy causes a temperature rise, and results in the adiabatic softening of the material. If the impact velocity exceeds the critical velocity and the thermal softening effect overwhelms the work hardening effect, the plastic flow will appear on the metal surface, and then a metal jet will occur. At the same time, adiabatic shear instability (ASI) will occur on the particle surface. Grujici et al. [29] conducted a more detailed analysis on the sensitivity of metallic materials to ASI during the CS based on the research of Assadi et al. [28]. It is considered that the metal jet produced by ASI breaks and extrudes the oxide film on the contact interface between the particles and the corresponding substrate, which increases the contact area of the clean metal surface and facilitates the metallurgical bonding between the particles and the substrate. The fragmentation mechanism of oxide films proposed by Li et al. [30] is also consistent with the viewpoints of Grujici [29]. On the contrary, the latest research conducted by Hassani-Gangardj et al. [31] revealed that ASI is not a prerequisite for particle bonding during the CS, and the adiabatic softening effect is not necessarily implicated in the generation of the metal jet. Hassani-Gangardj [31] believed that, similar to explosive welding, a large pressure gradient at the particle interface induces the generation of the jet. These contradictions in science indicate that the deposition mechanism of cold-sprayed coatings has not yet been completely solved, which needs further research and exploration.

Fardan et al. [32] intuitively elaborated the specific formation process of a metal jet in the cases of adiabatic shearing and jetting through model diagrams (Figure 2). As shown in Figure 2a, the impact of particles on the substrate leads to changes in the temperature and plastic strain, which induce a local temperature rise, causing plastic flow. This process explains the adiabatic shearing. When the rate of strain hardening is lower than that of thermal softening, a point of thermal instability known as ASI appears. At this point, it is found that jetting takes place at the periphery of the particles. However, Hassani-Gangardj [31] argued that this bonding is attributed to hydrodynamic plasticity rather than ASI, and likewise, jetting is triggered by pressure release instead of ASI. At the time the particles impact the substrate, compressed pressure waves are generated and unevenly distributed in the particles and substrate (Figure 2b). In the initial phase, *Ve* is higher than *Vs*, but at a threshold point, the hydrodynamic stress is higher than the flow strength of the material, and jetting occurs [33]. According to other studies on hypervelocity impacts, such as shaped charge jetting, explosive welding, and droplet impact, jetting is induced by a pressure release, which is in accordance with the above-mentioned mechanism [34].

On the basis of the ASI mechanism, researchers put forward four recognized bonding methods for coatings, namely, physical bonding, mechanical bonding, chemical bonding, and metallurgical bonding. Under the conditions of different materials and deposition processes, inter-particle bonding in coatings can be achieved by one or more of the above-mentioned methods. Hussain et al. [35] believed that after the ASI of particles, the locally generated metal jet can crack and clear the oxide film on the substrate surface, exposing the clean particles and substrate surface. Under relatively high pressure, physical bonding can be formed between particles and the corresponding substrate or among particles under the action of electrostatic forces or Van der Waals forces. Moridi et al. [36] explained the interface bonding mechanism in the particle deposition process using the mechanical bonding mechanism. They found that particles undergo the ASI and pressure results in the plastic deformation and metal jets of particles. After plastic deformation, the obtained flat particles are embedded with an uneven interface, which forms a mechanical interlocking

structure, resulting in mechanical bonding. Xie et al. [37] deposited a hard Ni coating on a soft aluminum (Al) substrate by the CS to clarify the bonding mechanism on the coating/substrate interface, and found the intermetallic compound Al_3Ni at the interface, demonstrating that the high temperature generated during the plastic deformation of particles will induce the chemical bonding between the coating and the corresponding substrate. Grujicic et al. [38] held that the ASI is attributed to particle impacts, during which a large amount of heat energy will be generated. Local high temperatures can melt the substrate interface and strengthen the bonding at the coating/substrate interface, thus forming metallurgical bonding at the coating/substrate interface and inside the coating.

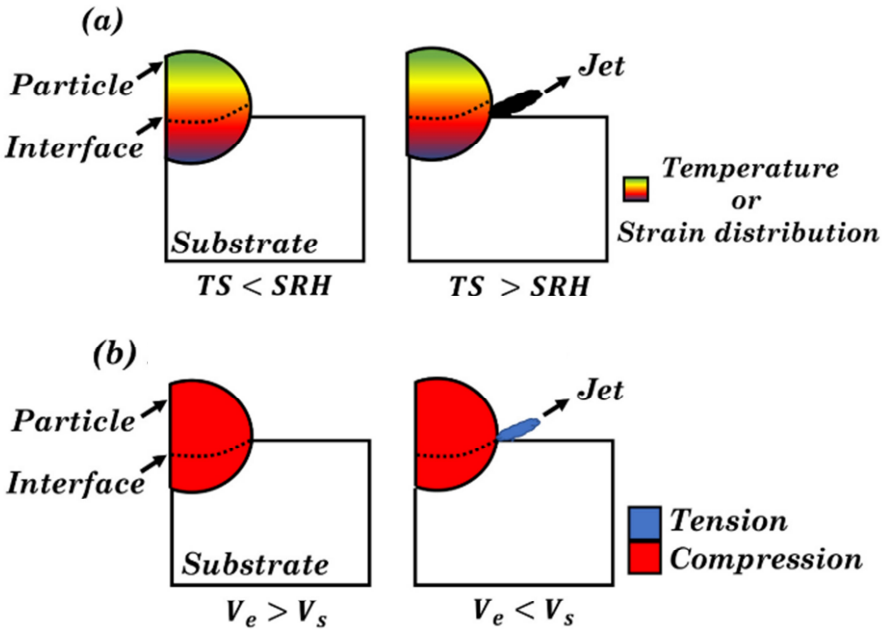

Figure 2. Schematic representation of the jet formation [32]. (**a**) Adiabatic shear instability, first proposed by Assadi et al. [28] and (**b**) hydrodynamic plasticity proposed by Hassani et al. [31]. TS = thermal softening, SRH = strain rate hardening, *Ve* = edge velocity, *Vs* = shock velocity.

To sum up, physical bonding and mechanical bonding occur almost at the same time. Under the action of Van der Waals forces, mechanical bonding is manifested as a non-chemical reaction. Theoretically, hard particles are mechanically captured by soft substrate materials to form interlocks, thus triggering the mechanical bonding. Regarding the whole deposition process of coatings, interfacial bonding is dominated by mechanical bonding. It is generally considered that metallurgical bonding results from chemical bonding between dissimilar materials, which is always accomplished by atomic diffusion. Moreover, the strength and plasticity of metallurgical bonding are far superior to those of mechanical bonding. Nonetheless, the CS is characterized by low-temperature solid-state deposition, by which the coating deposition is realized by means of the plastic deformation of particles, therefore mechanical bonding is the main bonding form of cold-sprayed coatings.

2.3. Deposition Mechanism of Cold-Sprayed Cu-Based Composite Coatings

2.3.1. Deposition Mechanism of Cu-Based Metal Composite Coatings

The deposition mechanism of the interfacial bonding between metals and metal alloy coatings is attributed to the severe deformation process caused by the high-velocity impact of metal/metal alloy solid particles, which directly influences the interfacial bonding quality of the coatings and finally determines the bonding strength and mechanical properties of the coatings. The deposition mechanism of Cu-based metal composite coatings is identical to that of cold-sprayed metal and metal alloy coatings, but it is remarkably different when ceramic particles are introduced into the Cu-based composite coatings. The metal-based ceramic composite powder has the characteristics of metal powder and the advantages

of ceramics, so its physical properties are different from those of the conventional metal powder. The deposition behavior of ceramic particles also dramatically differs from that of conventional metal particles. In the CS process, the ceramic particles as a hard reinforcing phase can hardly deform, while the metallic phase is prone to deformation due to the ASI, thus forming metallurgical and mechanical bonding with the substrate [24,39]. Hence, investigating the interfacial bonding process and deposition mechanism of the ceramic composite coatings is of vital significance to improve the performance of cold-sprayed Cu-based ceramic composite coatings.

2.3.2. Deposition Mechanism of Cu-Based Ceramic Composite Coatings

It has been revealed that the hardness, density, wear resistance, and mechanical properties of cold-sprayed coatings can be greatly enhanced and their bearing capacity can be strengthened through the addition of a hard reinforcing phase to the coatings [40]. Hence, the researchers added relatively harder metal particles and ceramic particles into metal feedstock particles, so as to analyze the role of the reinforcing phase in the deposition mechanism of metal-based composite coatings [41]. Fernandez et al. [42] proposed three hypotheses for the deposition mechanism of metal-based ceramic composite coatings to explain the increased deposition efficiency of coatings, including the shot peening (SP) effect, sandblasting effect, and cleaning effect. With ceramic particles as shots, the preceding soft particles are shot peened to increase their degree of deformation, thus increasing the deposition efficiency of the softer metal particles (Figure 3a). With the increase of the ceramic content, the interface between the coatings and the substrate becomes rougher due to the sandblasting effect of the ceramic particles on the substrate and the deposited particles (Figure 3b). When ceramic particles impact the metal or substrate, the oxide film on the surface of the metal particles or substrate is cleaned due to deformation, and the fresh metal surface can be exposed for the subsequent bonding of metal particles to produce more metallurgical bonding areas. Hence, ceramic particles can raise the deposition efficiency of metal particles (Figure 3c).

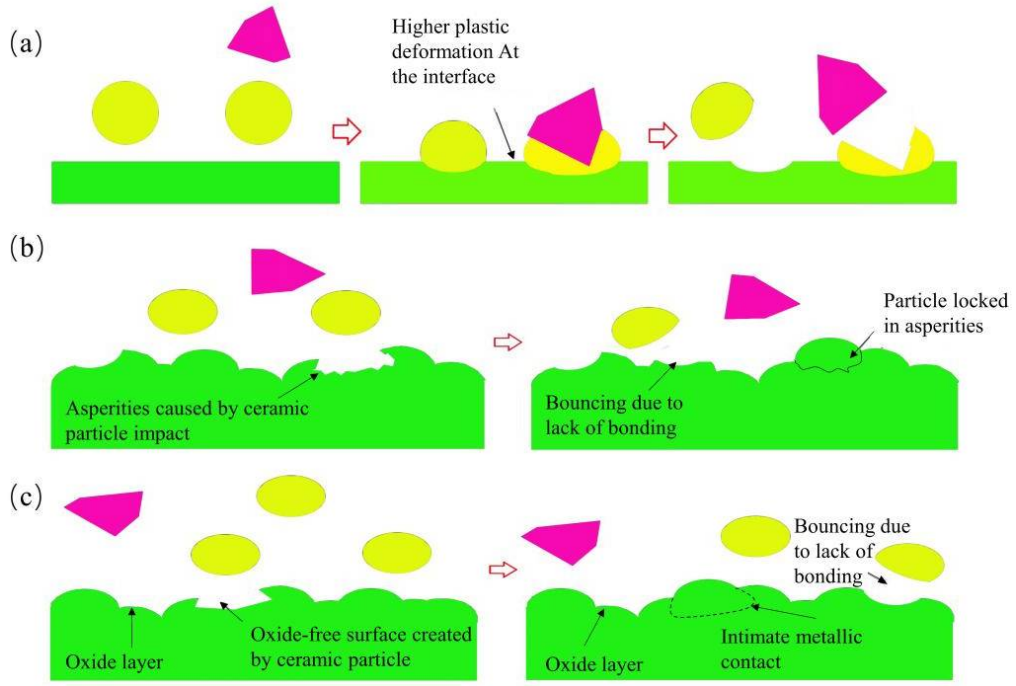

Figure 3. Schematic diagram of the three effects of metal–ceramic particles during deposition [42]. (**a**) Shot blasting effect; (**b**) sand blasting effect; (**c**) cleaning effect.

He and Chen et al. [43,44] summarized the impact effect between ceramic particles and metal particles in their research and concluded four effects according to the addition

order of ceramic particles, namely, the surface activation effect, the cushioning effect, the tamping effect, and the erosion effect (Figure 4). Firstly, the high-velocity impact of ceramic particles destroys the oxide layer on the substrate surface, and the pits generated by the impact increase the roughness of the substrate, so that the substrate surface maintains high activity (Figure 4a). Secondly, the metal surface can effectively accommodate plastic deformation, decrease the impact kinetic energy of the ceramic particles, provide an embedding mechanism for hard ceramic particles, and exert a buffering effect on the substrate (Figure 4b). Thirdly, with the formation of coatings, the continuous impact of the ceramic particles exerts a compression or SP effect, thus reducing the coating porosity and enhancing the metallurgical bonding between the metallic phase and the metal/ceramic interface (Figure 4c). At last, with the elevation of the number of ceramic particles, ceramic particles are vulnerable to fragmentation by impacts, and the erosion effect produced thereof exerts an adverse effect on deposition (Figure 4d).

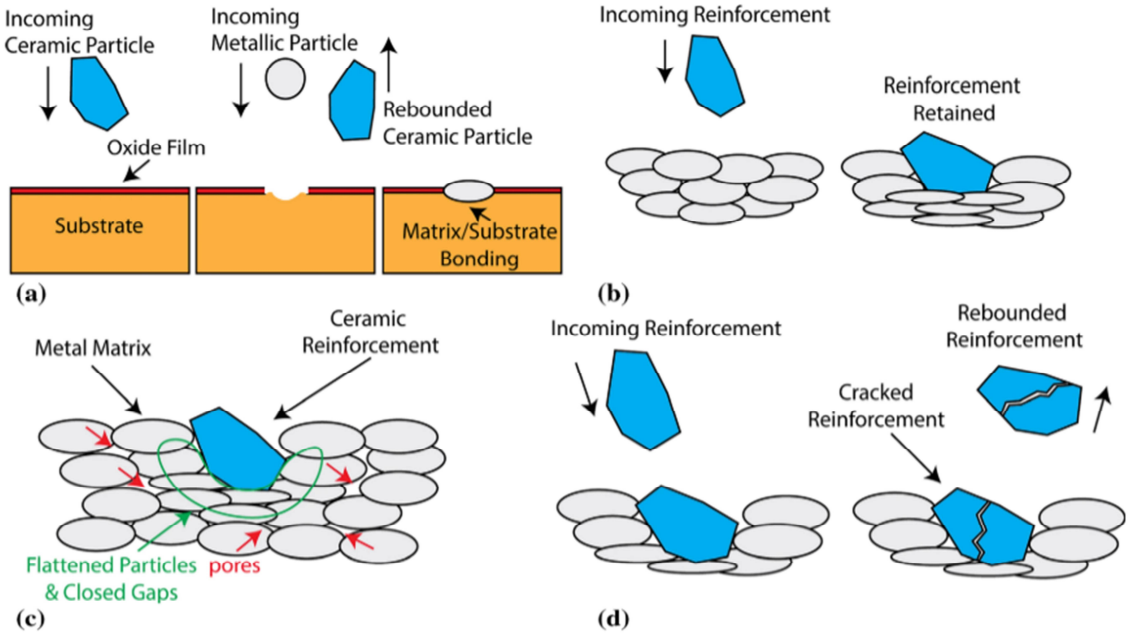

Figure 4. Schematic diagram of four effects of hard ceramic particles during deposition [43]. (**a**) Surface activation; (**b**) cushioning effect of the matrix; (**c**) tamping effect of ceramic reinforcement; (**d**) erosion effect.

According to the research above, the Cu-based composite coatings can be strengthened by the addition of ceramic particles during the CS from the following aspects: (1) Ceramic particles can activate metal particles by removing the oxide layer on their surface, which increases the deposition efficiency. (2) Ceramic particles can fill the gaps between metal particles and increase the compactness of composite coatings. (3) Ceramic particles play a role in compacting metal particles, which not only increases the hardness and bonding strength of the Cu-based composite coatings, but also improves the mechanical properties of the coatings. Therefore, it is of great value to make rational use of the reinforcing effect of ceramic particles to improve the mechanical properties of Cu-based composite coatings. Current research has provided no complete theoretical system elaborating the bonding mechanism of Cu-based ceramic composite coatings, mainly because the physical properties of Cu in the metallic phase and ceramic particles in the reinforcing phase are quite different. In addition, the impact time is very short (tens of nanoseconds), and the experimental technology is limited, so it is impossible to capture the specific impact and bonding process of ceramic particles. However, in recent years, researchers have been able to observe the impact and bonding process between ceramic particles in real time using in-situ scanning electron microscopy and femto-photography. The discovery of this

process can provide technical support for the design, preparation, and application of high-performance Cu-based ceramic composite coatings.

3. Effects of CS Parameters on the Coating Quality

There are many CS process parameters. Among them, the particle velocity is the most critical parameter in the CS process, which determines the deposition process of a given material and the final performance of the coatings. When the substrate material and particle size are constant, the particles can impact the substrate to form effective deposition only within a suitable velocity, and this velocity is defined as the critical velocity. If the particle velocity is less than the critical velocity, the particles will be rebounded by the substrate and erosion occurs, but if the particle velocity is greater than the critical velocity, coatings will be formed through deposition [45]. Additionally, if the particle velocity is much higher than the critical velocity, the particles will erode the substrate but not be deposited [46]. All in all, when the particles impact the substrate surface at different velocities, the particles will be rebounded by the substrate, deposited on the substrate, or pass through the substrate.

Other CS process parameters, such as gas pressure, gas temperature, stagnation pressure (pressure in the spray gun chamber), spray gun structure, spray distance, substrate condition, particle size and morphology, impact angle, and powder feeding rate, all affect the coating quality and performance by influencing the particle velocity [47]. In this paper, the effects of the particle velocity, particle morphology, and substrate condition on the coating deposition efficiency, microstructure properties, and bonding strength are mainly investigated. Table 1 summarizes the effect of the coating parameters on the coating properties of cold sprayed copper-based composite coatings.

Table 1. Effect of cold spray parameters on coating properties.

Coating	Composition	Particle Diameter	Gas	Pressure	Temperature	Hardness	Coating Properties	Application Field	Ref.
Cu/Al_2O_3	Cu/Al_2O_3 (50 wt%)	Cu/Al_2O_3 (−22 + 5 μm)	Air	6 bar	540 °C	127 ± 8.9 $HV_{0.3}$	High hardness, low porosity, high density	Conductive, anti-corrosion, wear-resistant	[48]
Cu/Ni	Cu/Ni (0/6/16/33/48 wt%)	Cu (20 μm) Ni (10 μm)	Air	0.6 MPa	600 °C	190 HV_{100g}	Low porosity, compact structure	Corrosion resistance	[49]
Cu/W	Cu (70/50/30 wt%) W (30/50/70 wt%)	Cu (15–53 μm) W (3 μm)	Air	2 MPa	500 °C	260 $HV_{0.05}$	Low porosity	Wear-resistant	[50]
$Cu/SiC/Al_2O_3$	Cu/SiC (15/35/45 wt%) Cu/Al_2O_3 (15/35/45 wt%)	SiC (7.7–22.4 μm) Al_2O_3 (9.4–23.8 μm)	Air	2.8 MPa	450 °C	215 HV	Low porosity, high hardness, low degree of oxidation	Wear-resistant and anti-corrosion	[51]
Cu/Ti_3SiC_2	Cu/Ti_3SiC_2 (20/35/50/66.7 wt%)	Cu/Ti_3SiC_2 (15–45 μm)	N_2	5 MPa	650 °C	2.61 GPa	High bonding strength and uniform density	Wear-resistant	[52]
Cu/MoS_2	Cu/MoS_2 (1.8 ± 0.99 wt%)	Cu (26 μm) MoS_2 (30 μm)	N_2	5 MPa	800 °C	124 $HV_{0.2}$	Low coefficient of friction	Self-lubricating	[53]
$Cu/MoS_2/WC$	Cu/MoS_2 (9 wt%) Cu/MoS_2 (9 wt%-WC 19 wt%)	Cu (26 μm) MoS_2 (68 μm) WC (30 μm)	N_2	5 MPa	800 °C	130 $HV_{0.2}$	Low wear rate	Self-lubricating, high wear resistance	[54]
	Cu/MoS_2 (5 wt%-WC 19 wt%)	Cu (26 μm) MoS_2 (30 μm) WC (30 μm)	N_2	5 MPa	800 °C	3.2 GPa	Significantly lower wear rate of dense coating		[55]
Cu/Al_2Cu	Cu/Al_2Cu (0/5/10/15 wt%)	Cu (68 μm) Al_2Cu (44 μm)	Air	6 bar	550 °C	132 ± 12 $HV_{0.025}$	Low porosity and high hardness	Conductive	[56]

3.1. Effect of the Particle Velocity on the Coating Deposition Efficiency

The cold-sprayed particle velocity directly affects the deposition efficiency and porosity of coatings. The low porosity of cold-sprayed coatings is mainly attributed to the fact that the coatings are formed by the gradual accumulation and superposition of deformed particles. At a high particle velocity, particles can be sufficiently deformed, which reduces the incomplete overlap between the particles. The continuous compaction effect of subsequent particles on the deposited coatings further reduces the porosity of the coatings [57]. Moreover, the change of the particle impact velocity will directly influence the deposition efficiency of the coatings mainly because the high-velocity impact of the sprayed particles on the substrate results in "ASI" at the interface, which gives rise to the violent plastic flow of the material and realizes the coating deposition effect. With the increase of the particle velocity, the compactness and quality of the coatings will also be improved, but the ultra-high velocity will lead to erosion rebound [58]. Figure 5a shows in a schematic sketch of how the critical deposition velocity (v_{crit}) and erosion velocity ($v_{erosion}$) vary with temperature. The area under v_{crit} signifies the lack of bonding or slight erosion. The area above $v_{erosion}$ denotes strong erosion or, in the case of soft particles hitting a hard substrate, no deposition. For example, some materials (tantalum, niobium, iron, and tungsten) are brittle at lower impact temperatures, so no deposition will occur under such conditions. The area between v_{crit} and $v_{erosion}$ describes the window of spray ability, WS, which can additionally be limited by a region of brittle material behaviour or limited ductility at lower temperatures. In the WS region, most of the impacting particles deposit as a coating on the substrate. PIC describes the distribution of the particle velocity and particle temperature of the selected spray parameter set, allowing cold spraying to be optimised by tuning the PIC for a maximum overlap with WS. The velocity range between the critical velocity and erosion velocity defines the window for CS deposition (Figure 5b). The particles having a velocity within this window can achieve a successful bonding and have high deposition efficiencies. The v_{crit} is primarily determined by the intrinsic properties of particles (material properties, morphology, and size) and the impact temperature of particles, nature of the carrier gas, and the effect of nozzle design. Under a very low particle velocity, the impact kinetic energy is insufficient, and the sprayed particles cannot be effectively deposited to form coatings. Coatings can only be formed within a certain range beyond the v_{crit}. Hence, the spray process parameters should be reasonably controlled in light of the actual working conditions, so that the velocity and temperature of the particles can exert a preferable synergic effect, thus further improving the coating performance.

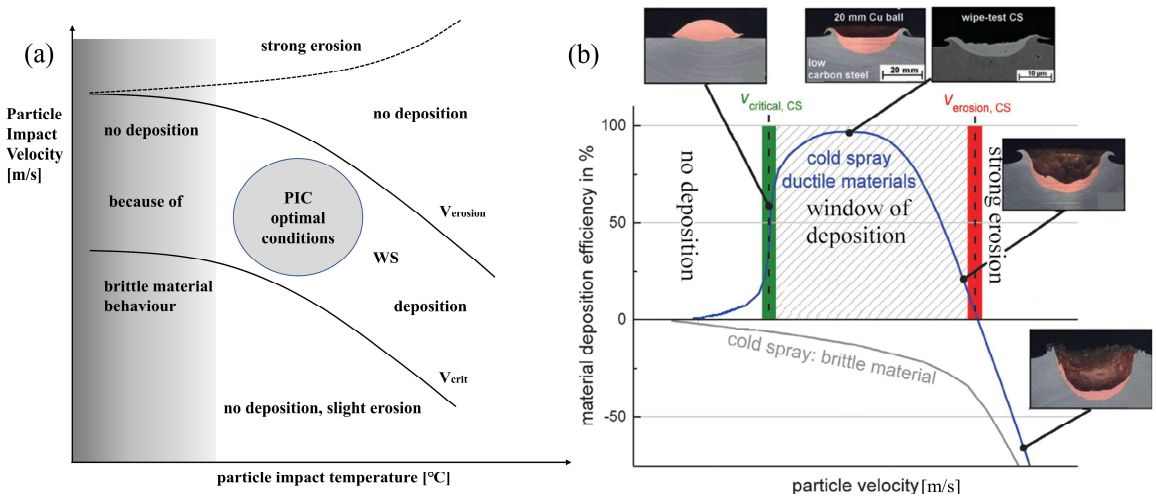

Figure 5. (**a**) Particle velocity versus particle temperature and the state of the spray ability window (WS) and particle impact condition (PIC) [46]; (**b**) successful combination of the relationship between particle velocity, deposition efficiency, and impact effect at a constant impact temperature occurs at the deposition window [59].

3.2. Effect of Particle Morphology on the Properties of Coatings

Particle morphology and particle size significantly affect the deposition process, microstructure, and performance of coatings. Particles with different morphology obtain different flight velocities during spraying, so the deposition efficiency is different, which leads to variations in the porosity, compactness, and bonding strength of the prepared coatings. It can be concluded that the morphology of particles indirectly influences the microstructure properties of coatings. Research on spherical particles has manifested that the particle velocity is inversely proportional to the particle diameter and is mainly affected by the cross-sectional area and drag coefficient of the particles [29,60]. It has also been shown that the morphology of non-spherical particles affects the deposition characteristics and coating quality. Gu et al. [61] combined a mathematical model with numerical simulation to explore the influence of sprayed particle morphology on particle dynamics. According to the results, non-spherical particles gain more kinetic energy and less heat than spherical particles in the process of high-velocity oxygen-fuel (HVOF), and non-spherical particles are closer to the gas jet center than spherical particles. Fukanuma et al. [62] used two different morphologies of powders, spherical and non-spherical, for cold spraying. The experimental results revealed that, under the same conditions, the airflow is accelerated, and the velocity of sprayed non-spherical particles is higher than that of spherical particles, which is mainly due to the larger drag coefficient of the non-spherical particles in the airflow. Venkatesh and Ma et al. [63,64] investigated the influence of the morphology of cold-sprayed powders on the deposition performance by means of a powder particle velocity test and a numerical simulation calculation. It was discovered that under specific airflow fields, a smaller particle size of the metal powder with irregular morphology will have a higher particle velocity, severer particle deformation, and higher deposition efficiency. The prepared coatings are characterized by better microstructure and no obvious pores and cracks, but poor powder fluidity, and the powder feeding faces challenges.

Studies have demonstrated that when certain quantities of ceramic particles or alloy powders showing differences in hardness are mechanically mixed into metal powders, some of these heterogeneous materials will remain in the deposit, changing the chemical composition of the deposit. There is a questionable scope of application in areas with strict requirements on mechanical properties, corrosion resistance, or electrical conductivity [65]. To tackle the problems above, the research team of Xi'an Jiaotong University found that the same metal powder with a porous structure and a solid structure can be mixed by virtue of the difference in the hardness of different metal powder structures, and then the compaction effect of solid high-hardness powders on porous soft powders can be utilized to improve the compactness of the deposit [66,67]. Furthermore, the addition of porous metal powders can obviously improve the deposition efficiency of solid structure powders. Figure 6a–c shows the cross-sectional microstructures of deposits prepared by solid gas atomized spherical Cu powder (GA Cu), porous electrolytic dendritic Cu powder (E Cu), mixed Cu powder (Mixed Cu), and corresponding powders, respectively. As shown in these figures, pores are easily formed among Cu particles in the GA Cu deposit, and some pores inside the E Cu are retained in the E Cu deposit, resulting in smaller voids therein. However, the Mixed Cu has no pores, and the coating possesses higher compactness. High compactness and high inter-particle bonding quality endow the Mixed Cu with better electrical and thermal conductivity, wear resistance, and corrosion resistance.

Ning et al. [68] investigated the effects of particle size and morphology on the particle velocity and deposition efficiency using B-Cu, C-Cu, and T-Cu particles with an average particle size of 12 μm as spray powders, in which the B-Cu and C-Cu were particles of irregular morphology, and the T-Cu particles were spherical particles. The results revealed that, under the same conditions, the particles of irregular morphology show a higher flight velocity than the spherical particles, and the deposition efficiency of the coatings formed by the particles of irregular morphology is significantly improved with better microstructure properties. Jodoin et al. [69] also discovered a similar phenomenon. In the range of the average particle size of less than 25 mm, the particle distribution is not affected, but the

velocity of non-spherical particles of the same size is higher than that of spherical particles. Under the same circumstance, the particle velocity declines with the increase of the average particle size. In addition, the morphology of larger particles dramatically influences the particle velocity. As the deposition efficiency is directly associated with the particle velocity, the higher the particle velocity is, the higher the deposition efficiency and the better the microstructure properties of the coatings will be.

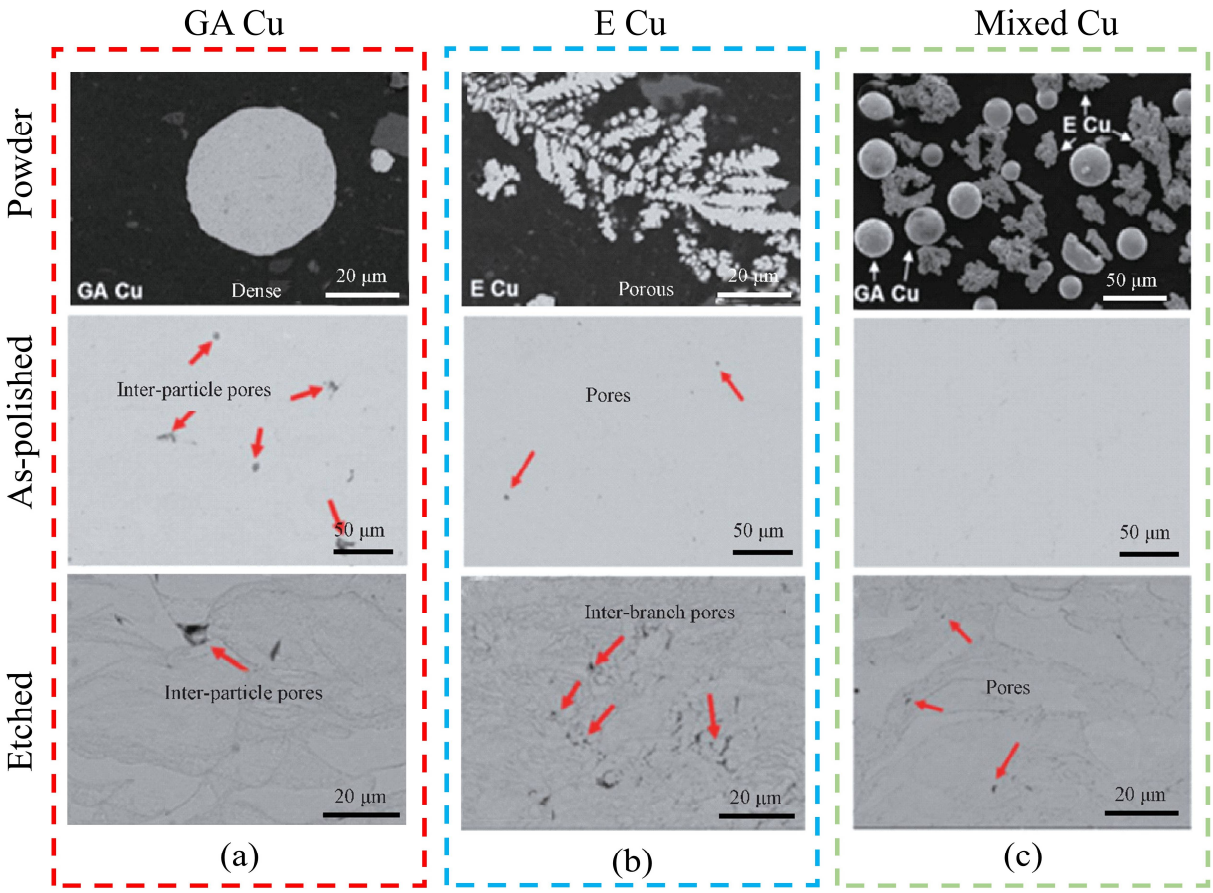

Figure 6. Cross-sectional organization of cold spray deposited bodies with different structure of Cu powder and its preparation [66,67]. (**a**) GA Cu powder and the corresponding deposit; (**b**) E Cu powder and the corresponding deposit; (**c**) Mixed Cu powder and the corresponding deposit.

In summary, the morphology and size of feedstock particles have impacts on the critical velocity of the particles, which affect the deposition efficiency and, finally, notably influence the microstructure properties of the coatings. The microstructure properties of the coatings include compactness, porosity, and cracks, which exert huge effects on the comprehensive properties of the coatings, such as bonding strength and mechanical properties. Therefore, selecting particles with reasonable morphology and size is of significance for the preparation of high-performance coatings with high compactness, high bonding strength, and low porosity.

3.3. Effect of the Substrate Condition on the Bonding Strength of Coatings

Researchers have made great efforts to improve the bonding strength and mechanical properties of cold-sprayed coatings, especially for materials that are difficult to deform. Most of the applied methods can only take effect by adjusting the process parameters and improving the particle condition before impact, such as increasing the particle velocity or changing the particle morphology. Nevertheless, the effect of the substrate condition on the coating performance has rarely been investigated. As an integral part of the coating system, the temperature, hardness, and surface roughness of the substrate greatly influence

the coating performance, especially the bonding strength, therefore, studying the effect of the substrate condition on the coating performance is of vital significance [70].

The substrate temperature affects the bonding strength between the particles and the substrate or among the particles to a certain extent, and primarily influences the microstructure and mechanical properties of coatings. Generally speaking, a higher temperature of the substrate leads to better adhesion between the particles and the corresponding substrate, because the thermal softening effect of the substrate material is enhanced with the increase of the temperature, and it is easier for the substrate to deform and generate metallurgical bonding when impacted by particles. However, the ultra-high temperature will cause the oxidation of the particle/substrate interface and the grain growth, thereby reducing the bonding force [71]. Song et al. [72] predicted the porosity of coatings undergoing multiple particle impacts in the process of metal CS by coupled Euler–Lagrange (CEL) numerical simulation and discovered that the substrate temperature has little effect on the coating porosity, but has a great influence on interfacial bonding. The bonding strength of the coatings is raised at a higher substrate temperature. Fukumoto et al. [47] studied the effect of the substrate temperature on the deposition behavior of Cu particles on the substrate surface during the CS and found that the deposition rate rises remarkably with the increase of the substrate temperature without any heating of the particles, indicating that heating the substrate is beneficial for the formation of the first layer with a high deposition rate. Yin et al. [73] conducted research on the effect of the substrate temperature on coating-substrate bonding through experiments combined with numerical simulations. As demonstrated by the results, with the increase of the substrate temperature, the heat input at the bonding interface between particles and the corresponding substrate rises significantly (Figure 7), which leads to an increase in the interface temperature, thereby increasing the dynamic recrystallization in the plastic deformation region, facilitating the formation of nanocrystals at the interface, and ultimately improving the yield strength and crack strength of the coatings. Additionally, due to the enhanced thermal softening effect, the high-temperature substrate will produce obvious metal jets and strong mechanical interlocks. Therefore, properly elevating the substrate temperature can improve the coating quality and the coating–substrate bonding strength.

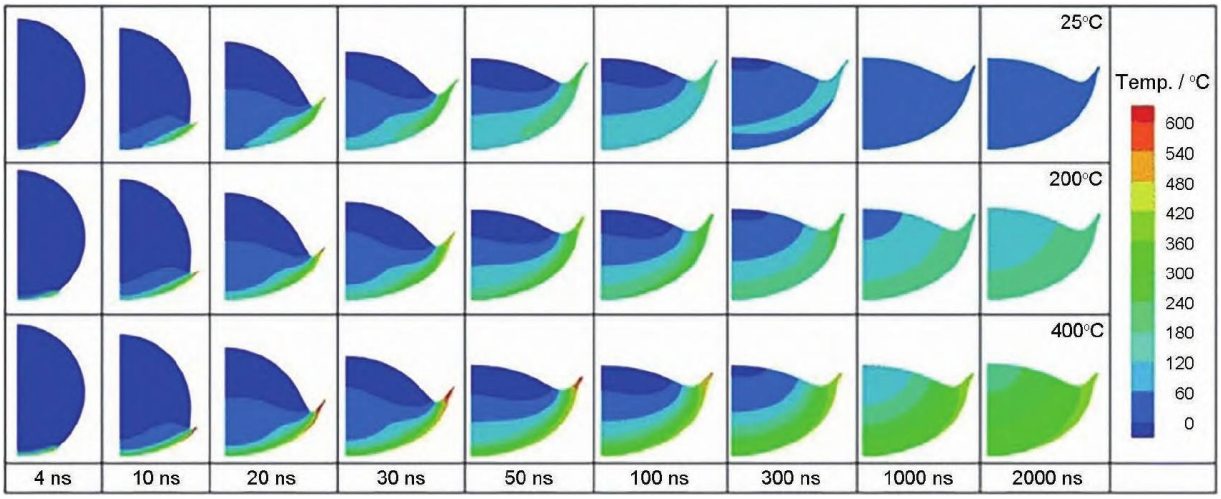

Color online

Figure 7. The temperature evolution of a single Ni particle deposited on a Cu substrate with the substrate temperatures of 25, 200, and 400 °C [73].

The substrate hardness greatly influences the interfacial bonding strength of coatings. Figure 8 is a schematic diagram of different groups of particles and substrate hardness. It can be seen that soft particles deform more severely and show better adhesion strength than hard particles. Hard particles induce the erosion of the substrate, whereas soft particles

deform on the substrate without causing erosion [74]. A relatively hard substrate can cause severer plastic deformation when soft particles are impacted, increase the deposition rate of flat particles, effectively reduce the porosity of the particle bonding interface, and enhance the bonding quality of cold-sprayed coatings [75]. Research conducted by Yin et al. [76,77] revealed that, compared with a hard substrate, a soft substrate can provide a larger contact area, and at the same time, it can reduce the oxide film residue on the surface of the powder and the substrate, which is beneficial for the metal bonding at the interface and improves the bonding strength of the coatings. Later, the research also verified that the substrate hardness greatly influences the deformation of subsequent incident particles and exerts a vital effect at the beginning of the coating formation. Therefore, the soft-to-soft interfacial bonding strength is better, mainly due to the formation of jets.

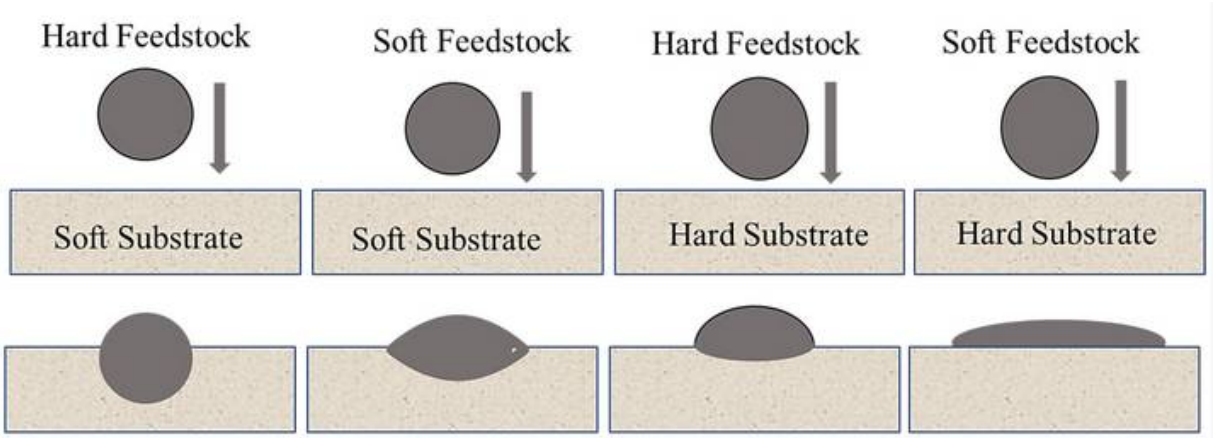

Figure 8. Schematic diagram of the impact behavior of different particle–matrix hardness [57].

Cao et al. [78] researched the effect of substrate hardness on the microstructure properties of cold-sprayed TC4 titanium alloy coatings. According to the results, when the TC4 particles with higher hardness impact the soft substrate of AA2024 Al alloy, a non-coordinated deformation occurs. In other words, hard particles can hardly deform, the deformation of hard particles is smaller than that of the substrate, and the hard particles will be embedded inside the substrate. At this time, the deposition process is dominated by mechanical bonding (Figure 9a). When the hardness of the TC4 particles approximates that of the TC4 substrate, the bonding interface will undergo coordinated deformation, and the deformation of the composite particles is similar to that of the substrate bonding interface. The interfacial bonding is dominated by mechanical bonding, and metallurgical bonding occurs in local areas, thus forming a dense coating on the substrate (Figure 9b).

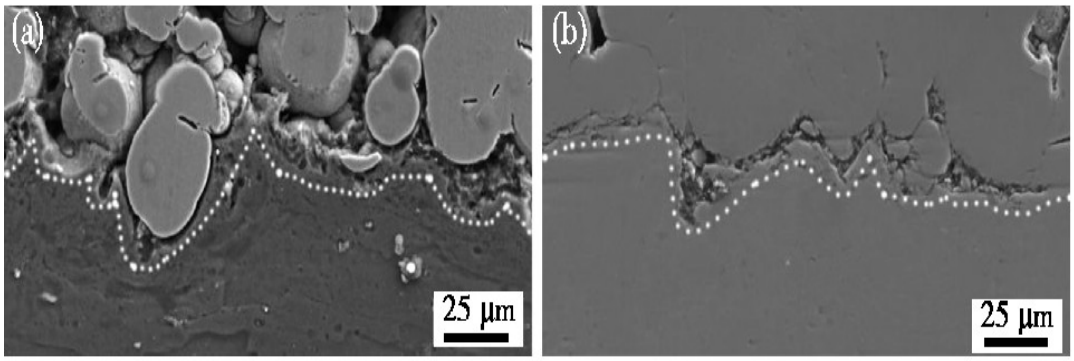

Figure 9. The influence of substrate hardness on the deposition characteristics of the first layer of coating [78]. (**a**) TC4/AA2024 coating; (**b**) TC4/TC4 coating.

Cetin et al. [79] explored the effect of substrate hardness on coating formation and performance. As illustrated in Figure 10a, the coating–substrate interface is dense and

uninterrupted, but there are pores above the coating. The substrate hardness increases from 55 to 107 HV, which exerts an obvious effect on the thickness and porosity of the coating at the initial stage, but with the continuous increase of hardness, the thickness and porosity of the coating do not change remarkably (Figure 10b,c). According to Figure 10d, the coating hardness increases with the increase of the substrate hardness. As demonstrated by the research results of Cetin et al. [79], the coating hardness is determined by the deformation rate of the particles. For a hard substrate, the deformation of the particles in the first layer absorbs almost all the kinetic energy, resulting in severe deformation of the particles and slight deformation of the substrate. In terms of a soft substrate, part of the kinetic energy of the particles in the first layer is used for the deformation of the substrate, which leads to weaker compression and smaller deformation of the particles. Hence, the coating hardness is also directly correlated with the substrate hardness.

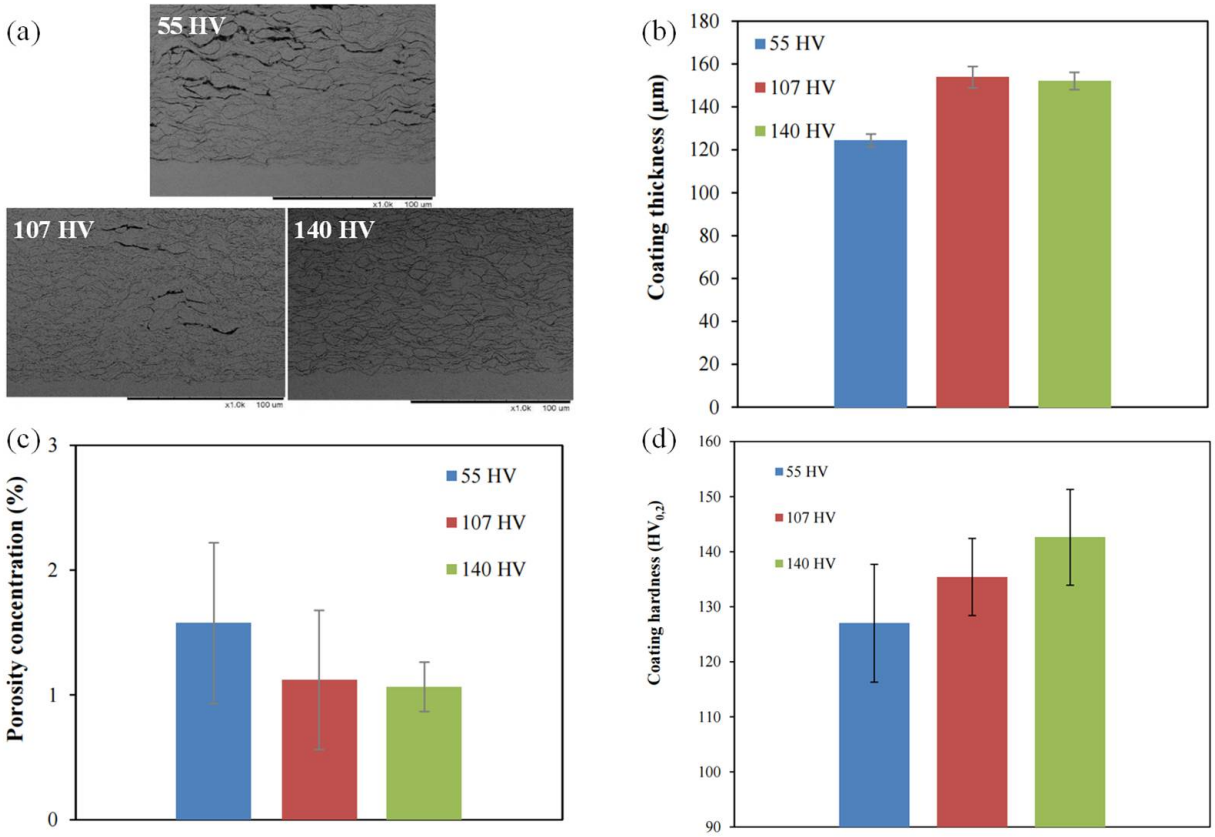

Figure 10. The effect of hardness of the substrate on coating properties [79]. (**a**) SEM images of the coatings produced on the substrate with different hardness; (**b**) substrate hardness–coating thickness relation; (**c**) substrate hardness–porosity concentration relation; (**d**) substrate hardness–coating hardness relation.

To sum up, the substrate hardness exerts a huge effect on the coating performance. Based on previous research results, the substrate hardness is mainly determined by the hardness of both the particles and the substrate. When the hardness of the particles is similar to that of the substrate, the bonding interface will undergo a coordinated deformation, which facilitates the formation of metallurgical bonding. At this time, the comprehensive performance of the coating is the best.

The surface roughness of the substrate plays a prominent role in the interfacial bonding mechanism. Marrocco et al. [80] changed the roughness of the substrate surface by grinding, polishing, and sandblasting. The results revealed that the bonding strength of the polished and ground surfaces is markedly higher (about 22 MPa), while that of the sandblasting surface was the lowest, with an average of 8 MPa. It is considered that the

surface hardening effect reduces the deformation capacity of the substrate, resulting in a small number of particles embedded at the bonding interface, as well as a mechanical interlocking effect. Kumar et al. [81] adopted different material combinations (soft/soft, soft/hard, hard/soft, and hard/hard) to improve the bonding state of the CS interface by optimizing the roughness of the substrate. According to the numerical simulation and experimental results, the optimum roughness for different material combinations was determined. It was also uncovered that the semi-polished low-carbon steel surface is the best source of sufficient adhesion strength for cold-sprayed Cu (soft/hard) coatings. However, Hussain et al. [35] argued that the smoother Al substrate (soft-to-soft) surface is more suitable for developing cold-sprayed Cu coatings in terms of adhesion strength. Surinder et al. [82,83] successfully prepared Cu coatings on untreated, semi-polished, and mirror-polished SS316L steel substrates. According to the results, the roughness of the substrate surface exerts a huge effect on the performance of Cu coatings. Compared with those prepared on untreated and semi-polished substrate surfaces, the Cu coatings prepared on the mirror-polished substrate surface exhibits the highest bonding quality. The roughness and waviness of the untreated substrate surface result in gaps at the interface, and the Cu particles are preferentially deposited at the deeper and wider peaks and troughs of the substrate, resulting in the energy loss of the deposited particles and poor adhesion (Figure 11a). Furthermore, the energy of the Cu particles is absorbed during the sharp peak deformation of the semi-polished substrate surface, which impedes the direct contact between the substrate surface and Cu particles, giving rise to insufficient bonding between Cu particles and the substrate (Figure 11b). On the mirror-polished substrates, Cu particles can be directly deposited and act on the plastic deformation of the particles in a concentrated amount, so that the bonding interface can be better mechanically interlocked, forming a coating with uniform compactness and high bonding strength (Figure 11c,d).

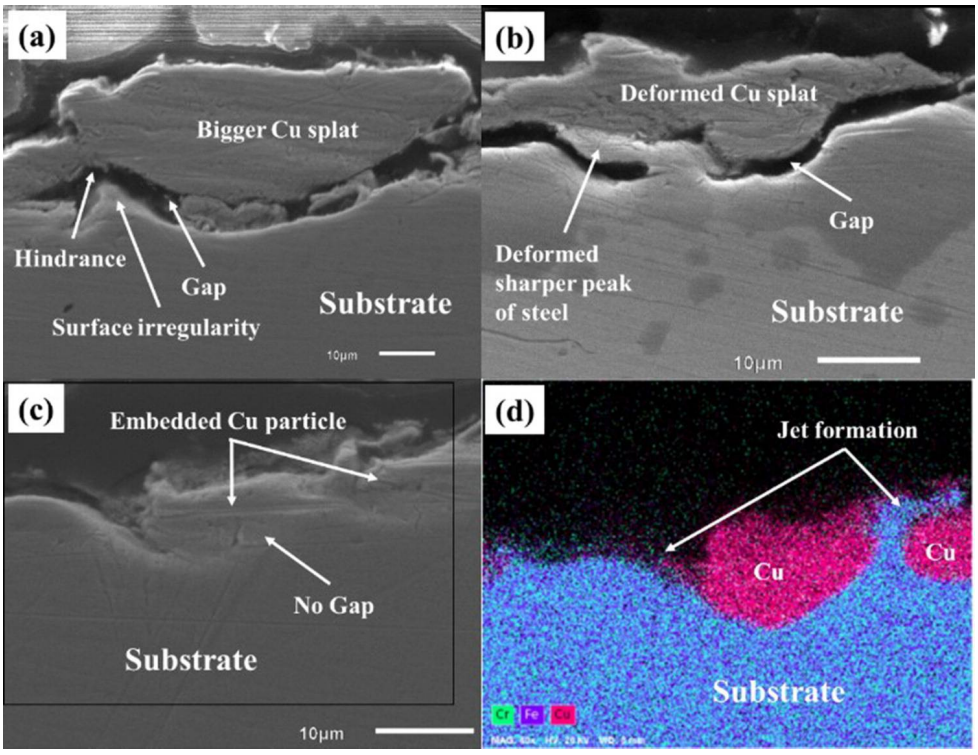

Figure 11. Cross-sectional SEM analysis of the cold-sprayed copper single particles deposited on steel [83]. (**a**) As-received; (**b**) semi-polished, and (**c**) mirror-finished SS316L steel substrates; (**d**) EDS analysis of (**c**).

In summary, the optimization of the morphology of the substrate surface before spraying mainly aims to reduce the kinetic energy loss during particle impacts and to

consume the kinetic energy in the plastic deformation of the substrate as much as possible, so that adiabatic shearing, metal jetting, and grain refinement occur as much as possible at the interface between the coating and the substrate, which will play a role in cleaning the oxide film on the substrate surface and improving the metallurgical bonding degree, thus improving the hardness and bonding strength of the Cu-based composite coatings.

This section mainly discussed the effects of the CS parameters on the coating quality. The effects of the particle velocity, particle morphology, and substrate condition on the coating quality were summarized. The above-mentioned studies have shown that the particle velocity directly affects the deposition efficiency of the coating, the particle morphology indirectly influences the microstructure properties of the coating by affecting the particle velocity, and the substrate condition exerts a direct effect on the bonding strength of the coating, especially the first-layer coating. Therefore, appropriate spray parameters can be selected in light of the actual engineering application requirements, so as to prepare the high-performance Cu-based composite coatings.

4. Research Status of Cold-Sprayed Cu-Based Composite Coatings

The Cu-based composite coatings are crucial metallic protective coatings, which have been widely used in the fields of energy and electricity, rail transit, aerospace, etc. In recent years, the CS technology has been applied by many scholars to prepare Cu-based composite coatings with different components and structures on different substrates. In addition, the microstructure, physical properties (microhardness, porosity, etc.), mechanical properties, corrosion resistance, self-lubricating properties, wear resistance, and electrical conductivity have been studied [84]. Mechanical equipment operating under special working conditions, such as heavy load and current-carrying friction, have extremely strict requirements on the tribological properties of the coatings. Under actual service conditions, severe wear and tear to the Cu-based composite coatings often result in the functional failure of the substrate material, which greatly shortens the service life of some key mechanical parts and components. Therefore, the preparation of Cu-based composite coatings with excellent mechanical properties and tribological properties has become a prerequisite for the safety and reliability of mechanical equipment [85]. The research status of cold-sprayed Cu-based functional coatings with corrosion resistance, wear resistance, high electrical conductivity, and self-lubricating properties is introduced below.

4.1. Cold-Sprayed Cu-Based Wear-Resistant Coatings

The metallic phase mainly includes Cu, Al, Ni, and their alloys, while the ceramic reinforcing phase is mainly composed of Al oxide (Al_2O_3), tungsten carbide (WC), silicon carbide (SiC), and ZrO_2 in common cold-sprayed metal-based ceramic composite wear-resistant coatings. The common and effective method to improve the wear resistance of the coating was the hard-particle reinforcement, a method of increasing the plastic deformation of mental particles by mechanical shocks and also enhancing the hardness and wear resistance of the coating by dispersion strengthening. Therefore, hard-particle reinforcement has been widely adopted in the design and preparation of Cu-based wear-resistant composite coatings [86].

Deng et al. [50] prepared tungsten (W)–Cu composite coatings with different W concentrations on the Al substrate by CS. It turned out that the W–Cu composite coatings featured low porosity and high hardness, and the wear resistance of 50 wt% W–Cu coatings was superior to that of 30 wt% W–Cu coatings, which was largely attributed to the W concentration and porosity in the coatings. Shikalov et al. [87] conducted experiments on the mechanical properties of W–Cu composite coatings with different W concentrations under the same conditions and found that the bonding strength and wear resistance of the coating were better with an increase of the W concentration in the coatings. Compared with that of pure Cu coatings, the bonding strength of coatings with 75 wt% W added into the raw composites can increase by 10 times (up to 31 MPa). Zhang et al. [88] explored the influence of different accelerating gas temperatures on the wear resistance of CuZn35

coatings by depositing CuZn35 coatings on the Al plate via high-pressure CS technology. The macroscopic observation result of the surface wear on the coatings is shown in Figure 12. According to the results, there are obvious differences in the wear scar depth of the coatings prepared by different accelerating gas temperatures under the same conditions of the friction experiment. The wear scar depth of the coatings prepared at 400, 600, and 800 °C was about 90, 65, and 55 μm, respectively. This indicates that the wear resistance of the coating is significantly enhanced with the increase of the accelerated gas temperature during the preparation process. In addition, the wear scar depth of the coating prepared at 800 °C was similar to that of the as-cast CuZn35 material, showing the best wear resistance.

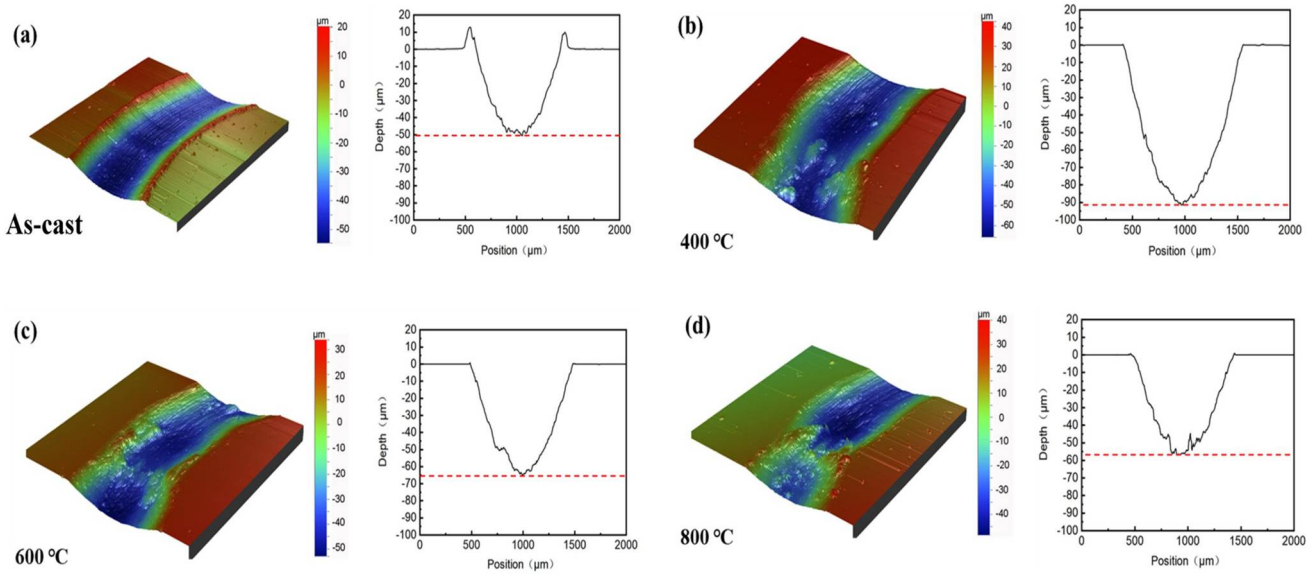

Figure 12. Surface wear scar morphologies of CuZn35 coatings and as-cast CuZn35 materials prepared under different accelerating gas temperatures [88]. (**a**) As-cast; (**b**) 400 °C; (**c**) 600 °C; (**d**) 800 °C.

Kostoula et al. [89] studied the tribological property of coatings where thick and compact Cu and Cu–Al_2O_3 composite coatings were prepared on the Al substrate. It turned out that the wear resistance of Cu–Al_2O_3 composite coatings was higher than that of Cu coatings. Similar results were obtained by Huang et al. [51] in their experiment where Cu–SiC and Cu–Al_2O_3 coatings were prepared by CS technology. The low coating porosity, high hardness, low oxidation degree, and significantly improved wear resistance could be attributed to the fact that the addition of SiC and Al_2O_3 ceramic phases enhances the plastic deformation of Cu particles and increases the deposition efficiency of the coatings. In order to further verify the good wear resistance of Cu-based composite coatings, Chen et al. [90] conducted more detailed experiments where they studied investigated the influence of different ceramics on the wear resistance of the coatings by adopting CS technology to prepare pure Cu, Cu–SiC, Cu–Al_2O_3, and Cu–WC coatings. The results verified that the Cu-based composite coating displays better wear resistance than the pure Cu coating. The low deposition rate of WC particles and numerous pores in the coatings result in the low hardness of the coatings and eventually affect their wear resistance, so Cu–SiC and Cu–Al_2O_3 coatings exhibit low porosity, good compactness, and excellent wear resistance, while Cu–WC coatings show poor wear resistance, largely differing from other research results. Yu et al. [52] prepared Cu–Ti_3SiC_2 composite coatings on Cu alloys. The experimental results manifested that the hardness and bonding strength of the coatings could be significantly enhanced by adding small quantities of Ti_3SiC_2 ceramic particles, and the wear scar volume of the coatings was about 1/3 of that of the Cu alloy substrate. Yin et al. [91] conducted experiments to prepare Cu–graphene (GNP) composite coatings by ball milling and the CS process below the melting point of the material. The results demonstrated that, compared

with those of the pure Cu substrate, the friction coefficient of GNP-enhanced Cu-based composite coatings was reduced by about 20%, and the wear resistance of the coatings was significantly improved, suggesting that GNP composite material plays an important role in improving the wear resistance of Cu-based composite coatings. Similarly, the application of magnesium alloys was generally limited by their poor corrosion and wear resistance. Zhang et al. [92] improved the properties of magnesium alloys by preparing Cu–Ni/Al_2O_3 and Cu–Zn/Al_2O_3 coatings via CS. The results demonstrated that the addition of Ni or Zn powders to the Cu–Al_2O_3 coating reduced the coating porosity and increased the coating compactness. As shown in Figure 13, the Cu–Zn/Al_2O_3 coating has the lowest friction coefficient and wear rate, indicating that it can protect the magnesium alloy substrate in the long term by virtue of its highest corrosion resistance and wear resistance.

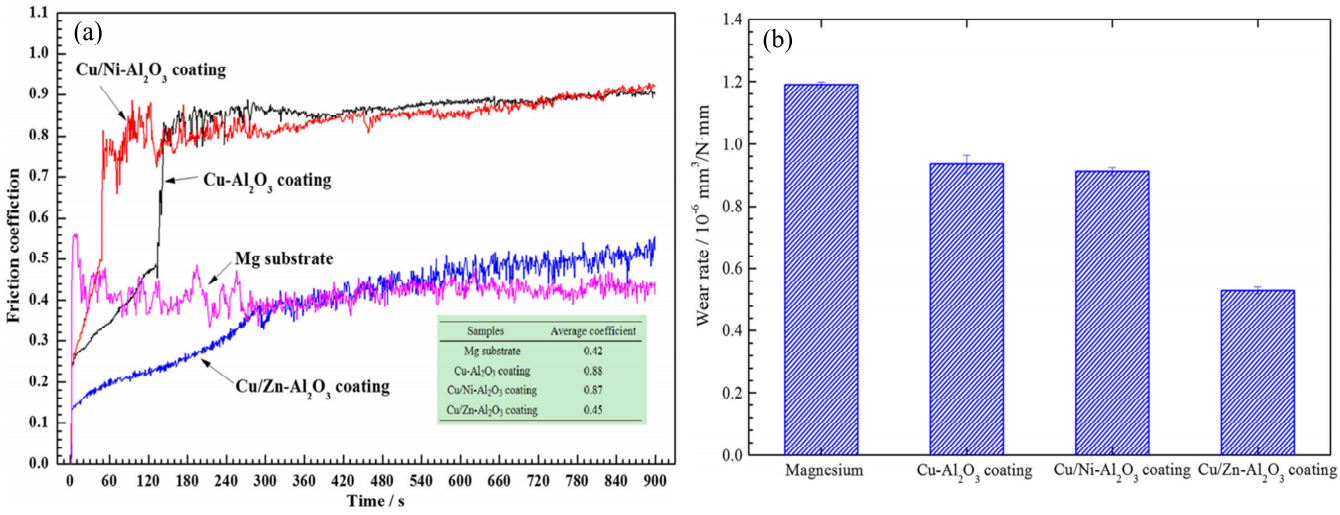

Figure 13. Time curve of the friction coefficient and wear rate of the Mg alloy substrate and the tested coating after sliding for 900 s [92]. (**a**) Friction coefficient; (**b**) wear rate.

The studies above prove that the bonding strength, hardness, compactness, and properties of wear resistance and corrosion of the cold-sprayed Cu-based composite coating have been significantly improved via adding ceramic particles (Al_2O_3, SiC, WC, Ti_3SiC_2, etc.) into the spray powder during the CS process. Therefore, the surface protection of Al, Mg, Cu alloy, and other materials with poor wear resistance using this method can meet the service performance requirements of key metal components and parts under special working conditions and extend their service lives, promoting the application of cold-sprayed Cu-based composite material in industrial fields.

4.2. Cold-Sprayed Cu-Based Self-Lubricating Coatings

In order to improve the tribological properties of the Cu-based composite coating and ensure its anti-friction and wear resistance, solid self-lubricating particles and appropriate reinforcing particles can be added into Cu-based composite coatings [93]. It is well known that graphite, molybdenum disulfide (MoS_2), WS_2, hexagonal boron nitride (h-BN), and boron nitride nanosheets (BNNSs) are often regarded as lubrication additives and the reinforcing phase of composite materials due to their excellent anti-friction and lubrication effects, which can significantly improve the self-lubricating property of Cu-based coatings [94–96].

Ling et al. [97] prepared Cu–Zn–graphite reinforcing composite coatings by low-pressure CS technology with a reasonable raw material design and graphite metal pretreatment, revealing that Cu–Zn–graphite composite coatings show excellent wear resistance and self-lubricating properties. Chen et al. [98] deposited Cu–Al_2O_3–graphite solid self-lubricating composite coatings on the 304 stainless steel substrate with mixed powder of Cu, Al_2O_3, and Cu-coated graphite as spraying powders. It was found that the addition

of Al_2O_3 particles could enhance the deformation degree of Cu, but it was detrimental to the deposition of Cu-coated graphite. The coating showed the highest bonding strength and best self-lubricating properties as the concentration of alumina and Cu-coated graphite was 10 wt% and the friction coefficient of the coating was 0.29. However, the self-lubricating properties weakened due to the separation of the coating as the concentration of Cu-coated graphite reached 20 wt%. Ling [99] prepared the graphene oxide/Cu composite coating via CS technology. The results demonstrated that the friction coefficient (0.2) of the graphene oxide/Cu composite coating was evidently lower than that of the pure Cu coating (0.8), and its wear rate was at least one order of magnitude lower than that of the pure Cu coating, exhibiting good wear resistance and anti-friction properties. Zhang et al. [53] prepared Cu–MoS_2 composite coatings by adding MoS_2 into Cu powders via CS technology and found that the addition of little MoS_2 [(1.8 ± 0.99) wt%] can significantly reduce the friction coefficient, exerting an obvious anti-friction effect as the addition value declines from 0.7 (pure Cu coating) before addition to 0.14–0.15. After the addition of WC into the MoS_2 powder, the friction coefficient of the Cu–MoS_2–WC composite coating was lower than that of the Cu–MoS_2 coating (Figure 14), suggesting that WC particles can reduce the friction coefficient and improve the wear resistance, thereby contributing to the formation of lubricant transfer films on the Cu–MoS_2 composite coating [54]. Subsequently, research on the influence of WC particles on the third bodies and wear resistance was conducted by changing the concentrations of Cu–MoS_2 and WC powders in the experiments, which yielded similar results. The presence of WC particles contributes to the formation of a continuous tribological transition structure (TTS) layer and a transfer film during the contact process, which makes the third-body flow smaller and more stable, so as to significantly improve the wear resistance of the Cu–MoS_2–WC coating [55].

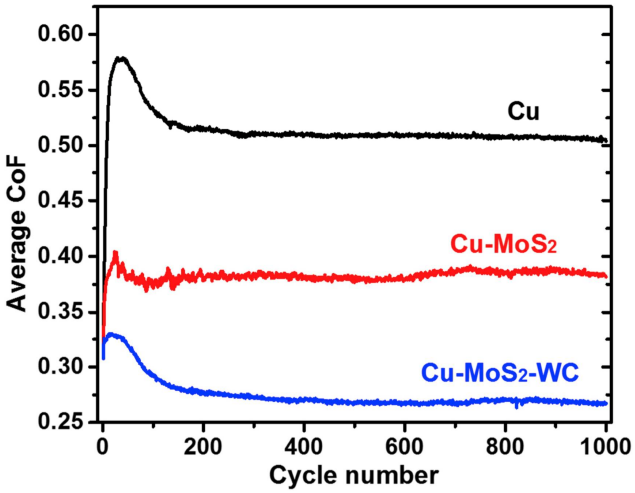

Figure 14. Average coefficients of friction (CoFs) of Cu–MoS2, Cu–MoS2–WC, and pure Cu in dry nitrogen [54].

In the preparation of Ni–hexagonal boron nitride (hBN) self-lubricating coatings by mechanical grinding and CS, Smid et al. [100] found that the self-lubricating and wear resistance of the coating achieved the optimal performance when the maximum amount of hBN in the cold-sprayed Ni coating is about 6 wt%. Wang et al. [101] prepared Cu–boron nitride nanosheets (Cu-BNNSs) composite coatings via the mechanical alloying method and CS. As shown in Figure 15, the tribological performance test results of the coating revealed that the friction coefficient of Cu–BNNSs coatings was the lowest, and their wear rates were about 34% and 20%, respectively, lower than that of the Cu substrate and the Cu coating. It can be concluded that BNNSs serve as lubricants and barriers that can improve the wear resistance of the coating. Therefore, it is expected that the Cu–BNNSs composite coating will be applied as an ideal coating material with low friction and high wear resistance.

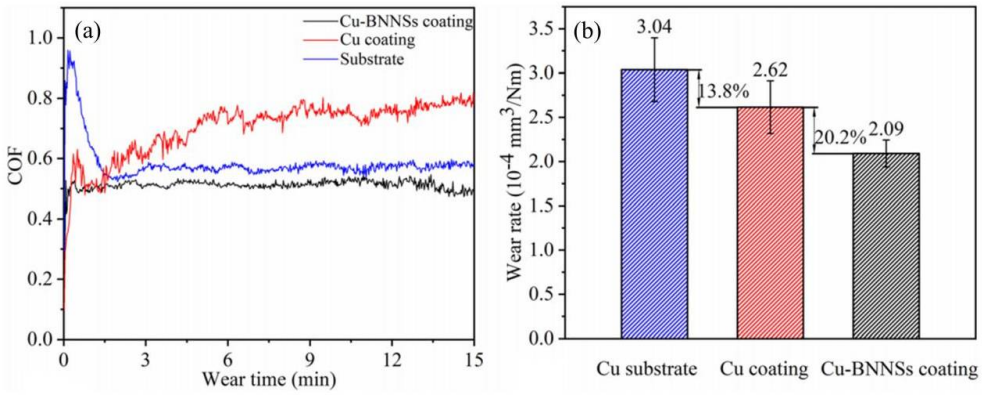

Figure 15. (**a**) Friction coefficients and (**b**) wear rates of Cu substrate, Cu coating and CuBNNSs composite coating [101].

In order to further verify the good wear resistance and lubrication effect of Cu–BNNSs composite coatings, Zhu [102] separated BNNSs from h-BN powders by the ball milling method and mixed it with electrolytic Cu powders to deposit Cu–BNNSs composite coatings on the TU1 Cu substrate via CS technology. The experimental results are basically consistent with those of Wang et al. [101], that is, the BNNSs adhering to the worn surface hindered the milling balls from contacting the composite coating to form a lubricating film, which prevented the material removal, thus achieving good self-lubricating and anti-friction properties. In addition, several experiments conducted by researchers have proved that the Cu-based self-lubricating composite coating prepared using the CS process shows a compact surface microstructure without obvious cracks and defects, and good interfacial bonding between the lubricants and metal substrates (Figure 16).

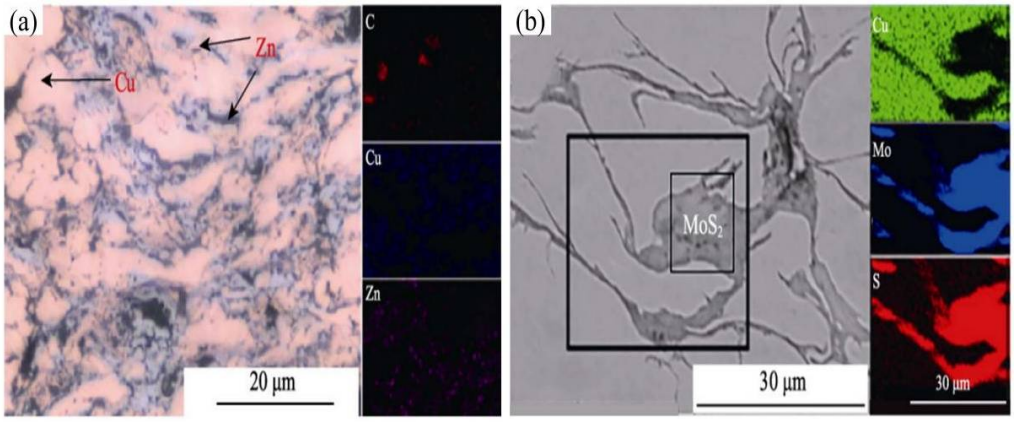

Figure 16. Cross-sectional morphology of cold-sprayed composite coatings. (**a**) Cu–Zn–graphite composite coating [97]; (**b**) Cu–MoS_2 composite coating [53].

Table 2 summarizes the properties of the cold-sprayed Cu-based wear-resistant self-lubricating coatings above. The preparation of the metal–solid lubricant composite coating with good tribological properties via CS faces challenges due to the low interfacial bonding strength between the solid lubricant and the metal substrate and the low compactness of the microstructure of the composite coating. In recent years, more and more studies on cold-sprayed Cu-based self-lubricating coatings have been conducted, obtaining great achievements from the selection of solid lubricants and preparation of coatings. At present, the development of Cu-based self-lubricating coatings focuses on the preparation of high-performance self-lubricating coatings with a low friction coefficient, heavy load, long lifetime, and strong environmental adaptability, so as to address the wear-caused failure of the components and parts under different working conditions.

Table 2. Cold sprayed copper-based wear-resistant and self-lubricating coatings.

Coating	Coating Composition	Test Conditions	Best Ratio	Friction Coefficient	Wear Rate	Conclusion	Ref.
Cu/W	Cu (70, 50, 30 wt%)/W (30, 50, 70 wt%)	steel ball, 5 N, 20 min, dry sliding friction	Cu (50 wt%)/W(50 wt%)	0.15–0.5	5.4×10^{-5} (mm^3/N·m)	Low porosity of the coating, high hardness, and enhanced wear resistance	[50]
Cu/SiC/Al_2O_3	Cu/SiC/Al_2O_3 (15, 35, 45 wt%)	WC–Co ball, Φ 6 mm, 5 N, 30 mm/s, dry sliding wear	Cu/Al_2O_3 (45 wt%)	0.2–0.5	$(11.29 \pm 1.65) \times 10^{-4}$ (mm^3/N·m)	Coatings with low porosity, high hardness, and low oxidation	[51]
Cu/Ti_3SiC_2	Cu/Ti_3SiC_2 (20, 35, 50, 66.7 wt%)	7075 aluminum ball, Φ 6 mm, 5 N, 5 min, reciprocating dry friction test	Cu/Ti_3SiC_2 (50 wt%)	0.4–0.5	6.15×10^{-5} (mm^3/N·m)	Mechanical properties and wear resistance of the coating are significantly improved.	[52]
Cu/MoS_2	Cu/MoS_2 (1.8 ± 0.99 wt%)	Al_2O_3 ball, 5 N, 2 mm/s, reciprocation	Cu/MoS_2 (1.8 ± 0.99 wt%)	0.14–0.15	0.12–0.22 nm/cycle	The tribological properties of the coating in dry air are very good, and the anti-friction effect is very obvious.	[53]
Cu/MoS_2/WC	Cu/MoS_2 (9 wt%) Cu/MoS_2 (9 wt%)-WC (19 wt%)	Al_2O_3 balls, Φ 6 mm 5 N, 4 mm, 2 mm/s, 100/1000 cycle,	Cu-MoS_2 (9 wt%)-WC (19 wt%)	0.27–0.28	~1.9×10^{-5} (mm^3/N·m)	During the sliding process, WC particles contribute to the formation of a transfer film, resulting in a lower coefficient of friction and a uniform wear trajectory.	[54]
	Cu/MoS_2 (5 wt%) Cu/MoS_2 (5 wt%)-WC (19 wt%)	ball-on-plate tribometer, 150 N, 200 μm, 5 Hz, 3500/10,000/30,000 cycle, (AISI 440C) ball, 50 mm	Cu-MoS_2 (5 wt%)-WC (19 wt%)	0.4–0.55	~8×10^{-5} (mm^3/N·m)		[55]
Cu/Zn/graphite	Cu/Zn/graphite (20/30 wt%)	52, 100 bearing steel ball, 2–6 N, 0.11 m/s ball on disc	Cu/Zn/graphite (20 wt%)	0.12–0.30	10^{-6}–10^{-8} (mm^3/N·m)	The Cu–Zn–graphite composite coating has excellent wear resistance and self-lubricating properties.	[97]
Cu/Al_2O_3/graphite	Cu/Al_2O_3/graphite (0–20 wt%)	304 ball, Φ 6 mm, 5 N, 6 mm/s, dry sliding wear	Cu/Al_2O_3/graphite (10 wt%)	0.29–0.55	~1.2×10^{-4} (mm^3/N·m)	The coating has a high bonding strength, low friction coefficient, and excellent lubricating performance.	[98]
Cu/graphite oxide	Cu/(1 wt% graphene oxide dispersion)	steel ball, Φ 10 mm, 0.5–6 N, 200 rmp, dry rub	Cu/(1 wt% graphene oxide dispersion)	0.1–0.4	~1.5×10^{-5} (mm^3/N·m)	The graphene/copper composite coating exhibits good wear resistance and antifriction properties.	[99]
Cu/BNNSs nanosheets	Cu/BNNSs nanosheets	GCr15 steel ball, Φ 6 mm, 4 N, 0.18 m/s, ball on disc,15min	Cu/BNNSs nanosheets	~0.51	~2.10×10^{-4} (mm^3/N·m)	The presence of BNNSs facilitates the formation of a lubricating film, prevents material shedding, significantly reduces the wear rate of the coating, and plays a good role in lubrication and wear reduction.	[101]
	Cu/BNNSs (1 wt%)	GCr15 steel ball, Φ 6 mm, 4 N, 0.18 m/s, ball on disc, 3 min	Cu/BNNSs (1 wt%)	~0.51	2.09×10^{-4} (mm^3/N·m)		[102]

4.3. Cold-Sprayed Cu-Based Corrosion-Resistant Coatings

Cu-based composite coatings have been widely adopted in surface protection for key components in aeroengines, marine ship bearings, and valves due to their good corrosion resistance. Koivuluoto et al. [48,103] prepared a Cu/Al_2O_3 composite coating via low-pressure spray technology. The results suggested that the low porosity and high compactness of the Cu/Al_2O_3 composite coating is caused by the hammer effect after the addition of Al_2O_3 particles, which develops its corrosion resistance of bulk Cu. Subsequently, NiCu and NiCr + 50% Al_2O_3 composite coatings were prepared on carbon steel (Fe52). The microstructure compactness of the coatings was improved, the density of its corrosion electric current decreased, the polarization resistance increased, and the coating showed good corrosion resistance in sulfuric acid and sodium chloride solutions due to the presence of the ceramic phase. Winnicki et al. [104] prepared Cu, Cu–Al_2O_3, and Cu–SiC composite coatings on the Al alloy substrate and analyzed the corrosion resistance of the coatings. The results uncovered that the coating hardness was 50% higher than that of the Al alloy substrate. In addition, the coating was relatively compact due to the hammer effect exerted by the Al_2O_3 and SiC particles, among which the coating porosity of Cu–Al_2O_3 was the lowest. The SEM after 18 cycles of the salt spray test is shown in Figure 17. The pure Cu coating has a high surface porosity, therefore it is easy for the corrosive liquid to penetrate the coating, thereby reducing the corrosion resistance of the coating. The corrosive liquid flowed into the deep coating along the crack gaps that appeared in the Cu–SiC coating, reducing the corrosion resistance of the coating. No obvious pores and cracks were found on the surface and cross-section of the Cu–Al_2O_3 composite coating, suggesting that the coating performed well in corrosion resistance.

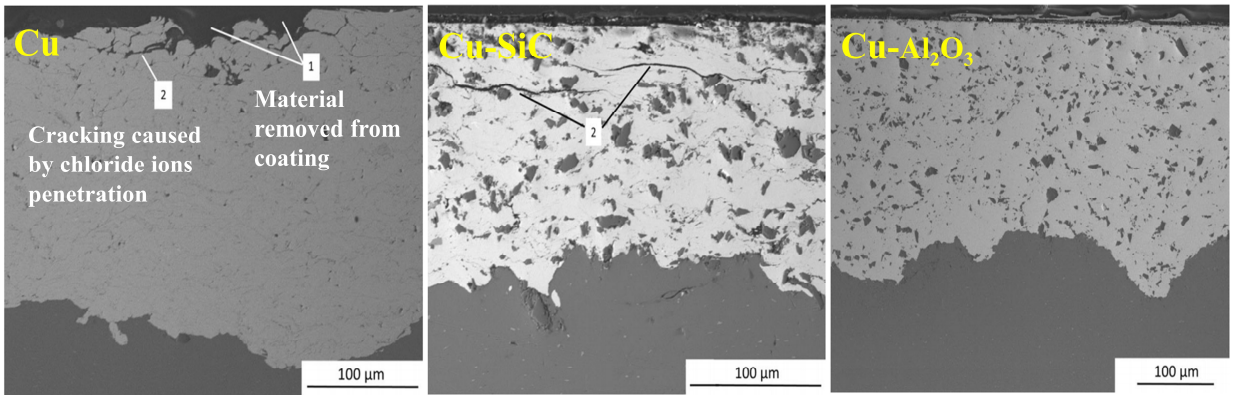

Figure 17. SEM images of Cu, Cu–Al_2O_3, and Cu–SiC after 18 cycles of a salt spray test [104].

In the preparation of Cu–Cu_2O composite coatings with different concentrations via CS technology, Ding [105] found that 30% Cu_2O–70% Cu composite coatings show the best antifouling and corrosion resistance. Sun et al. [106] prepared the Ni–Al bronze coating on the Ni–Al bronze 9422 substrate and tested the corrosion performance of the coating in the corrosion environment with pH values of 3, 7, and 11, respectively. From the test results, it can be seen that the corrosion resistance of the coating becomes worse as the pH value was 7, and the corrosion resistance of the Ni–Al bronze coating was better than that of the substrate as the pH values were 3 and 11. The passive regions were formed in these three pH environments, the cold hardening occurred during the CS process, and the pores on the coating accommodated wear debris, so as to enhance the wear resistance and corrosion resistance of the coating. Then, the Cu402F coating with a thickness of 200–300 μm was prepared on the 9442 Ni–Al bronze substrate. It was found that a stable Cu_2O passive film was formed on the surface of the coating in a corrosive environment, resulting in stronger corrosion resistance in the substrate [107]. In order to provide an effective anticorrosive Cu-based coating for magnesium alloys, Zhang et al. [49] deposited a series of Cu/Ni composite coatings with different Ni concentrations on the surface of magnesium alloys by

a composite process combining CS and ultrasonic shot peening (USSP). The coating porosity decreased, and the structure became compact after USSP treatment on the coating. The test results showed that the Cu/48% Ni composite coating displayed the worst corrosion resistance, while the Cu/16% Ni composite coating displayed the best (Figure 18). The porous structure led to the poor corrosion resistance of cold sprayed Cu/Ni coatings, but USSP could improve its structure and corrosion resistance. Therefore, Cu/Ni composite coatings after USSP treatment show good corrosion resistance, which can strongly safeguard the preparation of corrosion-resistant coatings on the surface of magnesium alloys.

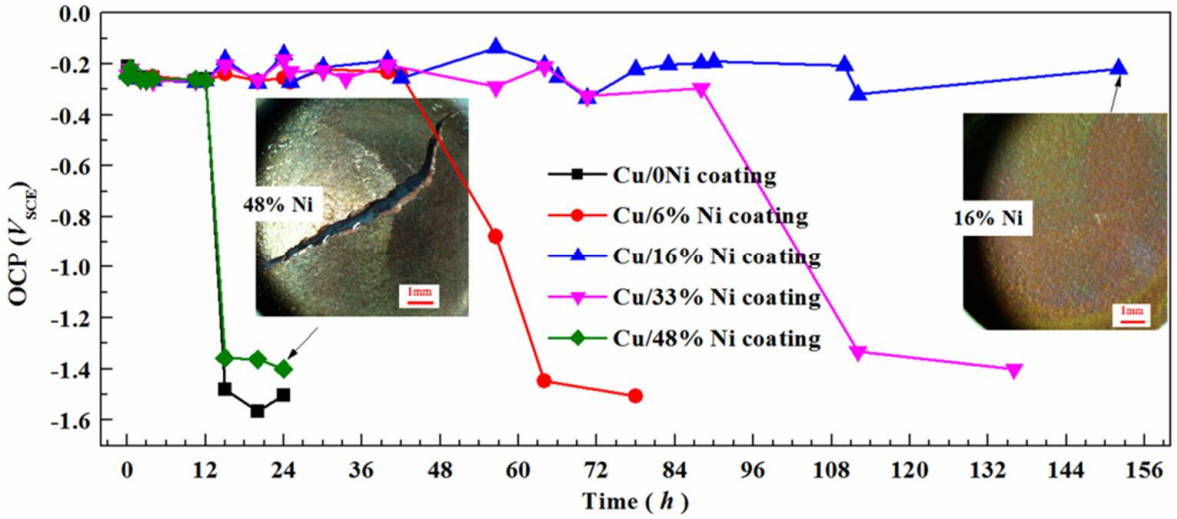

Figure 18. OCP vs. time curves of the USSPed Cu/Ni composite coatings immersed in 3.5 mass% NaCl solutions and the typical corrosion morphologies [49].

In conclusion, the protective effect of the coating on the substrate can be enhanced by an increase of the bonding strength of the coating and compactness of the coating in a corrosive environment, which can prolong the service life of the substrate. A wide prospect has been witnessed that, by virtue of the low porosity and high bonding strength, cold-sprayed Cu-based composite coatings with good corrosion resistance can be applied in Mg alloys and other parts with poor corrosion resistance in marine and aerospace. However, the mechanical bonding mode between ceramic particles and the coating interface in the cold sprayed Cu-based composite coating as well as cold hardening increase the material brittleness, which inhibits the improvement of the mechanical properties and corrosion resistance of the prepared coating to some extent. Therefore, a further study on the failure mechanism and corrosion resistance mechanism of the coating is needed.

4.4. Cold-Sprayed Cu-Based Electrically Conductive Coating

As a traditional, good electrically conducive material, the electrical conductivity of pure Cu at room temperature is 5.8×10^7 S/m. With high electrical conductivity and thermal conductivity, the pure Cu coating is essential for large-scale industrial development. However, it cannot be applied in adverse working conditions because of its low hardness, poor wear resistance, and mechanical properties, severely limiting its application in energy and power [108]. On this basis, the researchers used the mixed metal powders (Ag, Fe, Cr, Al) and Cu powders, and used cold spraying to prepare a high conductivity copper-based composite coating that can meet the conditions in severe environments [109].

Tazegul et al. [56] prepared Cu-based composite coatings using CS technology by adding Al_2Cu particles as a reinforcing phase into Cu powders to form a mixed powder. From the experiment, it can be seen that the interfacial bonding strength between the Al_2Cu particles and the Cu particles was high. The hardness, electrical conductivity, and wear resistance of the Cu-based composite coating were significantly improved, superior to those of the pure Cu coating. When the concentration of Al_2Cu was 5% and 10%, the

friction coefficient and wear rate of the coating were reduced by one-third and four-fifths, respectively. However, its hardness, electrical conductivity, and wear resistance are reduced when the concentration of Al_2Cu is 15%. The conductivity of the Cu coating prepared by Stoltenhoff et al. [110] by CS technology was equivalent to 90% of the conductivity of the pure Cu coating. In contrast, the conductivity of the Cu coating prepared by thermal spray technology, such as electric arc spraying, plasma spraying, or HVOF spraying, was only about 30% of that of the pure Cu, fully reflecting the advantages of CS in the preparation of electrically conductive Cu coating. Grigoriev et al. [111] studied the effect of the Cu–Al_2O_3–Zn powder mixture used for CS on coating properties in order to repair Cu contact lines. It turned out that 60% Cu–40% Al_2O_3 had the highest coating bonding strength and the best electrical conductivity when the spraying temperature is 500 °C, while the 40% Cu–50% Al_2O_3–10% Zn coating was the most wear-resistant, indicating that the addition of Zn powders exerted a great effect on the wear resistance of the coating, but a small effect on the electrical conductivity of the coating. The research results could lay a theoretical foundation for the preparation of Cu-based composite coatings with different functions in accordance with the requirements of different working conditions. Jiang et al. [112] prepared the elemental Cu coating on the surface of the 2A12 Al alloy substrate. The experimental results showed that, compared with arc spraying, the resistivity and roughness of the copper coating prepared by CS were lower, the bonding strength between the coating and the substrate was higher, and the bonding force was better, which signifies that the Cu coating performs well in surface lubrication and electrical conductivity. Coddet et al. [113] prepared a Cu–(0.1 wt%) Ag composite coating with high conductivity by CS technology, and the average electrical conductivity measured along three directions was close to 95.5% IACS. After heat treatment (HT), the conductivity in any direction maintained around (96.1 $\pm$ 0.5)% IACS. Yang et al. [114] prepared highly electrically conductive Cu–graphene nanosheets (Cu–GNS) composite coatings on the ABS (acrylonitrile–butadiene–styrene) substrate by electroplating and CS and tested the resistivity of the coating by the four-point probe method. According to the results, compared with that of the Cu coating, the resistivity of the Cu–GNS composite coating was reduced by nearly 40% at the same current density. The conductivity of the Cu–GNS composite coating prepared was obviously enhanced due to the deposition of GNS. Hence, this method is expected to be widely applied in electronic materials.

From the studies above, it can be seen that CS has been widely used in the preparation of Cu-based electrically conductive coatings. Cu-based composite coatings prepared by CS technology on metal materials or metal alloys show excellent electrical conductivity, which can meet the engineering application requirements in energy, electric power, and engineering machinery. At present, most Cu-based composite coatings with excellent electrical conductivity are prepared by adopting Cu and other metal materials or metal alloys. However, there are few reports on the preparation of conductive coatings from polymers such as polyether ether ketone (PEEK), the reasons for which need to be further investigated. Moreover, the conductivity of the Cu-based composite coating prepared by CS is inferior to that of the bulk Cu, so it is necessary to further improve the electrical conductivity of the coating through the post-process treatments of the coating. Table 3 lists the properties of some of these copper-based corrosion-resistant conductive coatings.

Table 3. Properties of copper-based corrosion-resistant conductive coatings.

Coating	Coating Composition	Best Ratio	Substrate	Self-Corrosion Potential (E_{corr}/V)	Electrical Conductivity	Microhardness	Conclusion	Ref.
Cu/Al_2O_3	Cu/Al_2O_3 (50 wt%)	Cu/Al_2O_3 (50 wt%)	Steel Fe52	−0.48	60% IACS	127 $HV_{0.3}$	Coating has the same corrosion resistance as bulk copper	[48]
Cu/Ni	Cu/Ni (0/6/16/33/48 wt%)	Cu/Ni (16 wt%)	AZ31D	−0.452		150 HV_{100g}	The coating porosity is reduced, and the corrosion resistance is the best.	[49]
Cu/Al_2Cu	Cu/Al_2Cu (0/5/10/15 wt%)	Cu/Al_2Cu (5 wt%)	Copper		32.7 ± 0.3 (MS/m)	159 ± 12 $HV_{0.025}$	Significantly improved electrical conductivity and wear resistance	[56]
$Ni/Cu/Cr/Al_2O_3$	$Ni/CuNiCr/Al_2O_3$ (50 wt%)	$NiCu/Al_2O_3$ (50 wt%)	Steel (Fe52)	−0.303		375 $HV_{0.3}$	Increased corrosion resistance of the coating	[103]
$Cu/SiC/Al_2O_3$	Cu Cu/SiC Cu/Al_2O_3	Cu/Al_2O_3	Aluminum alloy		62% IACS	120 $HV_{0.2}$	The coating has no obvious pores and cracks, and has the best corrosion resistance.	[104]
Cu/Cu_2O	Cu (90/80/70 wt%) Cu_2O (10/20/30 wt%)	Cu (70 wt%)/Cu_2O (30 wt%)	Q235 Steel	−0.313			Low coating porosity, best antifouling and corrosion resistance	[105]
$Cu/Al_2O_3/Zn$	Cu (40–70 wt%) Al_2O_3 (30–60 wt%) Zn (0–10 wt%)	Cu (40 wt%)/Al_2O_3 (60 wt%)	Copper contact wire		36 (MS/m)	143 HB	The coating is the most adhesive and has the best conductivity.	[111]
Cu/Ag	Cu/Ag (0.1/23.7 wt%)	Cu/Ag (0.1 wt%)	AISI 4130 steel		95.4 ± 0.5 IACS		Significantly improved conductivity	[113]

5. Post-Process Treatments of Cold-Sprayed Cu-Based Composite Coatings

During the CS process, a small number of micropores at the internal bonding interface of the deposition leads to a decline in compactness, poor malleability, and low tenacity of deposits, therefore the post-process treatments of the coating is needed. By post-process treatments, the microstructure of the coating can be homogenized, the interfacial bonding can be improved through solid diffusion, the residual stress can be reduced or eliminated, the coating porosity can be reduced, and the bonding strength of the coating can be improved [115]. In order to further improve the comprehensive performance of the cold-sprayed coating, researchers conducted post-process treatments to realize the transformation of the interfacial bonding between the coating and the substrate, as well as the bonding between the particles inside the coating from mechanical bonding to metallurgical bonding. In this way, the microstructure of the coating can be optimized, the bonding strength of the coating can be increased, the service performance of the coating can be improved, and the corrosion resistance, wear resistance, self-lubricating, and high conductivity of the coating can be enhanced [116]. The post-process treatments play a vital role in improving the comprehensive performance of the coating and promote the rapid development and application of CS technology in the industrial field, especially cold-sprayed Cu-based composite coatings.

At present, the post-process treatments of cold-sprayed Cu-based composite coatings have been widely studied, but there still is a lack of a comprehensive and systematic summary of these studies. In this paper, various post-process treatments of cold-sprayed Cu-based composite coatings are described comprehensively. First, the widely used heat treatment (HT) method is mainly reviewed, and their processes of different materials were compared. Secondly, the influence of FSP post-process treatments on cold-sprayed Cu-based composite coating was are discussed in detail. Finally, a brief introduction to the influence of other post-process treatments, such as shot peening (SP), laser remelting (LR), electric pulse processing (EPP), hot rolling (HR), and ball burnishing (BB) on cold-sprayed Cu-based composite coatings are briefly introduced.

5.1. Cold-Sprayed Cu-Based Composite Coatings Treated by HT

The lower porosity and the more compact microstructure of the cold-sprayed coating means that the coating has better mechanical and thermoelectric properties. However, solid particles can produce residual stress due to the strong impact deformation during the deposition process and lead to work hardening, posing a negative influence on the mechanical and thermoelectric properties. Therefore, appropriate post-process treatments of the coating are generally needed to eliminate the residual stress and work hardening in the coating and improve the comprehensive performance of the coating [117]. HT, as one of the most common post-process treatments of cold-sprayed coatings, has been widely applied in Cu-based composite coatings in recent years. Many studies have shown that HT can improve the microstructure, mechanical properties, corrosion resistance, and electrical conductivity of cold-sprayed Cu-based composite coatings. The changes of the coating during HT are shown in Figure 19, indicating that the microstructure changes of compact deposits differ from those of non-compact deposits. As for the non-compact deposits with large pores, the shrinkage of the pores decreases during HT, but it is difficult to completely repair these pores. However, the compact deposits can heal the inter-particle interface and form new grains and grain boundaries by the process of atomic diffusion, recrystallization, and grain growth during HT [118]. Similar to the HT of metal materials, the cold-sprayed coating undergoes the processes of recovery, phase diffusion, recrystallization, and grain growth with the increase of HT temperature and time, which can change the microstructure of the cold-sprayed coating to improve its plasticity [119].

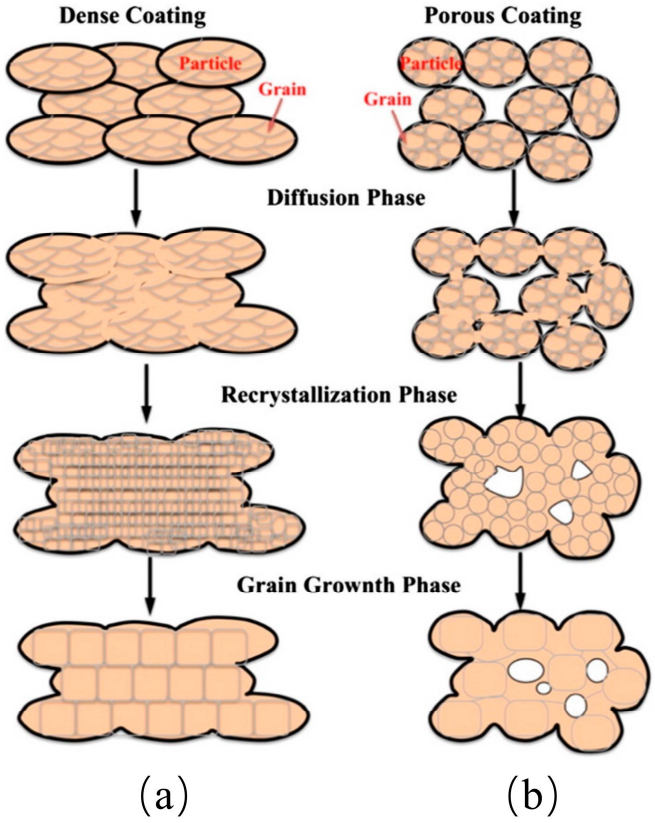

Figure 19. Schematic diagram of the evolution of the cold spray coating during heat treatment [120]. (**a**) Microstructural changes of the dense deposited layer; (**b**) microstructural changes of the non-dense deposited layer.

Price et al. [121] performed a short-time annealing HT of cold-sprayed Al/Cu composite coatings at 400 °C and found that the area of Al/Cu intermetallic compounds at the particle boundary increased with the elevated temperature, and obvious metallurgical bonding occurred at the particle interface inside the coating, which improved the bonding strength and reduced the porosity of the coating. The same results were obtained in Shen's [84] experiments where he conducted HT on the Cu–Al composite coating (Figure 20a). The Al particles in the sprayed coating were deformed from spherical to flat-shaped due to the impact with the substrate. The EDS spectrum analysis showed that no melting or elemental diffusion occurred in the Cu and Al particles in the coating, but only a simple mechanical bonding with the substrate and obvious pores in the coating. As shown in Figure 20b, there are no obvious Al particles inside the coating after HT at 450 °C, and the coating became compact with no obvious pores. EDS showed that after the sufficient elemental diffusion between the Cu–Al particles in the coating, the previous interface between the Cu–Al particles disappears, forming sintering products and effectively reducing the porosity of the Cu–Al composite coating, ensuring the highest bonding strength of the coating. All this proves that HT can be regarded as an effective measure to regulate coating properties.

Kang et al. [122] prepared Cu–metal–glass composite coatings by CS technology. After 300 °C/1 h HT, the particles showed good bonding with the Cu substrate, and the elongation of the coating increased from 6.6% to 26.1%, indicating that HT can significantly improve the ductility of the coating. However, the substrate softening caused by higher temperatures could increase the wear rate of the coating to 1.57×10^{-5} $mm^3/(N \cdot m)$. In the preparation of the pure Cu coating on the 6061 Al alloy using spraying, Xu et al. [123] found that the electrical conductivity of the Cu coating after HT was significantly higher than before HT. Stoltenhoff et al. [124] conducted research on the influence of the annealing treatment on the hardness, bonding strength, and electrical conductivity of the Cu coating.

The results revealed that grain restoration and grain recrystallization of the coating occurred at the annealing treatment, and the number of dislocations decreased, thus reducing the hardness of the Cu coating. The healing of the grain boundary defects caused by gaps, dislocations, vacancies, and inter-particle interactions due to poor bonding could not only improve the bonding strength of the coating, but also enable its electrical conductivity to reach 90% of the bulk material. Guo et al. [125] prepared Cu–6.5 wt% Sn tin bronze coatings by the CS process. It was found that the coating porosity was relatively high, but the value decreased from 4.7% to 1.4% after vacuum HT, showing a significant improvement. However, the hardness of the coating is reduced by HT, resulting in worse wear resistance. Phani et al. [126] prepared nanocrystalline Cu–Al_2O_3 coatings on the Cu substrate. The results proved that the porosity of nanocrystalline Cu–Al_2O_3 coatings decreased, the electrical conductivity increased significantly, and the hardness was higher than that of the pure Cu coating after HT because the grain size of the Cu–Al_2O_3 coatings under HT obviously rarely changes and Al_2O_3 particles effectively prevented the growth of grains. Zhang et al. [127] prepared Cu coatings on the surface of the 304 stainless steel substrate with 1 mm thickness by CS technology with helium as an accelerating gas. It was found that the compactness of the coatings increases, and the porosity decreases with the increment of the HT temperature. The microhardness of the Cu coating decreased continuously after HT due to the recrystallization of the microstructure, the disappearance of internal dislocation, and the elimination of the work hardening inside the coating after annealing. No significant decrease occurs in the bonding strength of the coating, and the electrical conductivity of the coating was higher than that of the coatings without HT, highly close to that of as-cast Cu. Tazegul et al. [128] prepared Cu and Cu–SiC composite coatings by CS, and conducted subsequent HT of the coatings. The results showed that after HT, the wear rate of the Cu–SiC composite coating was significantly reduced, and the wear resistance and electrical conductivity of the composite coating were significantly improved compared with those of the Cu coating. Huang et al. [120] prepared Cu coatings on Al alloy and stainless steel substrates to study the influence of the HT temperature on the microstructure and mechanical properties of the coatings. Figure 21a,b shows the microstructures of the Cu coating prepared by CS and HT at 500 °C, respectively. It can be seen that the cold-sprayed Cu grains underwent a severe deformation in the deposition process. The interface between the particles disappeared and the grains of Cu coating were fine and evenly distributed after HT at 500 °C. The stress–strain curves of the deposit under different HT conditions (Figure 21c) illustrated that the tensile strength of the cold-sprayed Cu exceeded that of the bulk, almost reaching 300 MPa, but the plasticity was poor (elongation was about 0.4%). With the increase of the HT temperature, the plasticity of the Cu coating rose, and the hardness weakened. In addition, a remarkable finding was that the electrical conductivity of the Cu coating approached 100% of that of the bulk Cu (Figure 21d). As such, HT can effectively improve the bonding strength, electrical conductivity, and mechanical properties of the Cu-based composite coating.

According to the studies above on HT of cold-sprayed Cu-based composite coatings, it has been widely accepted that HT technology can improve the performance of Cu-based composite coatings. The mechanism of HT is to modify the coating surface at high temperatures to enhance the cohesion between the deposited particles, so as to improve the performance of the coating. Reasonable HT technology can significantly improve the bonding strength and mechanical properties of cold-sprayed Cu-based composite coatings, but this technology has some defects. For example, HT technology could exert an adverse influence on the properties of the original coating because the coarsening of the precipitates and the growth of grains result in larger defects in the coating and an increase in porosity. Therefore, other technologies are needed to further improve the comprehensive performance of Cu-based composite coatings [129]. FSP, as another solid-state post-process treatments, has been applied to obtain Cu-based composite coatings with ultra-fine grains and high strength.

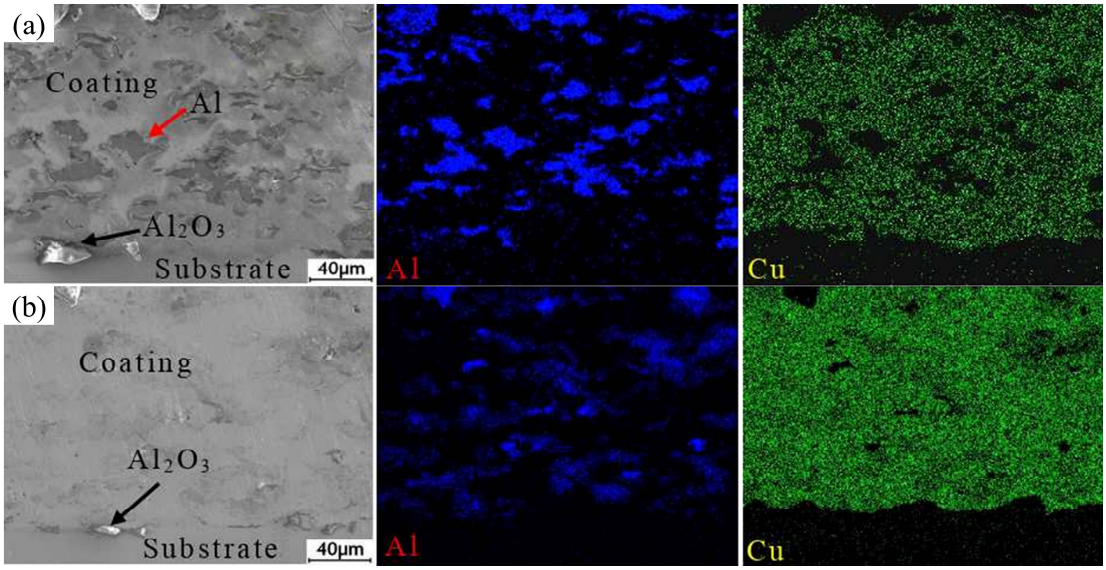

Figure 20. Microscopic morphology and EDS patterns of coated specimens at different heat treatment temperatures [84]. (**a**) Cold-sprayed state; (**b**) 450 °C.

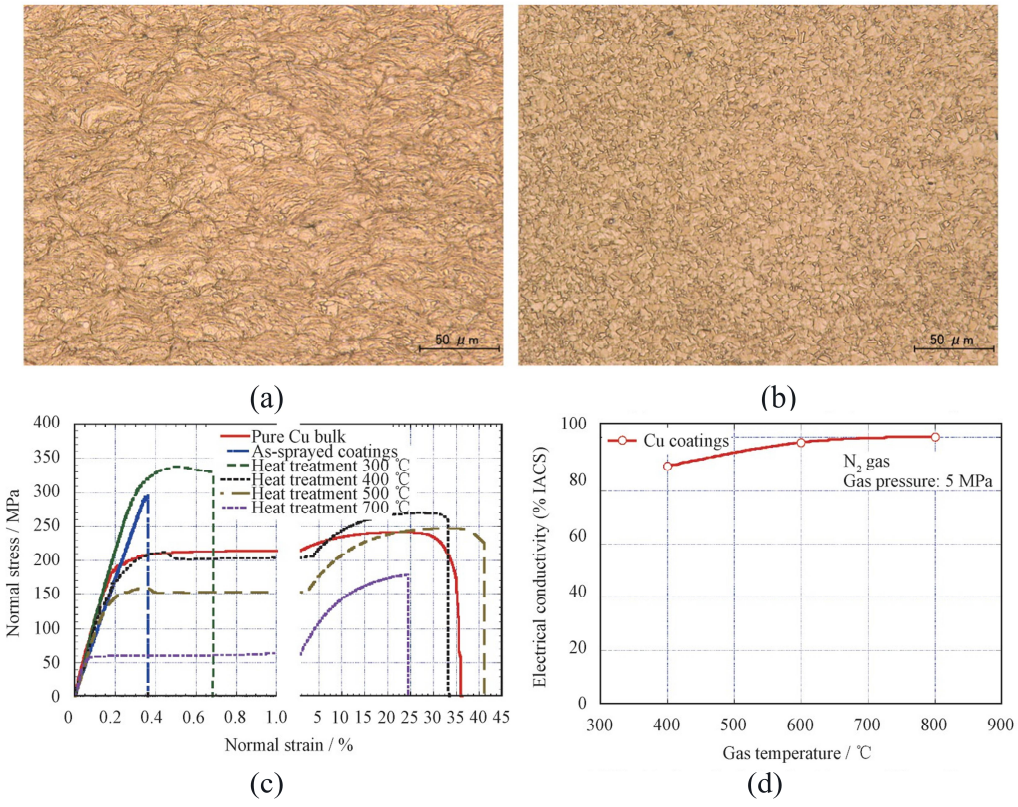

Figure 21. Microstructure and properties of a cold-sprayed copper coating [120]. (**a**) Microstructure of as-sprayed Cu coatings; (**b**) heat-treated at 500 °C; (**c**) tensile strength of cold-sprayed Cu coatings; (**d**) electrical conductivity of cold-sprayed Cu coatings.

5.2. Cold-Sprayed Cu-Based Composite Coatings Treated by FSP

FSP, a new post-process treatment of cold-sprayed coating developed in recent years, is a powerful thermal metal treatment method of thermo-mechanical coupling evolving from friction stir welding. As FSP can be employed to refine material grains and enhance material plasticization, it can densify the cold-sprayed coating, refine its grains, and im-

prove its microstructure, mechanical properties, and corrosion resistance [130–132]. The principle of FSP is shown in Figure 22. A rotating cylindrical tool with a specially designed shoulder and a pin is first inserted into the surface of the metal plate to be treated and then moved laterally along the surface of the workpiece, so that its high-velocity rotating shoulder contacts the coating surface to generate heat during friction, which softens the coating material. In the complex flow of the process from the front to the back, the material was extruded to form a solid stirring area. After FSP treatment, the coating surface has greater melting and high-stress deformation, and the particle sizes of the reinforced particles are uniformly distributed, remarkably modifying the coating's microstructure and properties [133]. Therefore, FSP is a promising post-process treatment to achieve structure uniformity in cold-sprayed coatings and eliminate their defects.

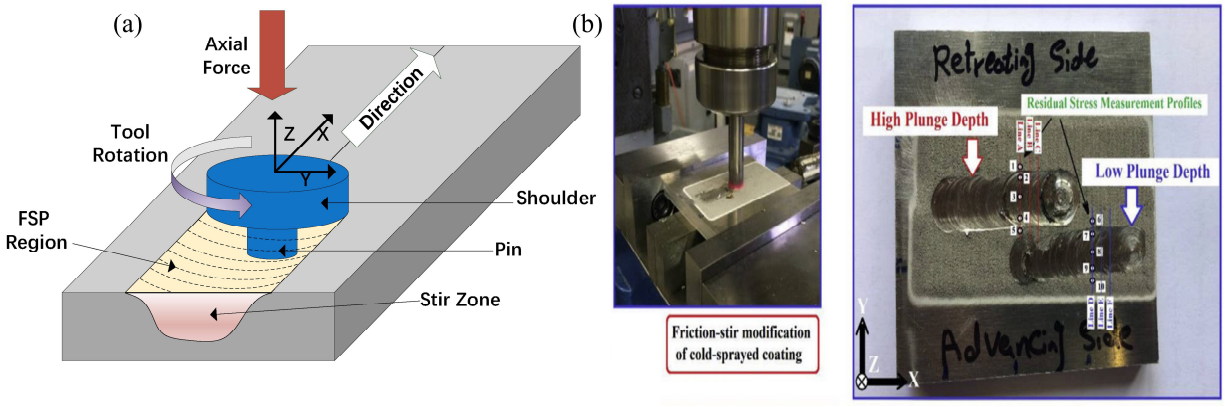

Figure 22. Schematic diagram of cold spray coating by stirring friction processing. (**a**) Schematic diagram [134]; (**b**) physical diagram [135].

Professor Li [136] pioneered the post-process treatments of FSP of cold-sprayed coatings. Based on FSP, the team brought up a new idea for additive manufacturing of friction-stir in-situ-assisted CS (Figure 23a). The detailed flow of the process is listed as follows. First, the spray gun and mixing tool are started and used for coating preparation and the treatment of in-situ synchronous modification, respectively, under the cooperative action of the first manipulator and the second manipulator. Second, the positions of the two manipulators are adjusted while maintaining a distance between the spray gun and mixing tool and the surface of the first layer of the deposited coating. Third, the surface of each layer (from the second layer to the last layer) of the metal-based composite bulk material will be continuously prepared and modified until the thickness of each layer reaches the requirement of the metal or the metal-based composite bulk material (Figure 23b). Afterwards, the team examined the effects of friction stir on the microstructure and mechanical properties of cold-sprayed Cu/Zn alloys [137]. As suggested by the research results, the particle interface disappeared after FSP, and the grain size in the coating was reduced to 1.9 μm. Meanwhile, the size distribution was uniform, and the tensile strength of the coating went up from 87.2 to 257.5 MPa. On this basis, Wang et al. [138] developed a CS and FSP composite additive manufacturing technology to prepare Al metal bulk materials and found from the experimental results that the strength (87 MPa) and elongation rate (60.3%) of the blocks prepared by composite technology turned out to be higher than those prepared by traditional CS (60 MPa and 4.2%).

Combining CS with FSP, Huang et al. [137] prepared high-strength Cu–Zn coatings with ultra-fine grains, as shown in Figure 24. Their experiment revealed that the coatings prepared by the composite technology had higher structural compactness than those prepared by cold-sprayed coatings. In addition, the defects such as cracks, pores, and weak bonding interfaces were all eradicated, as the excellent metallurgical bonding of recrystallization contributed to the formation of high-strength coatings.

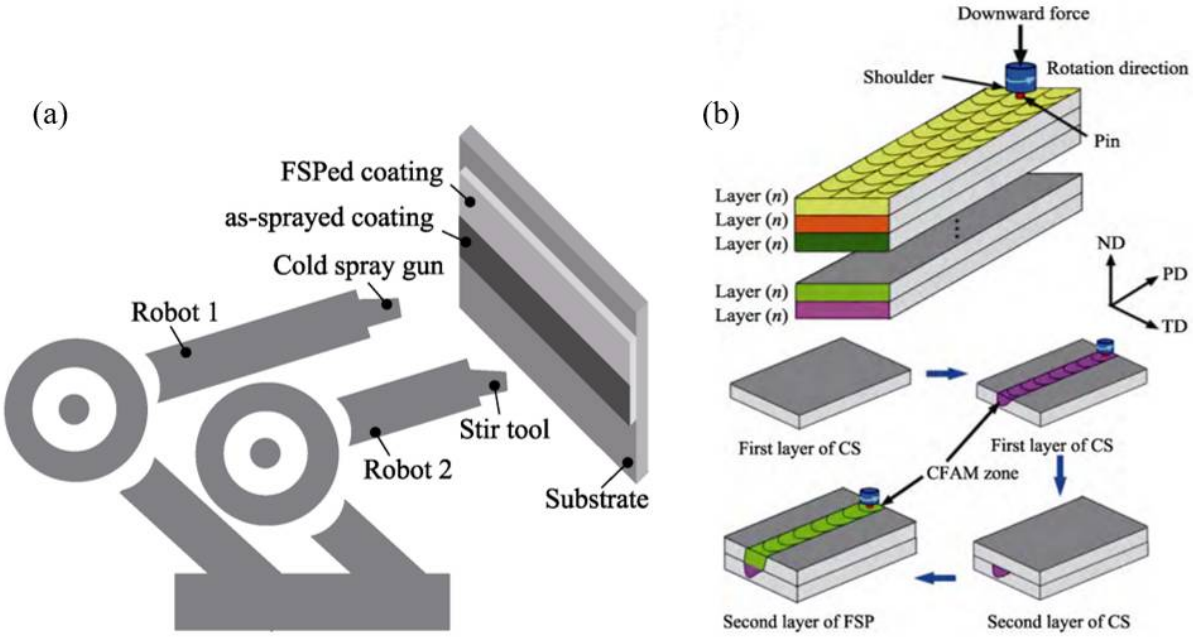

Figure 23. (**a**) Principle diagram of in-situ assisted cold spraying technology for stirring friction processing [27]; (**b**) cold spraying technology assisted by stirring friction processing [138].

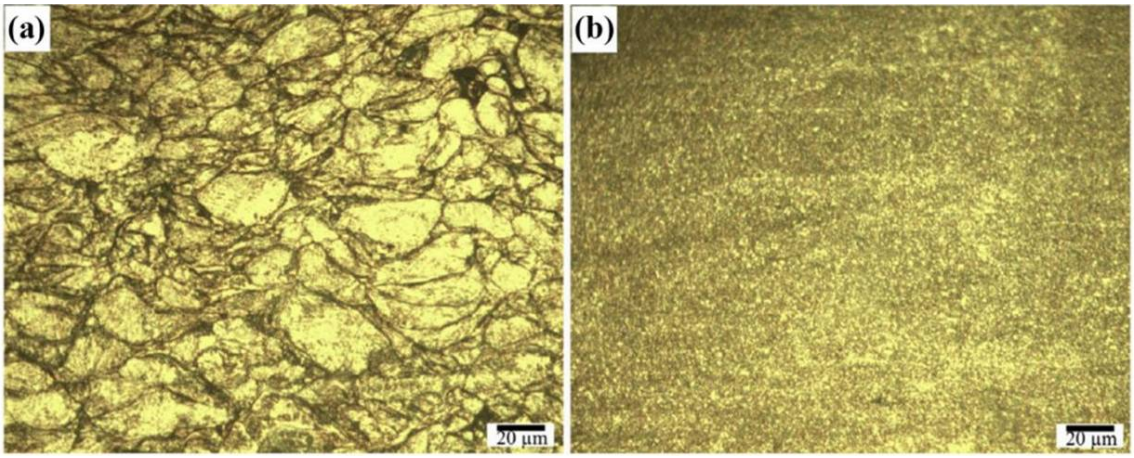

Figure 24. Cross-sectional micrographs of OM for (**a**) cold sprayed and (**b**) friction stirred coatings [137].

In the coating prepared by composite technology, the original sputtering granular grains turn into ultra-fine equiaxed crystals. After conducting further research into this phenomenon, Huang and Wang et al. [137,138] discovered that such a phenomenon resulted from discontinuous dynamic recrystallization assisted by dynamic recovery, where new fine subgrains grew continuously under the action of both high temperature and high stress. Subsequently, this conclusion was corroborated by electron backscatter diffraction (EBSD) analysis. Figure 24 illustrates the EBSD maps of coatings prepared by CS and CS–FSP. The white line represents low-angle grain boundary (LAGB). As demonstrated in the Figure, coatings prepared by CS contain many LAGBs (Figure 25a), while those prepared by CS–FSP contain many high-angle grain boundaries (HAGB) (Figure 25b). The formation of these fine grains largely resulted from the strong plastic deformation in the FSP process and from the dynamic recrystallization induced by friction heating. Subsequent tests revealed that the concentration of LAGB dropped from 77.4% to 9.5% and the concentration of HAGB increased from 22.6% to 90.5% (Figure 25c,d), which was largely due to the dynamic recrystallization that occurred in the cold-sprayed coating after the FSP treatment. Under

the effect of high temperature and stress, new grains were continuously nucleated and turned over, thus forming a large number of HAGBs. As the large quantity of HAGBs in the grain boundary of the coating could restrain the dislocation of displacement, the tensile strength and ductility of the coating were improved.

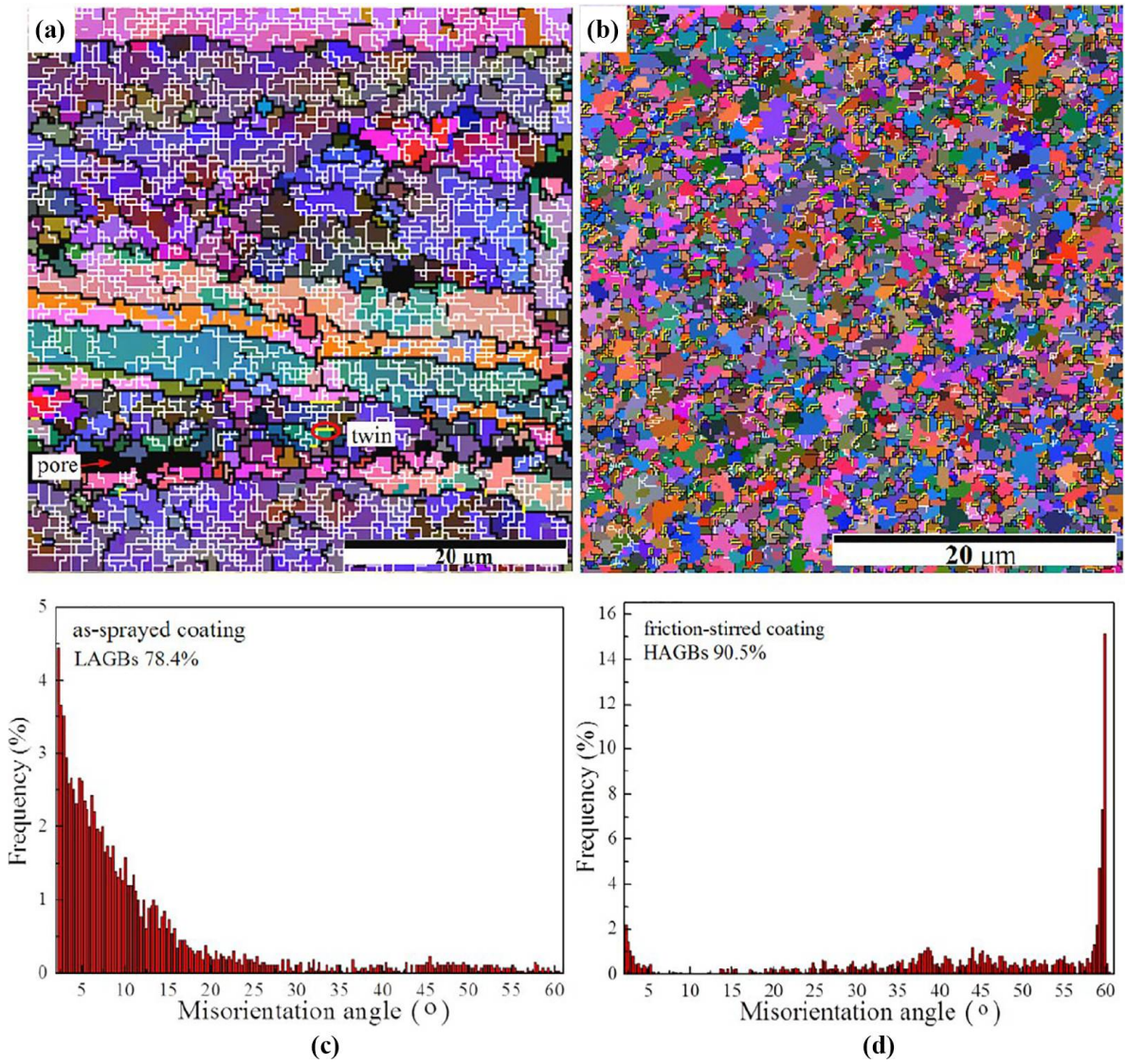

Figure 25. EBSD maps of (**a**) as-sprayed and (**b**) friction-stirred coatings. The black, white, and yellow lines in the EBSD maps correspond to the HAGBs ($\theta \geq 15°$), LAGBs ($15° \geq \theta \geq 2°$), and TBs, respectively. Misorientation angle distribution in (**c**) as-sprayed and (**d**) friction-sprayed coatings [137].

Dmitry et al. [139] prepared Cu–Al–Ni–Al_2O_3 composite coatings on AA2024 Al alloy substrates through an innovative hybrid process combining two effective surface modification techniques, CS and FSP, which can refine the microstructure of Cu–Al–Ni–Al_2O_3 composite coating materials. The results showed that cold sprayed CuAlNi–Al_2O_3 coating was dense, but porosity and microcracks still appeared (Figure 26a). After FSP treatment, the microstructure of the coating was significantly refined and the particle boundaries, microporosity, and microcracks disappeared (Figure 26b), and the mechanical properties of the coating were promoted and the wear rate of the CuAlNi–Al_2O_3 composite coating was slightly reduced. The FSP-S1 coating showed the lowest friction coefficient and wear rate (Figure 26c), which was almost twice lower than the untreated coating (Figure 26d), attributing to the excellent microstructure and mechanical properties of the FSP-treated coating.

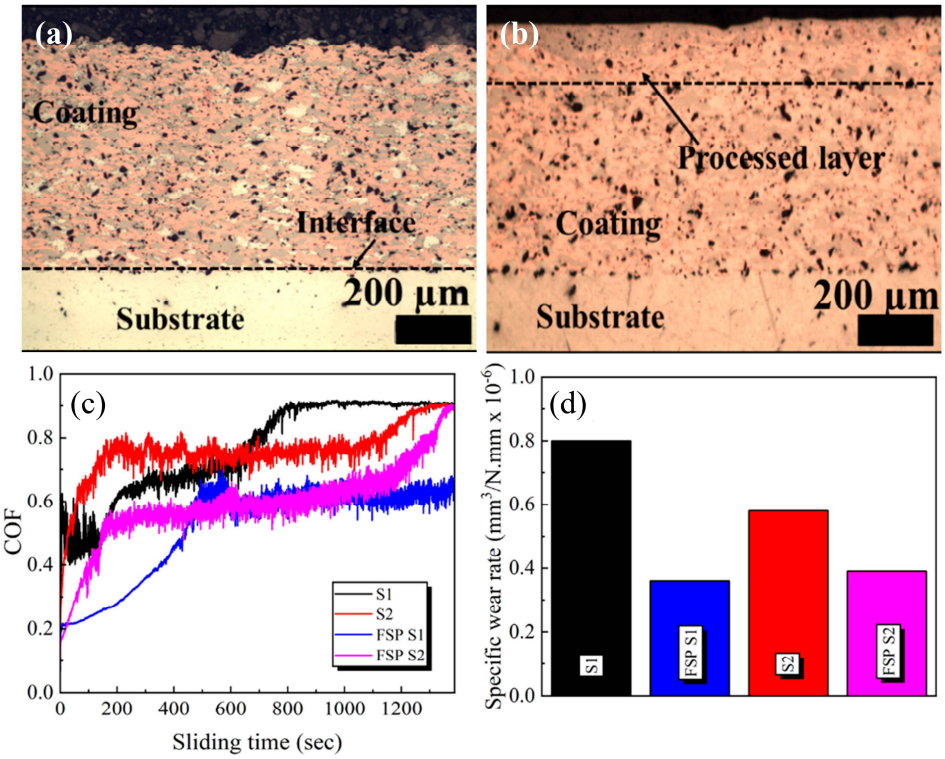

Figure 26. Optical micrographs of the cross-sectional cold sprayed coatings. (**a**) S1; (**b**) FSP-S1; (**c**) variation of the coefficient of friction as a function of time; (**d**) specific wear rate for a regular load of 2N of all developed coatings [139].

After reviewing the effects of the three post-treatment technologies, namely, FSP, EPP, and AHT, on the microstructure and mechanical properties of Cu-based composite coatings, Li et al. [140] found that EPP and HT could increase the grain size and reduce the residual stress in the coating, and FSP could enhance the uniformity of the grain sizes, as well as the plasticity and strength of the coating. Wang et al. [141] also summarized in more detail the post-process treatments of coatings such as HT, LR, FSP, HR, and SP. HT can reduce the porosity of coatings, but the process incurs grain growth and phase transformation in the deposits and reduces the hardness of the coatings. LR can improve the hardness of coatings, but there are large pores between the remelted layer and the substrate. FSP can improve the bonding strength of coatings, but the heat-affected zone (HAZ) generated during FSP affects the integrity of the coatings. HR can reduce the porosity of coatings, but the process is complex and costly. Finally, SP can generate compressive stress that can improve the compactness of coatings, but the process easily damages the surface morphology of the coatings and is inefficient.

5.3. Cold-Sprayed Cu-Based Composite Coatings Post-Treated by Other Processes

Regarding the current progresses made in the research on the post-process treatments of coatings, the application of HT and FSP in improving the performance of cold-sprayed Cu-based composite coatings has matured. However, there are few reports on the post-process treatments of laser remelting (LR), shot peening (SP), electric pulse (EPP), hot rolling (HR), and ball milling (BB) of Cu-based composite coatings, thus necessitating further research in this aspect, which will be a critical direction to enhance the comprehensive performance of Cu-based composite coatings [133,140,141]. As CS technology develops rapidly, researchers have successfully applied the post-process treatments of coatings above to Cu-based composite coatings and achieved great outcomes in their research.

LR treatment, which has gradually become an essential post-process treatment of coatings, is a laser surface strengthening technology that combines laser technology with

HT technology. Also serving as a method to quickly treat and modify coating surfaces, LR focuses the laser on the surface of cold-sprayed coatings (Figure 26a) so that the surface receives enormous heat input in a very short time, subjecting the coatings to instantaneous melting and concreting. As a result, along the direction of the coating depth, the microstructure of coatings forms three zones: the melted zone, the HAZ, and the substrate, the sizes of which change when the LR parameters change. Using CS technology, Kang et al. [142] prepared Al–Si composite coatings on an Al alloy substrate. The surface of the composite coating turned out to be rough, with almost no interaction between the Si particles and the Al substrates. As the coating was mechanically bonded to the substrate, the bonding strength was low (Figure 27c). Then, the post-treatment technology of LR was employed to improve the bonding strength. As suggested by the experimental results, since the Al–Si compound was completely melted and then rapidly cooled to form a supersaturated Al–Si phase, the microstructure of the coating was refined (Figure 27d) and the microhardness was increased (Figure 27b), effectively improving the performance of the Al–Si coating. Additionally, equiaxed grains were observed in the top area of the coating, while vertical columnar grains were observed in the bottom area. In between these two areas, a mixture of equiaxed grains and vertical columnar grains was observed (Figure 27(d1–d3)). However, after LR, large pores appeared on the coating surface between the remelted zone and the non-remelted zone, which would affect the microstructure and mechanical properties of the cold-sprayed coating. Therefore, the LR process needs to be further optimized to eliminate the pores.

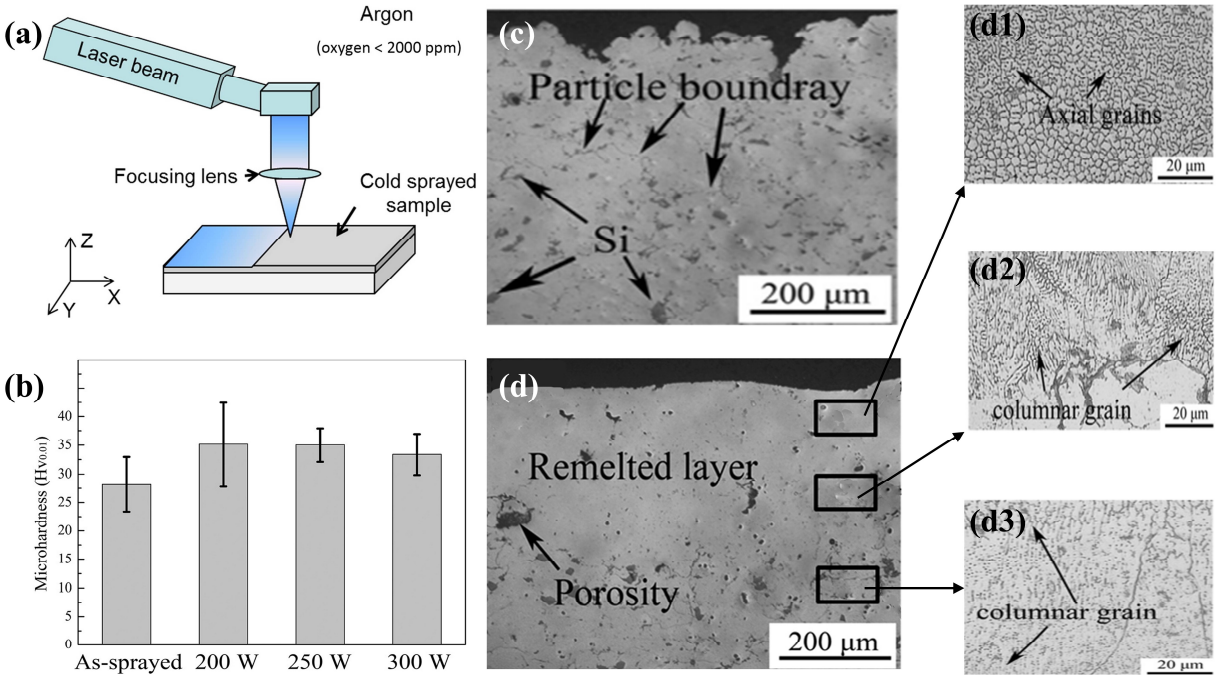

Figure 27. (**a**) Schematic diagram of the laser remelting post-treatment technique; (**b**) average values of microhardness of cold sprayed deposits before and after the laser remelting process; (**c**) cross-section of the sprayed Al–Si composite coating; (**d**) cross-section of the Al–Si composite coating after laser surface remelting at 250 W [142].

Chen et al. [143–146] adopted CS technology to prepare a Cu402F coating that was about 882.11 μm thick on the Ni–Al bronze 9442 alloy and deployed LR technology to modify the surface of the coating. As the results demonstrated, after LR, the coating took on a multilayer structure: the top remelted layer, the middle layer transitioning to remelting, and the bottom layer left out by CS. The coating surface was relatively flat and the coating was approximately 865.13 μm thick (Figure 28b), meaning that the advantages of the Cu402F coating were retained. The creation of passive films on the laser-remelted coating

was accelerated, which could tremendously help improve the wear resistance and corrosion resistance of the coating (Figure 28). Subsequently, a Ni–Al bronze coating was prepared on the surface of the Ni–Al bronze 9442 alloy. After LR, coating hardness was significantly improved, and both the corrosion resistance and the wear resistance of the coating proved to be better than those of the substrate.

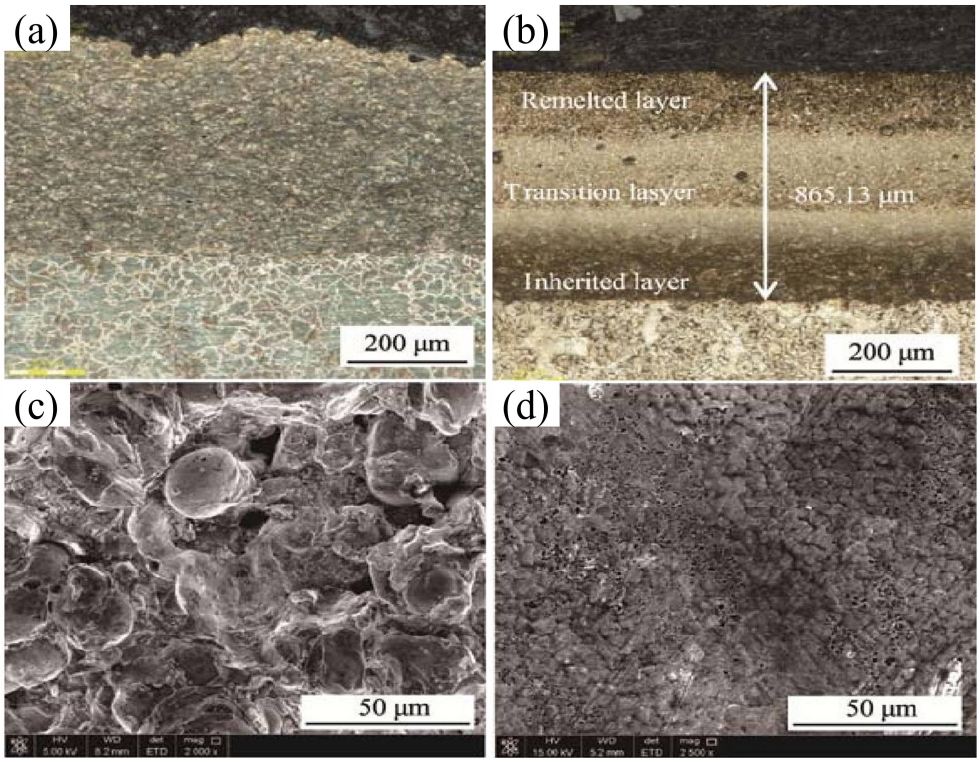

Figure 28. Coating microscopic morphology [143]. (**a**) Cross-section of cold sprayed coating; (**b**) cross-section of laser remelted coating; (**c**) surface of cold sprayed coating; (**d**) surface of laser remelted coating.

SP is an essential post-process treatment of cold-sprayed coatings. Due to the fact that during SP, plastic deformation will occur in the coating and a compressive stress layer will be generated near the surface, both the surface hardness and the fatigue property of the coating will be improved, achieving the compaction effect of the coating. Figure 29a is the schematic diagram of the post-treatment technology of SP. After the deposition of CS on the coating, SP particles are put into the CS system and sprayed on the coating surface again. High-velocity SP particles impact the coating, exerting a hammer effect, after which the SP particles will rebound. The cold-sprayed coating that has undergone the SP process will have a completely compact structure. However, due to a large number of intrinsic defects in the coating itself, SP may result in new cracks or enlarge the existing ones in the coating [147]. In order to solve this problem, based on SP, the research team of Xi'an Jiaotong University proposed the post-process treatments assisted by in-situ SP. As shown in Figure 29b, unlike SP, the post-process treatments of assistive in-situ SP mixes SP particles with the sprayed powder and affects the substrate in the meantime. Since the size of the SP particles is much larger than the sprayed particles, the SP particles will rebound after impacting the deposited particles or the substrate, thus contributing to the formation of a cold-sprayed coating that is fully compact inside.

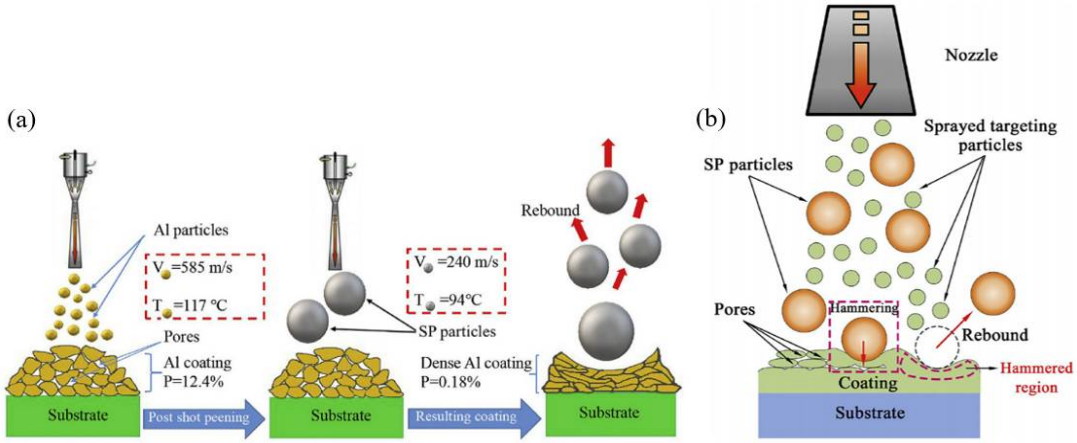

Figure 29. Schematic diagram of shot blasting post-treatment. (**a**) Schematic diagram of CS and SP processes for obtaining dense Al coatings on LA43M substrates [148]; (**b**) schematic diagram of in-situ shot blasting assisted cold spraying [149].

For cold-sprayed coatings, the bonding quality and the porosity depend on the degree of plastic deformation of the particles during deposition. The microforging effect of shot-peened particles can remarkably enhance the degree of plastic deformation of the sprayed particles, thereby optimizing the quality of bonding between the particles and the refining microstructure [150]. Li et al. [66] used a mixed raw material including soft/porous Cu powder and hard/compact Cu powder to CS fully dense Cu coatings. Based on the compaction effect of USSP, the coating was post-process treated to reduce the coating porosity. According to Moridi et al. [151], the traditional post-process treatments of SP would result in cracks in the cold-sprayed Al coating. By contrast, when SP was conducted on the substrate before the deposition of CS, the strengthening effect would be better, and the fatigue strength of the coating could be increased by 26%. In addition, the impact of SP on the coating structure is also determined by SP parameters and coating types. Brown et al. [152] adopted CS technology to prepare CuNi: Cr_3C_2–NiCr composite coatings. After the post-process treatments of ultrasonic consolidation, the mechanical properties of the coatings were greatly enhanced. As a post-process treatment of cold-sprayed coatings, ultrasonic consolidation offers a unique method for a completely solid treatment. In such a process, the mechanical properties of the coating can be improved through the concentration of carbide particles contained in the metal substrate. Similarly, Zhang et al. [49] adopted CS technology to prepare a Cu/Ni composite coating. After finding that the coating's porous structure contributed to its poor corrosion resistance, they adopted the post-process treatment of USSP to improve its properties. After the coating was treated by USSP, the structure and corrosion resistance of the Cu/Ni composite coating were tremendously improved. Maharjan et al. [153] adopted the two mechanical SP processes of deep cold rolling (DCR) and controlled hammer peening (CHP) to modify the cold-sprayed Ti–6Al–4V coating on the Ti–6Al–4V substrate. The micromorphology and porosity under different treatment processes are shown in Figure 30. After the post-process treatments of DCR and CHP, the bonding strength of the cold-sprayed coating that had loosely bonded coating interfaces due to large pores was increased because greater plastic deformation occurred at the interfacial bonding. Under the CPH conditions of high SP, the coating porosity was about 71% lower than that of the cold-sprayed coating. In light of this, the SP treatment plays a vital role in enhancing the properties of the coating.

After the SP treatment, as the porosity of the cold-sprayed coating decreases and the compactness increases, the comprehensive performance of the coating is significantly improved. As an indispensable post-process treatment to modify the coating surface, the post-treatment of SP has been applied to several cold-sprayed metal coatings. However, there are few reports on the SP treatment of cold-sprayed Cu-based composite coatings because the application of the SP treatment is limited, as this process easily deforms and

fails the key parts of Cu, Al, magnesium, and other light alloys, whose hardness is low. Therefore, it is necessary to comprehensively study the optimal SP process parameters so that they can serve to optimize the performance of Cu-based composite coatings.

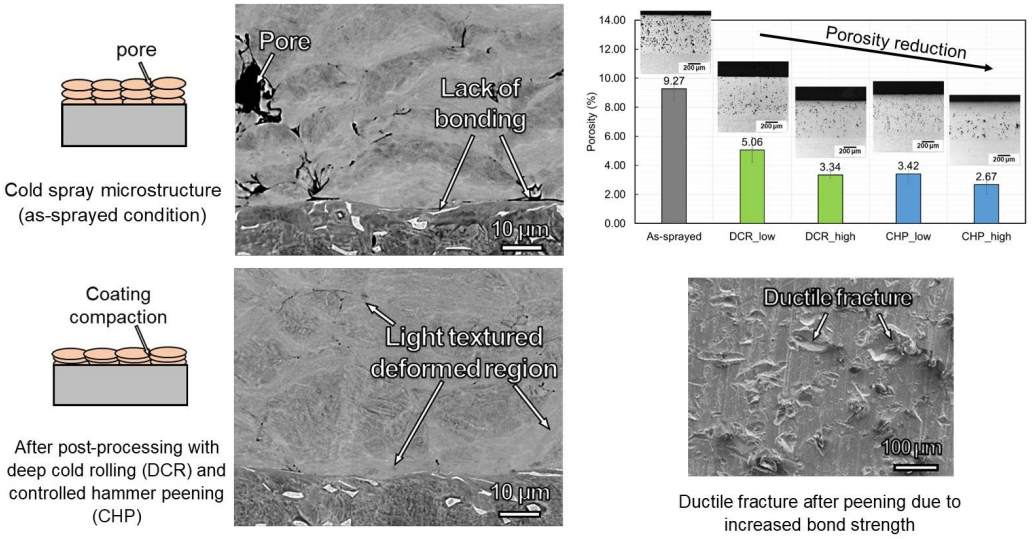

Figure 30. Microscopic morphology of post-treatment of a coating and the porosity of the post-treatment samples under various conditions [153].

As a new type of rapid HT treatment, electric pulse treatment or processing (EPP) remarkably changes the alloy's microstructure and mechanical behaviors, such as the distribution of precipitates, yield strength, elongation rate, and hardness, by applying high-density currents to create an electric, thermal, and strain non-equilibrium coupling magnetic field [154], as shown in Figure 31. Hu [155] studied the effect of the HT process of electric pulse on cold-sprayed Cu coatings. Figure 32 shows the comparison of the structures before and after the EPP of cold-sprayed Cu. Evidently, compared with sprayed Cu, the thermal effect of the currents promoted grains to grow, healing the unbound interfaces between a large number of particles and generating notable quantities of annealing twins inside the grains. As the existence of twins played a role in hardening the material, the hardness and bonding strength of the coating were improved, and the wear resistance of the coating was consequently enhanced.

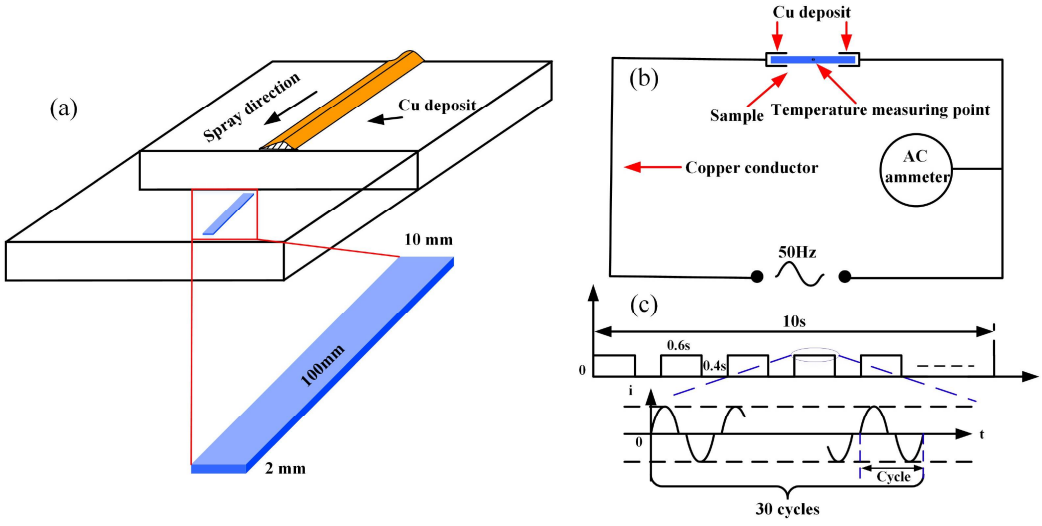

Figure 31. Schematic diagram of EPP post-processing [140]. (**a**) Sample preparation; (**b**) process; (**c**) circuit and pulse current curves.

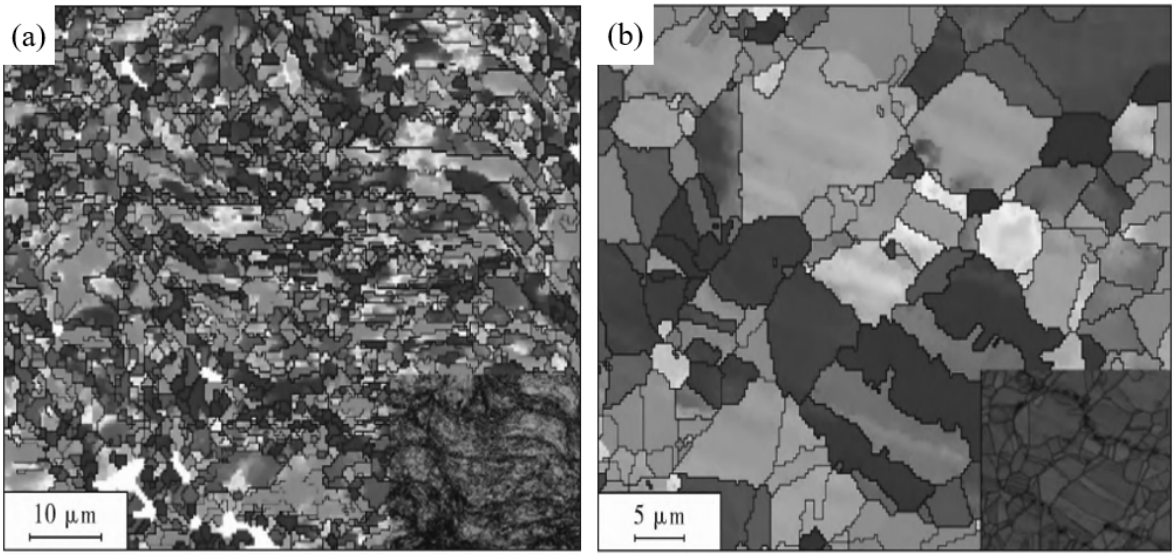

Figure 32. EBSD maps of the Cu deposit (**a**) before and (**b**) after EPP [155].

The HR treatment is another thermal treatment process of thermo-mechanical coupling. When the material is heated to the recrystallization temperature or above, strong plastic deformation and recrystallization occur during the rolling process to achieve the coordinated change of both the structure and the properties [156]. After HR, the coating thickness was markedly reduced (Figure 33), and the composite consisted of a mixed structure (including a large number of refined recrystallized particles and substructure particles) due to continuous dynamic recrystallization (Figure 33b–e). In addition, after HR, the tensile strength, yield strength, and elongation rate of the sample increased simultaneously and were higher than those of the sprayed sample and the conventionally treated sample (Figure 33f) because the enhancement of diffusion activity significantly improved the interfacial bonding degree of the coating [157]. Huang [158] hot rolled the cold-sprayed Cu. At a temperature of 500 °C and a compression of 30%, the tensile strength of the coating could be increased to 385 MPa. At the same time, the elongation rate remained at about 8.9%, while the microhardness was about 120 HV. Thus, the strength and plasticity of the coating were significantly improved. Although HR can remarkably improve the strength and plasticity of cold-sprayed coatings, the downside is that the HR treatment can notably reduce the coating thickness.

Ball burnishing (BB) and turning are also essential surface post-process treatments, in which the cold-sprayed coating is overturned and the surface conditions of cold-sprayed deposits are modified, as shown in Figure 34a. Sova et al. [159] studied how fine turning and BB affect the surface morphology, structure, and residual stress distribution of the CS 17-4 PH stainless steel coating. It was found that after turning and BB, the integrity of the coating was maintained without any cracks, layering, or torn particles (Figure 34b). The turning and BB processes can deform the grains near the surface of the cold-sprayed layer, turn them into the same direction, and reduce surface roughness. The residual stress test revealed that the coating after spraying was compressive stress, and that the residual stress after turning changed from the original compressive stress to tensile stress. After BB, the residual stress curve was smooth and the peak value was not obvious, eliminating the tensile residual stress previously seen. Subsequently, Courbon et al. [160] carried out a similar experimental study on residual stress, as shown in Figure 35, and obtained similar results. However, in order to further understand the microstructure evolution mechanism of the near-surface area during turning and BB, further research is required.

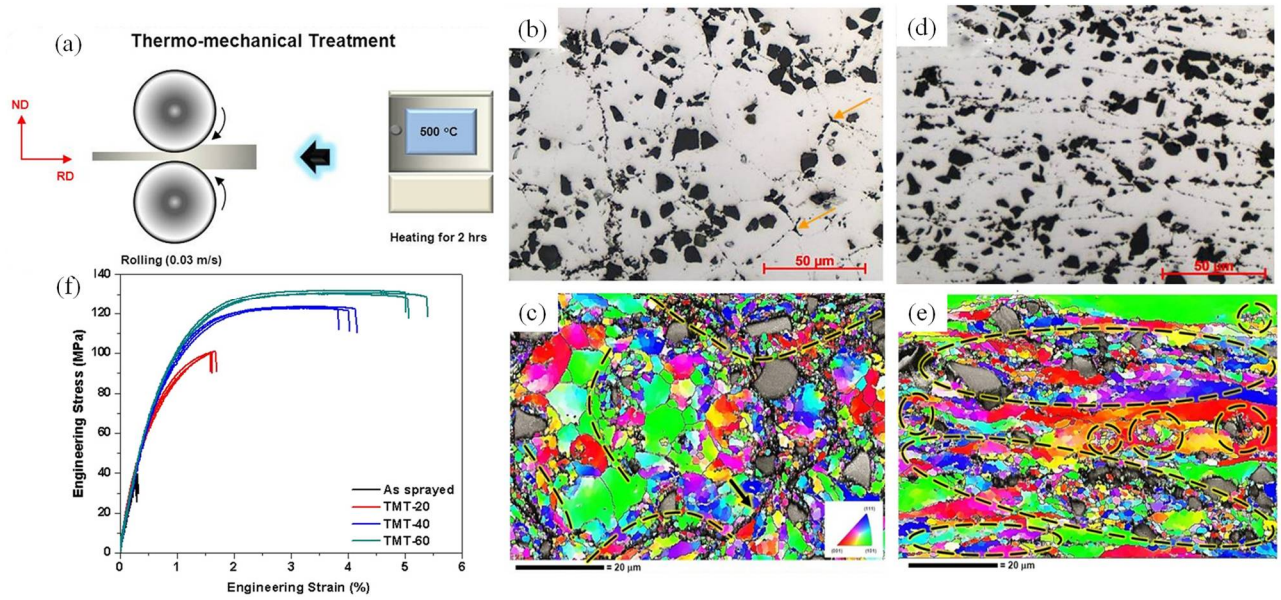

Figure 33. (**a**) Schematic diagram of the hot rolling process, (**b**–**e**) optical micrographs and EBSD results of cross-sections for (**b**,**c**) as-sprayed and (**d**,**e**) hot-rolled samples, and (**f**) stress–strain plots of as-sprayed and hot-rolled samples [157].

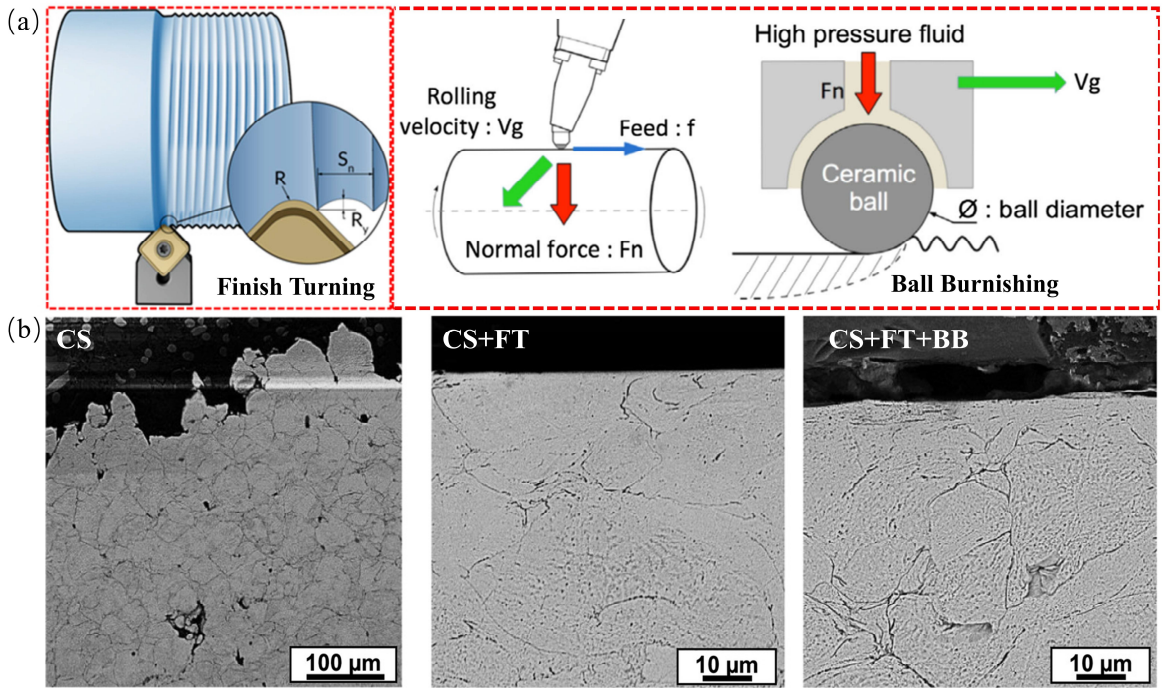

Figure 34. (**a**) Schematic diagram of the turning and ball polishing process; (**b**) SEM image of cold-sprayed, cold-sprayed after finishing turning, and cold-sprayed 17-4PH stainless steel coating after ball polishing after finishing turning [159].

In conclusion, post-process treatment is one of the most effective methods to improve the structure and properties of cold-sprayed coatings. Table 4 summarizes the improvements achieved in various properties of coatings by the seven post-process treatments discussed in this paper. By conducting profound research on various post-process treatments mechanisms and by selecting the appropriate post-process treatments based on the type of coating, the areas in which CS technology can be applied will be vastly expanded.

Table 4. Improvement, advantages, and disadvantages of seven post-treatment processes on various properties of coatings.

Post-Processing Technology	Mechanism	Used in Additive Manufacturing	Refinement and Dispersion of Ceramic Reinforcement Particles	Reduce Porosity	Corrosion Resistance	Hardness	Wear Resistance	Bond Strength	Ultimate Tensile Strength (UTS)	Advantage	Disadvantage
HT	Thermal action	0	1	0	3	4	3	3	4	Convenient operation, low cost, improved mechanical properties, and reduced residual stress	Limited performance improvement, reduced matrix performance, limited sample size
LR	Thermal action	1	1	0	3	3	3	2	2	The surface layer of the coating is densified to improve the wear resistance and corrosion resistance of the coating.	There are large pores at the bonding interface.
FSP	Strong thermal–mechanical coupling	0	0	0	3	3	3	3	3	Convenient operation, low cost, improved tissue performance, and reduced porosity	Coating internal residual stress, limited sample size
SP	Compaction	0	1	0	3	3	2	3	3	Compressive stress is generated, and the density of the coating is improved.	Easy to lose the microscopic topography of the coating surface
EPP	Thermal action	0	0	0	3	3	2	2	3	Local heat treatment, high efficiency	Not suitable for higher resistivity layers
HR	Strong thermal–mechanical coupling	0	0	0	3	3	2	2	3	Improved coating performance and reduced porosity	Complex process, high cost, limited sample size
BB	Compaction	2	1	0	2	2	2	2	2	The residual stress is reduced, and the corrosion resistance and hardness of the coating are enhanced.	There is destruction of the microstructure near the surface of the coating, causing severe deformation.

Notes: (0): Feasible, (1): Not feasible, (2): No research, (3): Obvious improvement, (4): No improvement/decrease.

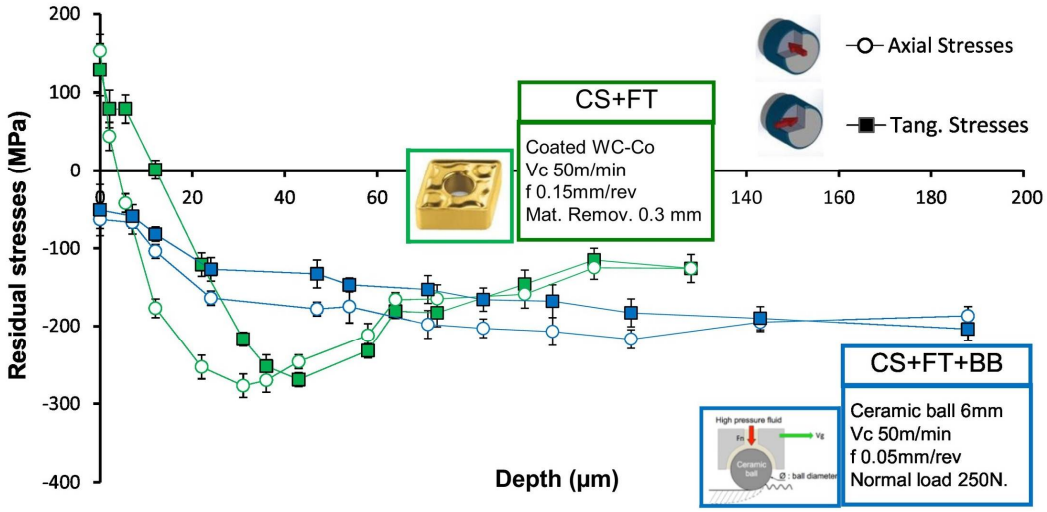

Figure 35. Residual stress profiles of the CS coating after finishing turning (FT) and finishing turning followed by ball-burnishing (BB) [159,160].

The post-process treatments of coatings can remarkably change the microstructure and properties of cold-sprayed coatings, but the currently available post-process treatments of CS can only improve one or two properties of coatings. In other words, no post-process treatments can fully improve the comprehensive performance of cold-sprayed coatings yet, as every post-process treatment of CS has its limitations and cannot meet all the requirements of specific working conditions. Therefore, composite post-process treatments will be the main development direction of the post-process treatments of CS. The composite post-process treatment needs to use two or more post-process treatments to improve the comprehensive performance of the coating. Such a process combines the advantages of various post-process treatments to comprehensively improve all the properties of cold-sprayed coatings. Therefore, a fundamental direction in future research on cold-sprayed coating is to use CS technology and the post-process treatments of coatings to devise a composite technology that can prepare cold-sprayed Cu-based composite coatings with excellent mechanical and tribological properties.

6. Conclusions and Prospects

As the CS equipment continues upgrading and iterating, CS technologies have been rapidly developed in both theoretical research and industrial applications. In the meantime, CS technology develops from a single CS technology to a composite "CS+" technology, while the post-process treatments of CS grow from a single post-process treatment to a composite post-process treatment. Accordingly, the research into cold-sprayed coatings also evolves from laboratory theoretical research to large-scale industrial production. As an emerging coating preparation technology, CS, by virtue of its high kinetic energy, low heat input, and high efficiency, has a broad prospect in the preparation and application of high-performance Cu-based composite coatings. CS mainly prepares high-performance Cu-based composite coatings under special working conditions by optimizing the spray process parameters, the composition of the sprayed powder, and the structure design. In recent years, promising results have been achieved in applying cold-sprayed Cu-based composite coatings to improve corrosion resistance, wear resistance, self-lubrication, and conductivity. However, there are few systematic studies on the post-process treatments of Cu-based composite coatings, the interface between the coating and the substrate, the bonding mechanism of the particle interface in the coating, and the morphology, composition, and structure of the sprayed particles that affect the microstructure, mechanical properties, and tribological properties of Cu-based composite coatings.

Therefore, the emphasis of research on cold-sprayed Cu-based composite coatings should be focused on the following aspects:

(1) Strengthening the research of the basic theory of cold spraying Cu-based composite coatings. The physical properties of the metal phase Cu and enhanced phase ceramic particles in the Cu-based composite coating differ greatly, therefore, the bonding mechanism of the metal composite coating cannot fully explain the role of ceramic particles, and the deposition characteristics of the cold sprayed Cu-based ceramic composite coating need to be studied in-depth. By optimizing the spraying process parameters and exploring the bonding process between metal and ceramic particles in the cold sprayed Cu-based composite coating, we can reveal the influence mechanism of the interfacial microstructure between ceramic particles on the performance of the Cu-based composite coating.

(2) The addition of ceramic reinforcement can indeed tremendously and comprehensively improve the wear resistance, mechanical properties, and other properties of Cu-based composite coatings. However, the interfacial bonding between cold-sprayed metal and ceramics is chiefly mechanical bonding, which has low bonding strength, fragile deposited layers, and other problems. This is because, during the deposition of cold-sprayed Cu-based ceramic composite coatings, ceramic particles will not deform during impacts as the temperature of the metal particles at the moment of impact cannot reach the melting point of the ceramics. For this reason, the focus of current research and the direction of future research remain to probe into the essence of the bonding mechanism of the coating, or to enhance the bonding strength of the metallization of cold-sprayed ceramics from the perspective of thermodynamics and dynamics based on existing technological means, including the combination of experimental and numerical simulations.

(3) Pores and cracks appear on the coating prepared only by CS technology due to poor plastic deformation and the high hardness of ceramic particles. However, surface-strengthening technologies, such as LR and ultrasonic rolling, can effectively rectify these defects. Therefore, developing appropriate "CS+" technologies for the different application directions of Cu-based composite coatings remains a hot research topic at present.

(4) Since cold-sprayed Cu-based composite coatings have low bonding strength, post-process treatment is needed to improve the microstructure and comprehensive properties of Cu-based composite coatings. As there are many types of post-process treatments of coatings, one or more composite post-process treatments can be employed, based on specific working conditions and the characteristics of coatings and post-process treatments, to improve the comprehensive performance of cold-sprayed Cu-based composite coatings, such as the strength of bonding with the substrate, ductility, cohesive strength, plasticity, anti-friction, wear resistance, and corrosion resistance.

Author Contributions: Conceptualization, P.L. and W.G.; writing—original draft preparation, P.L.; writing—review and editing, H.W. (Huipeng Wang), W.G., G.M., and H.W. (Haidou Wang); supervision, H.W. (Haidou Wang). All authors have read and agreed to the published version of the manuscript.

Funding: This paper is supported by the National Natural Science Foundation of China (52005511, 52122508, 52130509), Key Project (2021-JCJQ-ZD-302), the 14th Five-Year Plan Preliminary Research Project, and the 2022 Jiangxi Postgraduate Innovation Special Fund Project (YC2022-S672).

Institutional Review Board Statement: Not applicable.

Informed Consent Statement: Not applicable.

Data Availability Statement: Not applicable.

Conflicts of Interest: The authors declare no conflict of interest.

References

1. Xu, B. *Remanufacturing Engineering Basis and Its Application*; Harbin Institute of Technology Press: Harbin, China, 2005.
2. Guo, M.X.; Wang, M.P.; Cao, L.F.; Lei, R.S. Work softening characterization of alumina dispersion strengthened copper alloys. *Mater. Charact.* **2007**, *58*, 928–935. [CrossRef]
3. Guo, M.X.; Wang, M.P.; Shen, K.; Cao, L.F.; Lei, R.S.; Li, S.M. Effect of cold rolling on properties and microstructures of dispersion strengthened copper alloys. *Trans. Nonferrous Met. Soc. China* **2008**, *18*, 333–339. [CrossRef]
4. Wei, F.-J.; Chou, B.-Y.; Fung, K.-Z.; Tsai, S.-Y.; Yang, C.-W. Influence of Powder Plasticity on Bonding Strength of Cold-Sprayed Copper Coating. *Coatings* **2022**, *12*, 1197. [CrossRef]
5. Winnicki, M.; Małachowska, A.; Dudzik, G.; Rutkowska-Gorczyca, M.; Marciniak, M.; Abramski, K.; Ambroziak, A.; Pawłowski, L. Numerical and experimental analysis of copper particles velocity in low-pressure cold spraying process. *Surf. Coat. Technol.* **2015**, *268*, 230–240. [CrossRef]
6. Assadi, H.; Schmidt, T.; Richter, H.; Kliemann, J.O.; Binder, K.; Gärtner, F.; Klassen, T.; Kreye, H. On Parameter Selection in Cold Spraying. *J. Therm. Spray Technol.* **2011**, *20*, 1161–1176. [CrossRef]
7. Wang, J.Q.; Cui, X.Y.; Xiong, T.Y. Research Progress of Cold Sprayed Metal Matrix Composite Coatings and Materials. *China Surf. Eng.* **2020**, *33*, 51–67. [CrossRef]
8. Winnicki, M. Advanced Functional Metal-Ceramic and Ceramic Coatings Deposited by Low-Pressure Cold Spraying: A Review. *Coatings* **2021**, *11*, 1044. [CrossRef]
9. Chen, Y.; Yu, M.; Cao, K.; Chen, H. Advance on Copper-based Self-lubricating Coatings. *Surf. Technol.* **2021**, *50*, 91–100+220. [CrossRef]
10. Gärtner, F.; Stoltenhoff, T.; Voyer, J.; Kreye, H.; Riekehr, S.; Koçak, M. Mechanical properties of cold-sprayed and thermally sprayed copper coatings. *Surf. Coat. Technol.* **2006**, *200*, 6770–6782. [CrossRef]
11. Li, B.; Cao, Z. Metal-based Solid Self-lubricating Composite Coating and Its Preparation Technology. *Surf. Technol.* **2017**, *46*, 32–38. [CrossRef]
12. Poza, P.; Garrido-Maneiro, M.Á. Cold-sprayed coatings: Microstructure, mechanical properties, and wear behaviour. *Prog. Mater. Sci.* **2022**, *123*, 100839. [CrossRef]
13. Kumar, S. Influence of processing conditions on the mechanical, tribological and fatigue performance of cold spray coating: A review. *Surf. Eng.* **2022**, *38*, 324–365. [CrossRef]
14. Dykhuizen, R.C.; Smith, M.F. Gas Dynamic Principles of Cold Spray. *J. Therm. Spray Technol.* **1998**, *7*, 205–212. [CrossRef]
15. Sun, W.; Chu, X.; Lan, H.; Huang, R.; Huang, J.; Xie, Y.; Huang, J.; Huang, G. Current Implementation Status of Cold Spray Technology: A Short Review. *J. Therm. Spray Technol.* **2022**, *31*, 848–865. [CrossRef]
16. Karthikeyan, J. The advantages and disadvantages of the cold spray coating process. In *The Cold Spray Materials Deposition Process*; Elsevier: Cambridge, MA, USA, 2007; pp. 62–71.
17. Silvello, A.; Cavaliere, P.; Rizzo, A.; Valerini, D.; Dosta Parras, S.; Garcia Cano, I. Fatigue Bending Behavior of Cold-Sprayed Nickel-Based Superalloy Coatings. *J. Therm. Spray Technol.* **2019**, *28*, 930–938. [CrossRef]
18. Guerreiro, B.; Vo, P.; Poirier, D.; Legoux, J.-G.; Zhang, X.; Giallonardo, J.D. Factors Affecting the Ductility of Cold-Sprayed Copper Coatings. *J. Therm. Spray Technol.* **2020**, *29*, 630–641. [CrossRef]
19. Winnicki, M.; Baszczuk, A.; Gibas, A.; Jasiorski, M. Experimental study on aluminium bronze coatings fabricated by low pressure cold spraying and subsequent heat treatment. *Surf. Coat. Technol.* **2023**, *456*, 129260. [CrossRef]
20. Zhang, M.; Qiao, Y.; Zhang, Z.; Zhang, W.; Yu, H. Deposition Behavior and Corrosion Resistance of Cold Sprayed Cu-based Composite Coatings. *Mod. Salt. Chem. Ind.* **2019**, *46*, 35–36. [CrossRef]
21. Li, W.; Cao, C.; Wang, G.; Wang, F.; Xu, Y.; Yang, X. 'Cold spray +' as a new hybrid additive manufacturing technology: A literature review. *Sci. Technol. Weld. Join.* **2019**, *24*, 420–445. [CrossRef]
22. Li, F.; Li, D.; Chang, J.; An, G.; Li, W. Properties of Copper-Based Bulks Materials Produced by Low Pressure Cold Spray Additives. *Rare Met. Mater. Eng.* **2020**, *49*, 1729–1735. (In Chinese)
23. Alkhimov, A.P.; Kosarev, V.F.; Papyrin, A.N. A method of cold gas-dynamic deposition. *Sov. Phys. Dokl.* **1990**, *35*, 1047–1049.
24. Yin, S.; Cavaliere, P.; Aldwell, B.; Jenkins, R.; Liao, H.; Li, W.; Lupoi, R. Cold spray additive manufacturing and repair: Fundamentals and applications. *Addit. Manuf.* **2018**, *21*, 628–650. [CrossRef]
25. Assadi, H.; Kreye, H.; Gärtner, F.; Klassen, T. Cold spraying—A materials perspective. *Acta Mater.* **2016**, *116*, 382–407. [CrossRef]
26. Suo, X.; Yin, S.; Planche, M.-P.; Liu, T.; Liao, H. Strong effect of carrier gas species on particle velocity during cold spray processes. *Surf. Coat. Technol.* **2015**, *268*, 90–93. [CrossRef]
27. Huang, C.; Yin, S.; Li, W.; Guo, X. Cold Spray Technology and Its System: Research Status and Prospect. *Surf. Technol.* **2021**, *50*, 1–23. [CrossRef]
28. Assadi, H.; Gärtner, F.; Stoltenhoff, T.; Kreye, H. Bonding mechanism in cold gas spraying. *Acta Mater.* **2003**, *51*, 4379–4394. [CrossRef]
29. Grujicic, M.; Zhao, C.L.; DeRosset, W.S.; Helfritch, D. Adiabatic shear instability based mechanism for particles/substrate bonding in the cold-gas dynamic-spray process. *Mater. Des.* **2004**, *25*, 681–688. [CrossRef]
30. Li, W.-Y.; Li, C.-J.; Liao, H. Significant influence of particle surface oxidation on deposition efficiency, interface microstructure and adhesive strength of cold-sprayed copper coatings. *Appl. Surf. Sci.* **2010**, *256*, 4953–4958. [CrossRef]

31. Hassani-Gangaraj, M.; Veysset, D.; Champagne, V.K.; Nelson, K.A.; Schuh, C.A. Adiabatic shear instability is not necessary for adhesion in cold spray. *Acta Mater.* **2018**, *158*, 430–439. [CrossRef]
32. Fardan, A.; Berndt, C.C.; Ahmed, R. Numerical modelling of particle impact and residual stresses in cold sprayed coatings: A review. *Surf. Coat. Technol.* **2021**, *409*, 126835. [CrossRef]
33. Hassani-Gangaraj, M.; Veysset, D.; Champagne, V.K.; Nelson, K.A.; Schuh, C.A. Response to Comment on "Adiabatic shear instability is not necessary for adhesion in cold spray". *Scr. Mater.* **2019**, *162*, 515–519. [CrossRef]
34. Lienhard, J.; Crook, C.; Azar, M.Z.; Hassani, M.; Mumm, D.R.; Veysset, D.; Apelian, D.; Nelson, K.A.; Champagne, V.; Nardi, A.; et al. Surface oxide and hydroxide effects on aluminum microparticle impact bonding. *Acta Mater.* **2020**, *197*, 28–39. [CrossRef]
35. Hussain, T.; McCartney, D.G.; Shipway, P.H.; Zhang, D. Bonding Mechanisms in Cold Spraying: The Contributions of Metallurgical and Mechanical Components. *J. Therm. Spray Technol.* **2009**, *18*, 364–379. [CrossRef]
36. Moridi, A.; Hassani-Gangaraj, S.M.; Guagliano, M.; Dao, M. Cold spray coating: Review of material systems and future perspectives. *Surf. Eng.* **2014**, *30*, 369–395. [CrossRef]
37. Xie, Y.; Yin, S.; Chen, C.; Planche, M.-P.; Liao, H.; Lupoi, R. New insights into the coating/substrate interfacial bonding mechanism in cold spray. *Scr. Mater.* **2016**, *125*, 1–4. [CrossRef]
38. Grujicic, M.; Saylor, J.R.; Beasley, D.E.; DeRosset, W.S.; Helfritch, D. Computational analysis of the interfacial bonding between feed-powder particles and the substrate in the cold-gas dynamic-spray process. *Appl. Surf. Sci.* **2003**, *219*, 211–227. [CrossRef]
39. Li, W.; Yang, K.; Yin, S.; Yang, X.; Xu, Y.; Lupoi, R. Solid-state additive manufacturing and repairing by cold spraying: A review. *J. Mater. Sci. Technol.* **2018**, *34*, 440–457. [CrossRef]
40. Spencer, K.; Fabijanic, D.M.; Zhang, M.X. The use of Al–Al_2O_3 cold spray coatings to improve the surface properties of magnesium alloys. *Surf. Coat. Technol.* **2009**, *204*, 336–344. [CrossRef]
41. Fernandez, R.; Jodoin, B. Cold Spray Aluminum–Alumina Cermet Coatings: Effect of Alumina Morphology. *J. Therm. Spray Technol.* **2019**, *28*, 737–755. [CrossRef]
42. Fernandez, R.; Jodoin, B. Cold Spray Aluminum–Alumina Cermet Coatings: Effect of Alumina Content. *J. Therm. Spray Technol.* **2018**, *27*, 603–623. [CrossRef]
43. He, L.; Hassani, M. A Review of the Mechanical and Tribological Behavior of Cold Spray Metal Matrix Composites. *J. Therm. Spray Technol.* **2020**, *29*, 1565–1608. [CrossRef]
44. Chen, W.; Tan, H.; Cheng, J.; Zhu, S.; Yang, J. Research Progress and Prospect of Tribological Properties of Cold Sprayed Copper-based Composite Coatings. *Mater. Rep.* **2022**, *36*, 58–64. [CrossRef]
45. Zhang, H.; Shan, A.; Wei, L.; Wu, J.; Zhang, J.; Liang, Y.; Song, H. Developments of the Bonding Mechanism and Process in Cold Gas Dynamic Spray. *Mater. Rep.* **2007**, *21*, 80–91. [CrossRef]
46. Schmidt, T.; Gärtner, F.; Assadi, H.; Kreye, H. Development of a generalized parameter window for cold spray deposition. *Acta Mater.* **2006**, *54*, 729–742. [CrossRef]
47. Fukumoto, M.; Wada, H.; Tanabe, K.; Yamada, M.; Yamaguchi, E.; Niwa, A.; Sugimoto, M.; Izawa, M. Effect of Substrate Temperature on Deposition Behavior of Copper Particles on Substrate Surfaces in the Cold Spray Process. *J. Therm. Spray Technol.* **2007**, *16*, 643–650. [CrossRef]
48. Koivuluoto, H.; Coleman, A.; Murray, K.; Kearns, M.; Vuoristo, P. High Pressure Cold Sprayed (HPCS) and Low Pressure Cold Sprayed (LPCS) Coatings Prepared from OFHC Cu Feedstock: Overview from Powder Characteristics to Coating Properties. *J. Therm. Spray Technol.* **2012**, *21*, 1065–1075. [CrossRef]
49. Zhang, L.; Zhang, Y.; Wu, H.; Yang, S.; Jie, X. Structure and corrosion behavior of cold-sprayed Cu/Ni composite coating post-treated by ultrasonic shot peening. *SN Appl. Sci.* **2020**, *2*, 1–14. [CrossRef]
50. Deng, N.; Tang, J.; Xiong, T.; Li, J.; Zhou, Z. Fabrication and characterization of W Cu composite coatings with different W contents by cold spraying. *Surf. Coat. Technol.* **2019**, *368*, 8–14. [CrossRef]
51. Huang, C.J.; Wu, H.J.; Xie, Y.C.; Li, W.Y.; Verdy, C.; Planche, M.P.; Liao, H.L.; Montavon, G. Advanced brass-based composites via cold-spray additive-manufacturing and its potential in component repairing. *Surf. Coat. Technol.* **2019**, *371*, 211–223. [CrossRef]
52. Yu, T.; Ma, G.; Guo, W.; He, P.; Huang, Y.; Liu, M.; Wang, H. Microstructure and Properties of Cold Sprayed Cu-Ti_3SiC_2 Composite Coatings withDifferent Ceramic Contents. *Mater. Rep.* **2022**, *36*, 109–114. [CrossRef]
53. Zhang, Y.; Michael Shockley, J.; Vo, P.; Chromik, R.R. Tribological Behavior of a Cold-Sprayed Cu–MoS_2 Composite Coating During Dry Sliding Wear. *Tribol. Lett.* **2016**, *62*, 1–12. [CrossRef]
54. Zhang, Y.Y.; Epshteyn, Y.; Chromik, R.R. Dry sliding wear behaviour of cold-sprayed Cu-MoS_2 and Cu-MoS_2-WC composite coatings: The influence of WC. *Tribol. Int.* **2018**, *123*, 296–306. [CrossRef]
55. Zhang, Y.; Descartes, S.; Chromik, R.R. Influence of WC on third body behaviour during fretting of cold-sprayed Cu MoS2WC composites. *Tribol. Int.* **2019**, *134*, 15–25. [CrossRef]
56. Tazegul, O.; Dylmishi, V.; Cimenoglu, H. Copper matrix composite coatings produced by cold spraying process for electrical applications. *Arch. Civ. Mech. Eng.* **2016**, *16*, 344–350. [CrossRef]
57. Rokni, M.R.; Nutt, S.R.; Widener, C.A.; Champagne, V.K.; Hrabe, R.H. Review of Relationship Between Particle Deformation, Coating Microstructure, and Properties in High-Pressure Cold Spray. *J. Therm. Spray Technol.* **2017**, *26*, 1308–1355. [CrossRef]
58. Yang, S.; Wang, J.; Guo, Q. The Progress and Application Status of Cold Spraying Technology. *New Technol. New Process.* **2011**, *2*, 52–56. [CrossRef]

59. Hanft, D.; Exner, J.; Schubert, M.; Stöcker, T.; Fuierer, P.; Moos, R. An overview of the aerosol deposition method: Process fundamentals and new trends in materials applications. *J. Ceram. Sci. Technol.* **2015**, *6*, 147–182. [CrossRef]
60. Champagne, V.K.; Helfritch, D.J.; Dinavahi, S.P.G.; Leyman, P.F. Theoretical and Experimental Particle Velocity in Cold Spray. *J. Therm. Spray Technol.* **2010**, *20*, 425–431. [CrossRef]
61. Gu, S.; Kamnis, S. Numerical modelling of in-flight particle dynamics of non-spherical powder. *Surf. Coat. Technol.* **2009**, *203*, 3485–3490. [CrossRef]
62. Fukanuma, H.; Ohno, N.; Sun, B.; Huang, R. In-flight particle velocity measurements with DPV-2000 in cold spray. *Surf. Coat. Technol.* **2006**, *201*, 1935–1941. [CrossRef]
63. Venkatesh, L.; Chavan, N.M.; Sundararajan, G. The Influence of Powder Particle Velocity and Microstructure on the Properties of Cold Sprayed Copper Coatings. *J. Therm. Spray Technol.* **2011**, *20*, 1009–1021. [CrossRef]
64. Ma, W.; Xie, Y.; Chen, C.; Fukanuma, H.; Wang, J.; Ren, Z.; Huang, R. Microstructural and mechanical properties of high-performance Inconel 718 alloy by cold spraying. *J. Alloys Compd.* **2019**, *792*, 456–467. [CrossRef]
65. Luo, X.T.; Xie, T.; Li, C.J.; Li, C.X. Microstructure and Properties Tailoring of Cold Sprayed Metals. *China Surf. Eng.* **2020**, *33*, 68–81. [CrossRef]
66. Li, Y.-J.; Luo, X.-T.; Rashid, H.; Li, C.-J. A new approach to prepare fully dense Cu with high conductivities and anti-corrosion performance by cold spray. *J. Alloys Compd.* **2018**, *740*, 406–413. [CrossRef]
67. Li, Y.-J.; Luo, X.-T.; Li, C.-J. Dependency of deposition behavior, microstructure and properties of cold sprayed Cu on morphology and porosity of the powder. *Surf. Coat. Technol.* **2017**, *328*, 304–312. [CrossRef]
68. Ning, X.-J.; Jang, J.-H.; Kim, H.-J. The effects of powder properties on in-flight particle velocity and deposition process during low pressure cold spray process. *Appl. Surf. Sci.* **2007**, *253*, 7449–7455. [CrossRef]
69. Jodoin, B.; Ajdelsztajn, L.; Sansoucy, E.; Zúñiga, A.; Richer, P.; Lavernia, E.J. Effect of particle size, morphology, and hardness on cold gas dynamic sprayed aluminum alloy coatings. *Surf. Coat. Technol.* **2006**, *201*, 3422–3429. [CrossRef]
70. Zhou, H.X.; Li, C.X.; Li, C.J. Research Progress of Cold Sprayed Ti and Ti Alloy Coatings. *China Surf. Eng.* **2020**, *33*, 1–14. [CrossRef]
71. Klinkov, S.V.; Kosarev, V.F.; Rein, M. Cold spray deposition: Significance of particle impact phenomena. *Aerosp. Sci. Technol.* **2005**, *9*, 582–591. [CrossRef]
72. Song, X.; Ng, K.L.; Chea, J.M.-K.; Sun, W.; Tan, A.W.-Y.; Zhai, W.; Li, F.; Marinescu, I.; Liu, E. Coupled Eulerian-Lagrangian (CEL) simulation of multiple particle impact during Metal Cold Spray process for coating porosity prediction. *Surf. Coat. Technol.* **2020**, *385*, 125433. [CrossRef]
73. Yin, S.; Suo, X.; Xie, Y.; Li, W.; Lupoi, R.; Liao, H. Effect of substrate temperature on interfacial bonding for cold spray of Ni onto Cu. *J. Mater. Sci.* **2015**, *50*, 7448–7457. [CrossRef]
74. Go, T.; Sohn, Y.J.; Mauer, G.; Vaßen, R.; Gonzalez-Julian, J. Cold spray deposition of Cr2AlC MAX phase for coatings and bond-coat layers. *J. Eur. Ceram. Soc.* **2019**, *39*, 860–867. [CrossRef]
75. Liu, H.; Ren, Y.; Li, T.; Cui, X.; Wang, J.; Xiong, T. Pores in Cold Sprayed Deposits and Their Control Methods. *Mater. Prot.* **2022**, *55*, 1–21. [CrossRef]
76. Yin, S.; Wang, X.; Li, W.; Liao, H.; Jie, H. Deformation behavior of the oxide film on the surface of cold sprayed powder particle. *Appl. Surf. Sci.* **2012**, *259*, 294–300. [CrossRef]
77. Yin, S.; Wang, X.-f.; Li, W.Y.; Jie, H.-e. Effect of substrate hardness on the deformation behavior of subsequently incident particles in cold spraying. *Appl. Surf. Sci.* **2011**, *257*, 7560–7565. [CrossRef]
78. Cao, C.; Li, W.; Yang, K.; Li, C.; Ji, G. Influence of Substrate Hardness and Thermal Characteristics on Microstructure and Mechanical Properties of Cold Sprayed TC4 Titanium Alloy Coatings. *Mater. Rep.* **2019**, *33*, 277–282. (In Chinese) [CrossRef]
79. Cetin, O.; Tazegul, O.; Kayali, E.S. Effect of Parameters to the Coating Formation during Cold Spray Process. In Proceedings of the 2nd World Congress on Mechanical, Chemical, and Material Engineering, Budapest, Hungary, 22–23 August 2016; pp. 1401–1407.
80. Marrocco, T.; McCartney, D.G.; Shipway, P.H.; Sturgeon, A.J. Production of Titanium Deposits by Cold-Gas Dynamic Spray: Numerical Modeling and Experimental Characterization. *J. Therm. Spray Technol.* **2006**, *15*, 263–272. [CrossRef]
81. Kumar, S.; Bae, G.; Lee, C. Influence of substrate roughness on bonding mechanism in cold spray. *Surf. Coat. Technol.* **2016**, *304*, 592–605. [CrossRef]
82. Singh, S.; Singh, H.; Chaudhary, S.; Buddu, R.K. Effect of substrate surface roughness on properties of cold-sprayed copper coatings on SS316L steel. *Surf. Coat. Technol.* **2020**, *389*, 125619. [CrossRef]
83. Singh, S.; Singh, H.; Buddu, R.K. Microstructural investigations on bonding mechanisms of cold-sprayed copper with SS316L steel. *Surf. Eng.* **2019**, *36*, 1067–1080. [CrossRef]
84. Chang, J. Study on Corrosion Resistance of Low Pressure Cold Sprayed Copper Matrix Composite Coatings Alloy. Master's Thesis, Lanzhou University of Technology, Lanzhou, China, 2019.
85. Jiang, Y.; Zhu, H. Research Status of Friction and Wear Properties of Copper Matrix Composites. *Mater. Rep.* **2014**, *28*, 33–36+65. [CrossRef]
86. Lei, Q.; Yang, Y.; Zhu, X.; Jiang, Y.; Gong, S.; Li, Z. Research Progress and Prospect on High Strength, High Conductivity, and High Heat Resistance Copper Alloys. *Mater. Rep.* **2021**, *35*, 15153–15161. [CrossRef]
87. Shikalov, V.S.; Filippov, A.A.; Vidyuk, T.M. Cold Spray Deposition of Composite Copper-Tungsten Coatings. *Mater. Phys. Mech.* **2021**, *47*, 787–795. [CrossRef]

88. Zhang, L.; Huang, J.; Diao, P.; Li, D.; Huang, R.; Zhang, N.; Xie, Y. Structure and wear behavior of CuZn35 coating prepared by cold spraying. *Surf. Technol.* **2022**, 1–13. Available online: http://kns.cnki.net/kcms/detail/50.1083.tg.20220512.20221722.202200 31.html (accessed on 6 February 2023).
89. Triantou, K.I.; Pantelis, D.I.; Guipont, V.; Jeandin, M. Microstructure and tribological behavior of copper and composite copper+alumina cold sprayed coatings for various alumina contents. *Wear* **2015**, *336–337*, 96–107. [CrossRef]
90. Chen, Q.; Yu, M.; Cao, K.; Chen, H. Thermal conductivity and wear resistance of cold sprayed Cu-ceramic phase composite coating. *Surf. Coat. Technol.* **2022**, *434*, 128135. [CrossRef]
91. Yin, S.; Zhang, Z.; Ekoi, E.J.; Wang, J.J.; Dowling, D.P.; Nicolosi, V.; Lupoi, R. Novel cold spray for fabricating graphene-reinforced metal matrix composites. *Mater. Lett.* **2017**, *196*, 172–175. [CrossRef]
92. Zhang, L.; Yang, S.; Lv, X.; Jie, X. Wear and Corrosion Resistance of Cold-Sprayed Cu-Based Composite Coatings on Magnesium Substrate. *J. Therm. Spray Technol.* **2019**, *28*, 1212–1224. [CrossRef]
93. Yang, J.; Zhang, Y.J.; Zhao, X.Q.; An, Y.L.; Zhou, H.D.; Chen, J.M.; Hou, G.L. Tribological behaviors of plasma sprayed CuAl/Ni-graphite composite coating. *Tribol. Int.* **2015**, *90*, 96–103. [CrossRef]
94. Zhen, W.; Liang, B. Tribological Behavior of Plasma Sprayed MoS_2/CuComposite Coating Under Vacuum Atmosphere. *J. Mater. Eng.* **2013**, *3*, 16–22. [CrossRef]
95. Chen, S.; Bi, Y.; Zhang, H.; Liang, J.; Wellburn, D.; Chang-sheng, L.I.U. Effect of BN fraction on the mechanical and tribological properties of Cu alloy/BN self-lubricating sleeves. *J. Compos. Mater.* **2015**, *49*, 3715–3725. [CrossRef]
96. Shahar, C.; Zbaida, D.; Rapoport, L.; Cohen, H.; Bendikov, T.; Tannous, J.; Dassenoy, F.; Tenne, R. Surface functionalization of WS_2 fullerene-like nanoparticles. *Langmuir* **2010**, *26*, 4409–4414. [CrossRef] [PubMed]
97. Ling, H.J.; Mai, Y.J.; Li, S.L.; Zhang, L.Y.; Liu, C.S.; Jie, X.H. Microstructure and improved tribological performance of graphite/copper-zinc composite coatings fabricated by low pressure cold spraying. *Surf. Coat. Technol.* **2019**, *364*, 256–264. [CrossRef]
98. Chen, W.; Yu, Y.; Cheng, J.; Wang, S.; Zhu, S.; Liu, W.; Yang, J. Microstructure, Mechanical Properties and Dry Sliding Wear Behavior of Cu-Al_2O_3-Graphite Solid-Lubricating Coatings Deposited by Low-Pressure Cold Spraying. *J. Therm. Spray Technol.* **2018**, *27*, 1652–1663. [CrossRef]
99. Ling, H. Preparation and Tribological Properties of Cold Sprayed Copper-Based Self-lubricating Composite Coatings. Master's Thesis, Guangdong University of Technology, Guangzhou, China, 2019.
100. Smid, I.; Segall, A.E.; Walia, P.; Aggarwal, G.; Eden, T.J.; Potter, J.K. Cold-Sprayed Ni-hBN Self-Lubricating Coatings. *Tribol. Trans.* **2012**, *55*, 599–605. [CrossRef]
101. Wang, Y.; Zhu, Y.; Li, R.; Wang, H.; Tian, L.; Li, H. Microstructure and Wear Behavior of Cold-Sprayed Cu-BNNSs Composite Coating. *J. Therm. Spray Technol.* **2021**, *30*, 1482–1492. [CrossRef]
102. Zhu, Y. Microstructure and Wear Behavior of Cold-Sprayed Cu-BNNSs Composite Coating. Master's Thesis, Jiangsu University, Zhenjiang, China, 2021. (In Chinese)
103. Koivuluoto, H.; Vuoristo, P. Structural Analysis of Cold-Sprayed Nickel-Based Metallic and Metallic-Ceramic Coatings. *J. Therm. Spray Technol.* **2010**, *19*, 975–989. [CrossRef]
104. Winnicki, M.; Baszczuk, A.; Jasiorski, M.; Małachowska, A. Corrosion Resistance of Copper Coatings Deposited by Cold Spraying. *J. Therm. Spray Technol.* **2017**, *26*, 1935–1946. [CrossRef]
105. Ding, R. Study on Preparation, Anticorrosion and Antifouling Properties of Copper Composite Coatings Prepared by Cold Spray Technology. Ph.D. Thesis, Ocean University of China, OUC, Qingdao, China, 2014.
106. Sun, X.; Chen, Z.; Li, Z.; Huang, Y.; Shi, Y. Tribocorrosion properties of nickel aluminum bronze coating prepared by cold spraying in different pH environment. *Chin. J. Eng.* **2017**, *39*, 1055–1061. [CrossRef]
107. Sun, X.F.; Chen, Z.H.; Li, Z.M.; Huang, Y.L.; Song, W. Cold Sprayed Cu402F Coating for Large Marine Propeller Remanufacturing. *China Surf. Eng.* **2017**, *30*, 159–166. [CrossRef]
108. Calli, C.; Tazegul, O.; Kayali, E.S. Wear and corrosion characteristics of copper-based composite coatings. *Ind. Lubr. Tribol.* **2017**, *69*, 300–305. [CrossRef]
109. Kang, N.; Coddet, P.; Liao, H.; Coddet, C. Cold gas dynamic spraying of a novel micro-alloyed copper: Microstructure, mechanical properties. *J. Alloys Compd.* **2016**, *686*, 399–406. [CrossRef]
110. Stoltenhoff, T.; Kreye, H.; Richter, H.J. An Analysis of the Cold Spray Process and Its Coatings. *J. Therm. Spray Technol.* **2002**, *11*, 542–550. [CrossRef]
111. Grigoriev, S.; Gershman, E.; Gershman, I.; Mironov, A. Properties of Cold Spray Coatings for Restoration of Worn-Out Contact Wires. *Coatings* **2021**, *11*, 626. [CrossRef]
112. Jiang, S.; Li, B. Microstructure and Property of Cold Sprayed Copper Coatings on 2A12 Aluminium Alloy. *Plat. Finish.* **2017**, *39*, 9–12. (In Chinese)
113. Coddet, P.; Verdy, C.; Coddet, C.; Debray, F. On the mechanical and electrical properties of copper-silver and copper-silver-zirconium alloys deposits manufactured by cold spray. *Mater. Sci. Eng. A* **2016**, *662*, 72–79. [CrossRef]
114. Yang, S.; Kang, Z.; Guo, T. Preparation and conductive property of Cu coatings and Cu-graphene composite coatings on ABS substrate. *Nanotechnology* **2020**, *31*, 195710. [CrossRef] [PubMed]
115. Li, W.; Cao, C.; Yang, X.; Xu, Y. Cold spraying hybrid processing technologyand its application. *J. Mater. Eng.* **2019**, *47*, 53–63. [CrossRef]

116. Ge, W.; Li, X.; Cheng, X.; Zhang, Q. Research Progress of Preparation and Surface-treatment Technology of Metal-Ceramic Composite Coatings. *Dev. Appl. Mater.* **2011**, *26*, 95–99. [CrossRef]
117. Deng, N.; Dong, H.; Che, H.; Li, S.; Zhou, Z. The Research Progress on Preparation of Metal Coatings by Cold Spraying and Its Application in Additive Manufacturing. *Surf. Technol.* **2020**, *49*, 57–66. [CrossRef]
118. Ren, y.; Qiu, X.; Liu, H.; Li, T.; Cui, X.; Wang, J.; Xiong, T. Application of Heat Treatment in Cold Spraying Additive Manufacturing. *Therm. Spray Technol.* **2020**, *12*, 1–17+29. [CrossRef]
119. Guo, Z.; Zhang, D.; He, W.; Yang, G.; Li, J.; Fu, L. Research Status and Prospect of Metal Multi-Material Additive Manufacturing. *J. Netshape Form. Eng.* **2022**, *14*, 129–137. [CrossRef]
120. Huang, R.; Sone, M.; Ma, W.; Fukanuma, H. The effects of heat treatment on the mechanical properties of cold-sprayed coatings. *Surf. Coat. Technol.* **2015**, *261*, 278–288. [CrossRef]
121. Price, T.S.; Shipway, P.H.; McCartney, D.G.; Calla, E.; Zhang, D. A Method for Characterizing the Degree of Inter-particle Bond Formation in Cold Sprayed Coatings. *J. Therm. Spray Technol.* **2007**, *16*, 566–570. [CrossRef]
122. Kang, N.; Coddet, P.; Liao, H.; Coddet, C. The effect of heat treatment on microstructure and tensile properties of cold spray Zr base metal glass/Cu composite. *Surf. Coat. Technol.* **2015**, *280*, 64–71. [CrossRef]
123. Xu, L.; Zhou, X.; Sun, C.; Xie, C. Preparation and Study of Copper Coating by Cold Spray Technology on Electric Conduction and Thermal Conductivity. *Therm. Spray Technol.* **2017**, *9*, 7–12. (In Chinese)
124. Stoltenhoff, T.; Borchers, C.; Gärtner, F.; Kreye, H. Microstructures and key properties of cold-sprayed and thermally sprayed copper coatings. *Surf. Coat. Technol.* **2006**, *200*, 4947–4960. [CrossRef]
125. Guo, X.; Zhang, G.; Li, W.-Y.; Dembinski, L.; Gao, Y.; Liao, H.; Coddet, C. Microstructure, microhardness and dry friction behavior of cold-sprayed tin bronze coatings. *Appl. Surf. Sci.* **2007**, *254*, 1482–1488. [CrossRef]
126. Sudharshan Phani, P.; Vishnukanthan, V.; Sundararajan, G. Effect of heat treatment on properties of cold sprayed nanocrystalline copper alumina coatings. *Acta Mater.* **2007**, *55*, 4741–4751. [CrossRef]
127. Zhang, L.; Huang, J.; Li, D.; Deng, C.; Huang, R.; Zhang, N.; Xie, Y. Preparation and Properties of Cold Sprayed Copper Coating on Stainless Steel Surface. *Surf. Technol.* **2022**, 1–11. Available online: http://kns.cnki.net/kcms/detail/50.1083.TG.20220817.2022 0927.20220006.html (accessed on 6 February 2023). (In Chinese).
128. Tazegul, O.; Meydanoglu, O.; Kayali, E.S. Surface modification of electrical contacts by cold gas dynamic spraying process. *Surf. Coat. Technol.* **2013**, *236*, 159–165. [CrossRef]
129. Li, W.-Y.; Yang, C.; Liao, H. Effect of vacuum heat treatment on microstructure and microhardness of cold-sprayed TiN particle-reinforced Al alloy-based composites. *Mater. Des.* **2011**, *32*, 388–394. [CrossRef]
130. Ma, Z.Y.; Feng, A.H.; Chen, D.L.; Shen, J. Recent Advances in Friction Stir Welding/Processing of Aluminum Alloys: Microstructural Evolution and Mechanical Properties. *Crit. Rev. Solid State Mater. Sci.* **2017**, *43*, 269–333. [CrossRef]
131. Hodder, K.J.; Izadi, H.; McDonald, A.G.; Gerlich, A.P. Fabrication of aluminum–alumina metal matrix composites via cold gas dynamic spraying at low pressure followed by friction stir processing. *Mater. Sci. Eng. A* **2012**, *556*, 114–121. [CrossRef]
132. Yang, K.; Li, W.; Xu, Y.; Yang, X. Using friction stir processing to augment corrosion resistance of cold sprayed AA2024/Al_2O_3 composite coatings. *J. Alloys Compd.* **2019**, *774*, 1223–1232. [CrossRef]
133. Sun, W.; Tan, A.W.Y.; Wu, K.Q.; Yin, S.; Yang, X.W.; Marinescu, I.; Liu, E.J. Post-Process Treatments on Supersonic Cold Sprayed Coatings: A Review. *Coatings* **2020**, *10*, 123. [CrossRef]
134. Li, K.; Liu, X.; Zhao, Y. Research Status and Prospect of Friction Stir Processing Technology. *Coatings* **2019**, *9*, 129. [CrossRef]
135. Khodabakhshi, F.; Marzbanrad, B.; Yazdanmehr, A.; Jahed, H.; Gerlich, A.P. Tailoring the residual stress during two-step cold gas spraying and friction-stir surface integration of titanium coating. *Surf. Coat. Technol.* **2019**, *380*, 125008. [CrossRef]
136. Huang, C.J.; Li, W.Y.; Zhang, Z.H.; Fu, M.S.; Planche, M.P.; Liao, H.L.; Montavon, G. Modification of a cold sprayed SiCp/Al5056 composite coating by friction stir processing. *Surf. Coat. Technol.* **2016**, *296*, 69–75. [CrossRef]
137. Huang, C.; Li, W.; Feng, Y.; Xie, Y.; Planche, M.-P.; Liao, H.; Montavon, G. Microstructural evolution and mechanical properties enhancement of a cold-sprayed Cu Zn alloy coating with friction stir processing. *Mater. Charact.* **2017**, *125*, 76–82. [CrossRef]
138. Wang, W.; Han, P.; Wang, Y.; Zhang, T.; Peng, P.; Qiao, K.; Wang, Z.; Liu, Z.; Wang, K. High-performance bulk pure Al prepared through cold spray-friction stir processing composite additive manufacturing. *J. Mater. Res. Technol.* **2020**, *9*, 9073–9079. [CrossRef]
139. Dzhurinskiy, D.; Babu, A.; Dautov, S.; Lama, A.; Mangrulkar, M. Modification of Cold-Sprayed Cu-Al-Ni-Al_2O_3 Composite Coatings by Friction Stir Technique to Enhance Wear Resistance Performance. *Coatings* **2022**, *12*, 1113. [CrossRef]
140. Li, W.Y.; Wu, D.; Hu, K.W.; Xu, Y.X.; Yang, X.W.; Zhang, Y. A comparative study on the employment of heat treatment, electric pulse processing and friction stir processing to enhance mechanical properties of cold-spray-additive-manufactured copper. *Surf. Coat. Technol.* **2021**, *409*, 126887. [CrossRef]
141. Wang, Z.; Han, C.; Huang, G.; Han, B.; Han, B. Cold spray micro-defects and post-treatment technologies: A review. *Rapid Prototyp. J.* **2021**, *28*, 330–357. [CrossRef]
142. Kang, N.; Verdy, C.; Coddet, P.; Xie, Y.; Fu, Y.; Liao, H.; Coddet, C. Effects of laser remelting process on the microstructure, roughness and microhardness of in-situ cold sprayed hypoeutectic Al-Si coating. *Surf. Coat. Technol.* **2017**, *318*, 355–359. [CrossRef]
143. Chen, Z.; Sun, X.; Li, Z.; Shi, Y.; Liu, X. Tribological Behavior of Cold Sprayed Cu402F Coating after Laser Remelting. *Surf. Technol.* **2017**, *46*, 161–167. [CrossRef]
144. Chen, Z.; Sun, X.; LI, Z.; Shi, Y.; Song, W.; Shuai, G. Corrosion Resistance of Ni-Al Bronze Based Coatings Prepared by Laser Remelting and Cold Spraying. *Surf. Eng. Remanuf.* **2017**, *17*, 23–27. (In Chinese)

145. Chen, Z.; Sun, X.; Li, Z.; Liu, X.; Shi, Y. Effect of laser remelting on microstructure and properties of nickel aluminum bronze coating prepared by cold spraying. *Trans. Mater. Heat Treat.* **2017**, *38*, 116–122. [CrossRef]
146. Chen, Z.; Sun, X.; Li, Z.; Shi, Y. Mechanical Properties of Cold Sprayed Cu402F and Cu Coating Deposited on Nickel Aluminum Bronze. *Mater. Rep.* **2018**, *32*, 1618–1622. [CrossRef]
147. Luo, X.-T.; Wei, Y.-K.; Wang, Y.; Li, C.-J. Microstructure and mechanical property of Ti and Ti6Al4V prepared by an in-situ shot peening assisted cold spraying. *Mater. Des.* **2015**, *85*, 527–533. [CrossRef]
148. Lu, F.F.; Ma, K.; Li, C.X.; Yasir, M.; Luo, X.T.; Li, C.J. Enhanced corrosion resistance of cold-sprayed and shot-peened aluminum coatings on LA43M magnesium alloy. *Surf. Coat. Technol.* **2020**, *394*, 125865. [CrossRef]
149. Wei, Y.-K.; Li, Y.-J.; Zhang, Y.; Luo, X.-T.; Li, C.-J. Corrosion resistant nickel coating with strong adhesion on AZ31B magnesium alloy prepared by an in-situ shot-peening-assisted cold spray. *Corros. Sci.* **2018**, *138*, 105–115. [CrossRef]
150. Zhang, W.; Luo, X.; Liu, Q.; Li, C. Research Progress in Metallic Coatings Prepared with the In -Situ Micro-Forging Assisted Cold Spraying. *Mater. Prot.* **2022**, *55*, 34–43. [CrossRef]
151. Moridi, A.; Hassani-Gangaraj, S.M.; Vezzú, S.; Trško, L.; Guagliano, M. Fatigue behavior of cold spray coatings: The effect of conventional and severe shot peening as pre-/post-treatment. *Surf. Coat. Technol.* **2015**, *283*, 247–254. [CrossRef]
152. Brown, R.F.; Smith, G.M.; Hehr, A.; Eden, T.J. Ultrasonic Consolidation Post-Treatment of CuNi:Cr_3C_2-NiCr Composite Cold Spray Coatings: A Mechanical and Microstructure Assessment. *J. Therm. Spray Technol.* **2021**, *30*, 2069–2082. [CrossRef]
153. Maharjan, N.; Bhowmik, A.; Kum, C.W.; Hu, J.K.; Yang, Y.J.; Zhou, W. Post-Processing of Cold Sprayed Ti-6Al-4V Coatings by Mechanical Peening. *Metals* **2021**, *11*, 1038. [CrossRef]
154. Yang, J.; Li, W.; Xing, C.; Yin, S. Research Progress in Cold Spraying of Copper Coating. *Mater. Prot.* **2022**, *55*, 58–70+85. [CrossRef]
155. Hu, K. Research on Microstructure and Strong Plasticity Improvement of Cold Sprayed Cu Deposits. Master's Thesis, Northwestern Polytechnical University, Xi'an, China, 2019.
156. Qiu, X.; Tariq, N.U.H.; Qi, L.; Wang, J.Q.; Xiong, T.Y. A hybrid approach to improve microstructure and mechanical properties of cold spray additively manufactured A380 aluminum composites. *Mater. Sci. Eng. A-Struct.* **2020**, *772*, 138828. [CrossRef]
157. Tariq, N.H.; Gyansah, L.; Qiu, X.; Du, H.; Wang, J.Q.; Feng, B.; Yan, D.S.; Xiong, T.Y. Thermo-mechanical post-treatment: A strategic approach to improve microstructure and mechanical properties of cold spray additively manufactured composites. *Mater. Des.* **2018**, *156*, 287–299. [CrossRef]
158. Huang, Q. Effect of Post-Treatment Process on Microstructure and Mechanical Properties of Cold Sprayed Pure Copper Coating. Master's Thesis, Southwest Jiaotong University, Chengdu, China, 2021.
159. Sova, A.; Courbon, C.; Valiorgue, F.; Rech, J.; Bertrand, P. Effect of Turning and Ball Burnishing on the Microstructure and Residual Stress Distribution in Stainless Steel Cold Spray Deposits. *J. Therm. Spray Technol.* **2017**, *26*, 1922–1934. [CrossRef]
160. Courbon, C.; Sova, A.; Valiorgue, F.; Pascal, H.; Sijobert, J.; Kermouche, G.; Bertrand, P.; Rech, J. Near surface transformations of stainless steel cold spray and laser cladding deposits after turning and ball-burnishing. *Surf. Coat. Technol.* **2019**, *371*, 235–244. [CrossRef]